Receptor switching controls human parvovirus B19 tropism and cell entry

Inaugural dissertation

of the Faculty of Science,

University of Bern

presented by

Jan Bieri

from Schangnau, BE

Supervisor of the doctoral thesis:

PD Dr. Carlos Ros

Department of Chemistry, Biochemistry and Pharmaceutical Sciences

Receptor switching controls human parvovirus B19 tropism and cell entry

Inaugural dissertation

of the Faculty of Science,

University of Bern

presented by

Jan Bieri

from Schangnau, BE

Supervisor of the doctoral thesis:

PD Dr. Carlos Ros

Department of Chemistry, Biochemistry and Pharmaceutical Sciences

Accepted by the Faculty of Science.

Bern, 07.04.2022

The Dean,

Prof. Dr. Zoltan Balogh

Acknowledgements

While the idea of completing a PhD seemed daunting initially, I am looking back fondly on the four-year-long commitment at the University of Bern. It is not easy to summarize or even recall all my feelings about this period. Still, what is clear to me is that I did not have to deal with over-long work hours and enormous mental stress that might be associated with a PhD position. Instead, I look back fondly at the time spent in the Ros lab. I have had the luxury of never regretting or second-guessing my decision to accept the position back in 2018. I believe this stems from both the enjoyable environment at work and the support I received from my friends and family. It certainly is not something that can be taken for granted. Primarily I am grateful to Carlos and his constant support throughout the past ve and a half years and for his abundance of patience. I also want to thank the various members of the Ros group throughout the years*. They have made the time both within and outside the lab thoroughly enjoyable. Being able to look forward to going to work is something that I hope to continue to experience in the future. I am also extremely grateful to my family for their support for my work and personal struggles.

*Remo, Maelle, Oli, Marcus, Andrea, Lukas, Cornelia, Minela, Corinne and Ruben.

Abstract

Cellular receptors are essential for virus entry and spread. Their identi cation is fundamental to understand the tropism and pathogenesis of the infection. Parvovirus B19 (B19V) is a human pathogen with global prevalence and has a marked tropism for erythroid progenitor cells (EPCs) in the bone marrow. Globoside, a highly abundant membrane glycosphingolipid (GSL), is required for the infection and has been historically considered the primary receptor of the virus. However, the pathogenicity and narrow erythroid tropism of B19V do not correlate with the wide expression pro le of globoside. Another receptor that is exclusively expressed in EPCs, here named VP1uR, was recently shown to be required and su cient for virus entry. While VP1uR is the receptor required for entry and infection in EPCs, the role of globoside is not yet clear.

To clarify the function of globoside in B19V infection, we knocked out the gene B3GalNT1 coding for the enzyme globoside synthase in UT7/Epo cells. The loss of this enzyme leads to the elimination of globoside and downstream GSLs. The B3GalNT1 KO cell line was used to investigate the contribution of globoside to virus entry. We con rmed that globoside does not have the expected function as the primary receptor required for B19V entry into permissive cells, a function that corresponds to VP1uR. Instead, we found that globoside has an essential role at a postentry step by facilitating the escape of the incoming viruses from the acidic endosomal vesicles. We also uncovered that the interaction of B19V with globoside occurs exclusively at mildly acidic pH values, similar to those encountered in early endosomes. In an arti cially induced acidic environment, the virus interacts with globoside on the surface of UT7/Epo cells which enables internalization. The nding that B19V a nity for globoside is tightly controlled by the pH has major consequences in the overall virus infection. Under neutral conditions, which are characteristic of the extracellular milieu, B19V does not interact with the ubiquitously expressed globoside. This strategy prevents the redirection of the virus to nonpermissive tissues facilitating the selective targeting of the EPCs in the bone marrow. However, considering the broad expression pro le of globoside, naturally occurring acidic niches in the body, such as the nasal mucosal surface, become potential targets for the virus, which may facilitate entry through the respiratory route.

Taken together, pH-dependent receptor switching between the widely expressed GSL globoside and the restricted VP1uR represents an evolutionary adaptation controlling the erythroid tropism of B19V.

Contents

1 Introduction

1.1 A world of viruses

Viruses are obligate, acellular parasites infecting every living organism. In the most basic way, viruses consist of a DNA or RNA genome which is encapsulated in a protein shell or capsid. Enveloped viruses have an additional lipid bilayer surrounding the capsid. Their small size and simplistic structure do not allow viruses to pack all the genes and proteins required for self-su cient replication. Regardless of their degree of complexity, they all lack the machinery necessary for protein synthesis. They also lack any metabolic activity of their own. Viruses are not only small, but they are also highly abundant. The total amount of viruses in the world is estimated to be 10^{31} [1], which is more than all living entities on earth combined. Lines up, all these viral particles would stretch over 100 million light-years into space [2].

The ongoing COVID-19 pandemic has showcased the colossal impact that such tiny, inanimate particles can have on humanity. Around 500'000 people die each year from in uenza infections alone [3]. Viral infections in animals and plants can lead to severe economic losses. Still, viruses are a crucial element of our ecosystem and, as such, they often play an important regulatory role. As an example, it is estimated that everyday viruses infect and kill roughly 20 % of bacteria in marine ecosystems [4]. The organic molecules released from the dead bacterial cells stimulate the growth of new bacterial and algae, which impacts the whole food chain. Another example is the viruses present in the gut, which have an immunomodulatory role similar to intestinal bacteria [5]. Accordingly, viruses should not be viewed only as foreign invaders causing disease, but also as an integral part of the animal and human biology promoting health.

1.2 A tale of receptors

The rst step required for a virus to initiate the infection is the interaction with molecules present on the plasma membrane. The rst contact with the cell generally relies on charge-based interactions [6], often mediated by sulfated glycan side chains of proteoglycans [6]. Viruses require speci c receptors to gain entry into permissive cells, a process that may require the contribution of co-receptors [7]. Virus binding to speci c receptors may trigger conformational changes leading to the fusion of the viral envelope with the cell membrane or induce penetration [7]. Alternatively, receptor binding can trigger receptor-mediated endocytosis, which may require the transport of virions to a speci c site on the cell surface [8]. Any molecule on the cell surface can serve as a viral receptor, e.g., proteins of the immunoglobulin superfamily (human immunode ciency virus [HIV], human rhinovirus), integrins (rotavirus), tetraspanins (hepatitis C virus [HCV]), lectins (ebola virus) or sialic acid (in uenza virus) [6]. While some viruses interact with a single receptor and it is su cient to trigger internalization,

others require multiple interactions with receptors and co-receptors before internalization is possible (e.g. Coxsackie B virus, HCV) [9]. The interaction of a virus with a cellular receptor is inherently non-physiological, and cells do not bene t from such interaction.

Viruses evolve to recognize speci c cell surface receptors under the pressure of the immune system. They must nd an equilibrium to maintain e cient receptor binding while evading the immune system. Cells also evolve to hamper the interaction with viruses, which increases chances of survival. By altering their surface molecules, cells may reduce viral a nity while maintaining the function of the receptor [10][11]. Some viruses were also observed to completely swap to another receptor of a similar structure and exploit another entry pathway into the host if necessary. Alternative receptors can also lead to a di erent set of symptoms than ordinarily observed [12].

The identi cation of viral receptors is fundamental to understanding the host range and tropism of the virus and facilitates the development of antiviral strategies. For example, vaccines that elicit a strong immune response against viral receptor-binding domains are most e cient in preventing infections [13][14].

1.3 The parvovirus family

The name "parvovirus" derives from the Latin word $parvus$, meaning "small". The parvovirus family thus contains some of the smallest viruses known. The parvovirus capsid is a robust, non-enveloped particle made out of 60 protein monomers, forming a T=1 icosahedral symmetry. The rst parvovirus identi ed was the Kilham rat virus in 1959 [15], followed by other rodent viruses with similar characteristics, including minute virus of mice (MVM) in 1966 [16]. However, it soon became evident that parvoviruses infect a plethora of di erent animals, having been found in practically all vertebrates as well as arthropods.

The $Parvoviridae$ family is divided into subfamilies based on host range and phylogenetic similarities. Members of the $Parvovirinae$ subfamily infect exclusively vertebrates whereas members of the $Densovirinae$ and $Hamaparvovirinae$ subfamilies infect arthropods.

1.3.1 Parvovirus infection in humans

The rst parvovirus found to infect and cause disease in humans was parvovirus B19 (B19V) in 1974 [17]. B19V has been assigned to the Erythroparvovirus genus. Since then, new parvoviruses with the ability to infect humans have been discovered in a total of ve di erent genera.

In 1967, adeno-associated viruses (AAV) were found in various human tissues [18]. AAVs belong to the Dependoparvovirus genus and do not cause disease. These viruses are defective and only replicate

in cells that are co-infected with another DNA virus, generally adenovirus or herpesvirus. Human bocavirus (HBoV) was first described in 2005 [19]. The virus belongs to the Bocaparvovirus genus and infects the lower respiratory tract. It is mostly found in children where it can cause respiratory disorders, such as bronchitis and pneumonia, as well as gastroenteritis [19][20]. Other, more recently discovered and less well studied human parvoviruses include the bufavirus (BuV) [21], tusavirus (TuV) [22] and cutavirus (CutaV) [23] from the genus Protoparvovirus as well as the human parvovirus 4 (PARV4) from the genus Tetraparvovirus [24]. The clinical significance of those viruses has not been fully determined.

1.3.2 Parvovirus infection in animals

Every major farm animal, such as chickens [25], sheep [26], horses [27], cattle [28] and pigs [29] can be infected by a member of the *Parvoviridae* family, causing diseases that vary in severity. In chickens, stunted growth has been observed [25][30], and infections in cattle and pigs during gestation can leads to fetal death and abortions [29]. Acute outbreaks of parvovirus infections cause serious economic costs for agricultural services [31]. Parvoviruses are also a concern for pets, especially for cats and dogs where the infection is often lethal [32]. Feline panleukopenia virus (FPV) can cause diarrhea, vomiting, fever, and leukopenia (decrease in blood leukocytes) [33] as well as cerebellar hypoplasia in kittens [34]. The canine parvovirus (CPV) can cause myocarditis as well as enteritis, leading to severe complications such as leukopenia, vomiting, diarrhea and sudden death [35][36]. Vaccines for FPV and CPV are available and widely used, but efficiency is oftentimes limited [32][33][37].

1.3.3 The *Parvoviridae*, a family with multiple faces

The *Parvoviridae* is a large virus family encompassing multiple human and animal pathogens as well as viruses with therapeutic applications. Research that focuses on human viruses is, among other things, important for the development of novel vaccines to combat infections and limit spread. Similarly, vaccines against the animal viruses of the family aim to improve prospects for both pets and farm animals. Multiple parvoviruses have also been employed for therapeutic applications: AAV is an extremely promising vector for gene therapy, with preclinical trials having been conducted for diseases such as cystic fibrosis [38][39] and muscular dystrophy [40]. Further, the oncolytic virus H1 (H1-PV), a rodent protoparvovirus, has been shown to infect and lyse tumor cells and has thus found applications in cancer therapy [41]. The marked advantage of this virus compared to conventional therapies is that it does not affect ordinary human cells, ensuring a high safety in its application and has been verified in phase I/IIa trials for glioblastoma [42]. Lastly, members of the *Parvoviridae* are useful model viruses. Due to their small genomes with limited coding capabilities, parvoviruses are ideal to study virus-host

interactions. Moreover, parvoviruses are interesting for viral inactivation studies, as they possess one of the most robust viral capsids. Lastly, their diminutive size makes them outstanding candidates for worst-case models in virus- ltration, an important process for the plasma industry [43]

1.4 Parvovirus B19: An introduction

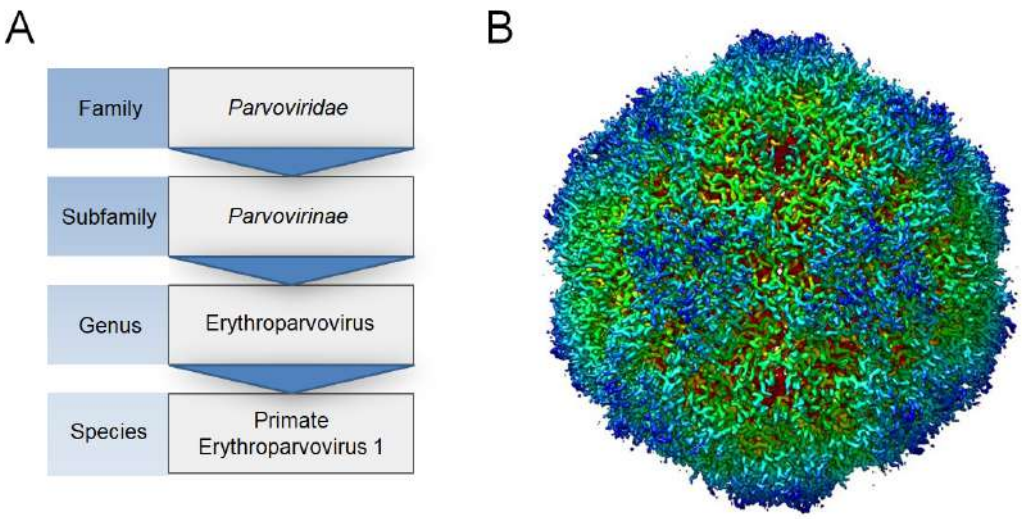

Figure 1: (A) Within the family *Parvoviridae*, the subfamily *Parvovirinae* and the genus Erythroparvovirus lies the species primate erythroparvovirus 1, most commonly known as parvovirus B19 or B19V [44]. (B) Detailed structure of the B19V capsid resolved by cryo-electron microscopy. Data was recorded using recombinant VP2 particles. Resolution: 2.8 Å, image provided by S. Hafenstein.

B19V was discovered in 1974 by Yvonne Cossart [17]. The name B19V derives from the sample (labeled 19 in panel B) in which the virus was discovered by accident when screening for hepatitis B surface antigen. B19V is a highly prevalent human pathogen belonging to the Erythroparvovirus genus (Figure 1A). As the name of the genus indicates, B19V has a marked tropism for erythroid progenitor cells, and the lytic infection in these cells accounts for the erythroid disorders typically associated with the infection. Transmission occurs via aerosol droplets that come into contact with the nasal mucose and the risk of infection increases in winter and spring [45]. No vaccine is currently available to prevent the infection.

The genome of the virus is protected by a nonenveloped icosahedral capsid with a diameter of roughly 25 nm (Figure 1B). The capsid is composed of 60 protomers, i.e. the minor viral protein 1 (VP1, 86 kDa) and the major viral protein 2 (VP2, 61 kDa) [46]. VP1 shares the same C-terminal amino acid sequence with VP2, but has an additional 227 amino acids at the N-terminus, the so-called VP1 unique region (VP1u). The VP2 and the VP1 make up 95 % (57 copies) and 5 % (3 copies) of the capsid, respectively. Inactivation studies have shown that B19V possesses a highly stable capsid against UV

light [47] and gamma rays [48]. However, heat and acidic pH have been shown to inactivate the virus [49][50][51]. Viral capsids are metastable structures and, as such, must be able to disassemble at the right cellular compartment during infection. The susceptibility of B19V to acidic pH may facilitate the required capsid conformational changes during the endocytic transit of the incoming virus, promoting nuclear targeting and uncoating.

1.4.1 The viral genome

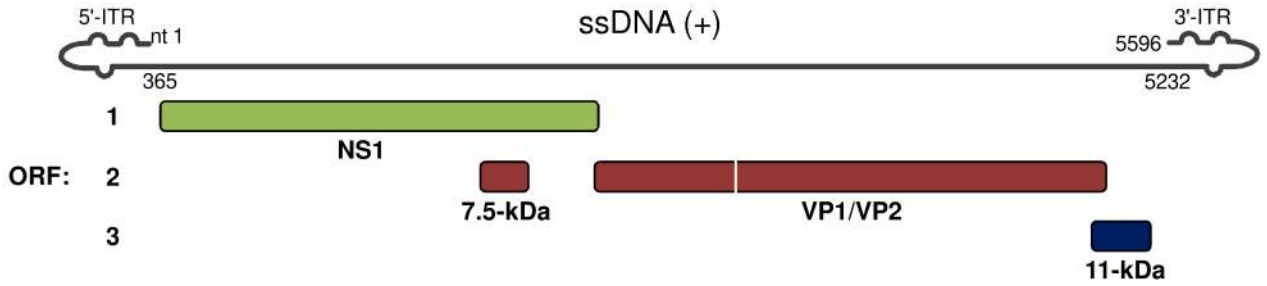

Figure 2: Properly scaled depiction of a positive sense genome of B19V. It is a 5596 long ssDNA with the ITRs flanking the genome on either side. At least five proteins are produced from a total of three different ORFs. The nonstructural protein 1 (NS1) and the 7.5-kDa on the left side of the genome are translated in the early stages of the infection. The structural proteins (VP1 and VP2), as well as the non-structural protein 11-kDa are important for later infection stages.

As with all parvoviruses, the genome is a short single-stranded DNA (ssDNA) molecule [52]. The virus packages positive and negative genomes in equal numbers [52]. Structurally, the ssDNA genome is 5996 nucleotides (nt) in length, and it is anked by two complementary inverted terminal repeats (ITRs, see Figure 2). The distal 365 nt of each ITR self hybridize, forming hairpin-like structures at the ends of the genome. The 3' hairpin forms a self-priming structure that is used for the initiation of DNA replication. It is not yet clear which structural conformation is adopted by the viral DNA within the virion. However, a highly ordered and dense secondary structure is necessary to t the roughly 2000 nm long genome into the 25 nm capsid [53]. After delivery inside the host nucleus, the ssDNA genome needs to be converted into a transcriptionally active double-stranded DNA (dsDNA) molecule. Unlike many other parvoviruses, such as MVM, H1-PV, and AAV, B19V (and other Erythroparvoviruses) only possesses a single promoter at the left-hand side of the genome [54]. This promoter was shown to be unusually strong and drives transcription of a single precursor-mRNA [54]. Figure 2 shows the transcriptional organization of the B19V genome, consisting of a total of three open reading frames (ORF). To express the proteins encoded at the left (proximal) and right (distal) sides of the genome, the precursor mRNA undergoes alternative polyadenylation and splicing. A more in-depth look into the transcriptional strategies and proteins of B19V is presented in subsection 1.5.

1.4.2 B19V receptors and tropism

Viral receptors are essential for virus entry and spread. Accordingly, their identi cation is fundamental to understanding the host range, tropism, and pathogenesis of the infection and to developing e ective antiviral strategies. In 1993, the small membrane glycosphingolipid (GSL), globoside (Gb4) (see subsection 1.6), was identi ed as the cellular receptor of B19V [57]. The hemagglutination of red blood cells (RBCs) by B19V could be inhibited in the presence of soluble globoside [57]. More importantly, individuals lacking globoside due to a rare mutation were found to be resistant to the infection [58]. These ndings represent strong evidence that globoside is the cellular receptor of B19V. However, attempts to demonstrate the interaction of B19V with globoside have yielded contradictory results. While some studies con rmed the interplay [59], others were unable to detect the interaction using various sensitive techniques [60].

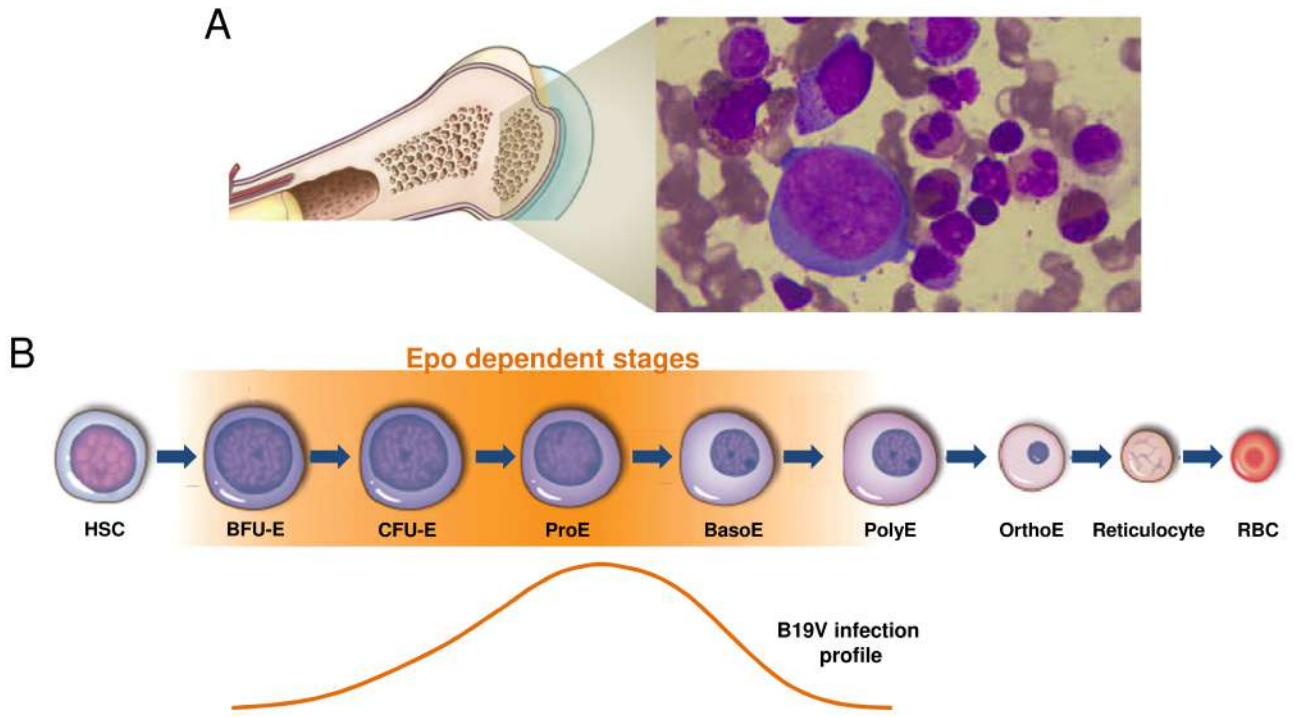

Figure 3: (A) B19V infects cells in the bone marrow. Prominently visible on the right is a giant proerythroblast with visible inclusions in the nucleus as well as a malformed cytoplasmic membrane. This represents a classical phenotype of B19V infection. Image adapted from [55]. (B) Schematic depiction of erythropoiesis. The orange hue represents the Epo dependent stages of differentiation. This coincides with the susceptibility and permissiveness for B19V infection. HSC: hematopoietic stem cell, BFU-E: burst-forming unit erythroid, CFU-E: colony-forming unit erythroid, E: erythroblast. Image adapted from [56].

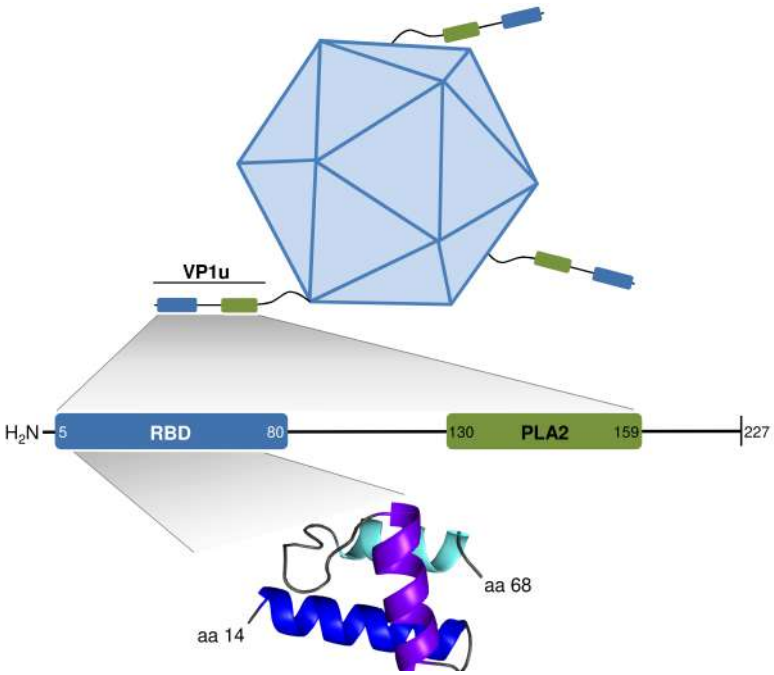

Figure 4: Representation of the B19V capsid with three exposed VP1u regions. In the native capsid, the VP1u, containing the RBD and PLA2 domain, is inaccessible [61]. The central amino acids of the RBD (14-68) are predicted to form three alpha-helices, depicted in dark blue, purple, and light blue. Generated with QUARK [62].

B19V has an extraordinarily restricted tropism for progenitor cells of the erythroid lineage. Speci cally, the virus infects cells at the erythropoietin (Epo)-dependent stages of di erentiation in the bone marrow (Figure 3A)[63][64]. Figure 3B shows the strong correlation between Epo-dependent di erentiation stages and permissiveness to B19V infection. Cells from the CFU-E to early basophilic erythroblasts, notably proerythroblasts, are permissive to the infection. The restricted erythroid tropism of B19V contrasts with the wide expression pro le of globoside (see subsection 1.6.1). As the tropism of B19V cannot be explained by globoside alone, another receptor or co-receptor has to be involved. In an attempt to explain the dissonance between globoside expression and B19V tropism, molecules such as Ku80 autoantigen [65] and integrin $\alpha 5\beta 1$ [66][67] have been proposed as co-receptors. However, follow-up studies have shown that neither of the two molecules is exclusively expressed in B19V susceptible cells [68].

A receptor-binding domain (RBD) was found in the VP1u. The RBD spans amino acids (aa) 5-80 of the N-terminal of VP1u (see Figure 4)[69]. The phospholipase A2 (PLA2) domain (aa 130-159), which is also present in the VP1u is not required for uptake and likely plays a role in intracellular tra cking of incoming virus [69]. The VP1u RBD interacts with an as yet unknown cellular receptor for uptake [70]. Only cells expressing the VP1u cognate receptor (VP1uR) are permissive for B19V infection [70]. Furthermore, the VP1uR on its own has proven to be required and su cient for virus

uptake [71][70], and its expression pro le corresponds precisely with the erythroid tropism of B19V [72].

1.4.3 B19V associated diseases

B19V is an endemic virus with a worldwide distribution. The main route of transmission occurs via droplets that come into contact with the upper respiratory mucosa [73]. Alternatively, B19V can be transmitted through blood transfusion or contaminated plasma-derived therapeutic products [74][73]. B19V infects and kills erythroid progenitor cells (EPCs) in the bone marrow, which leads to a temporary cessation of erythropoiesis [75]. Roughly half of young adults (18-24 years old) have been infected by the virus [76][77], and in people older than 65, the prevalence increases to almost 80 % [76][78]. B19V infection can cause various illnesses and a myriad of symptoms varying in severity. Chie y, B19V is known as the causative agent of the childhood disease *erythema infectiosum*, also known as fth disease [79]. Often found in schoolchildren, *erythema infectiosum* is characterized by a mild rash, usually on the face and/or extremities [80]. In adults, B19V can cause u-like symptoms and temporary arthralgia [80]. Moreover, in some cases, infections with more dangerous manifestations are observed. Severe symptoms include transient aplastic crisis, which can lead to severe anemia [75]. In patients with a compromised immune system, persistent anemia can be established [81]. Patients with HIV may have elevated risks of persistent anemia during B19V infection [82]. Similarly, malaria patients may su er from severe anemia in the case of a B19V co-infection due to an already diminished RBC count [83][84]. Myocarditis [85], cardiomyopathy [86] and a general in ammatory response in a variety of tissues, such as the heart, the brain, and the liver [87] has also been attributed to B19V infections.

B19V infection during pregnancy can lead to perinatal complications. It is estimated that 1-5 % of women become infected during pregnancy [88][89], and vertical transmission is estimated to take place in roughly a quarter of cases [90][91]. *Hydrops fetalis* can develop in roughly 10 % of pregnant mothers infected with B19V [92][85][90]. *Hydrops fetalis* is a condition in which an abnormal buildup of uid is present in various tissues of the fetus and has an up to 50 % perinatal mortality rate [93]. B19V may also cause spontaneous abortion due fetal organ damage [94]. Despite the recognized risk for an adverse pregnancy outcome, the mechanism involved in the dissemination of the virus from the infected mother to the developing fetus remains unknown.

1.4.4 Immune response to B19V infection

The incubation period of the infection can range anywhere from four days to three weeks, with a median value of seven days [95][74][96]. During the infection, a viremia is established reaching concentrations

of up to 10^{14} viruses per ml of plasma [97][98]. The peak of viremia coincides with the onset of the first clinical symptoms similar to the flu or common cold. More specific symptoms, such as rash and arthralgia start approximately three to four weeks post-infection.

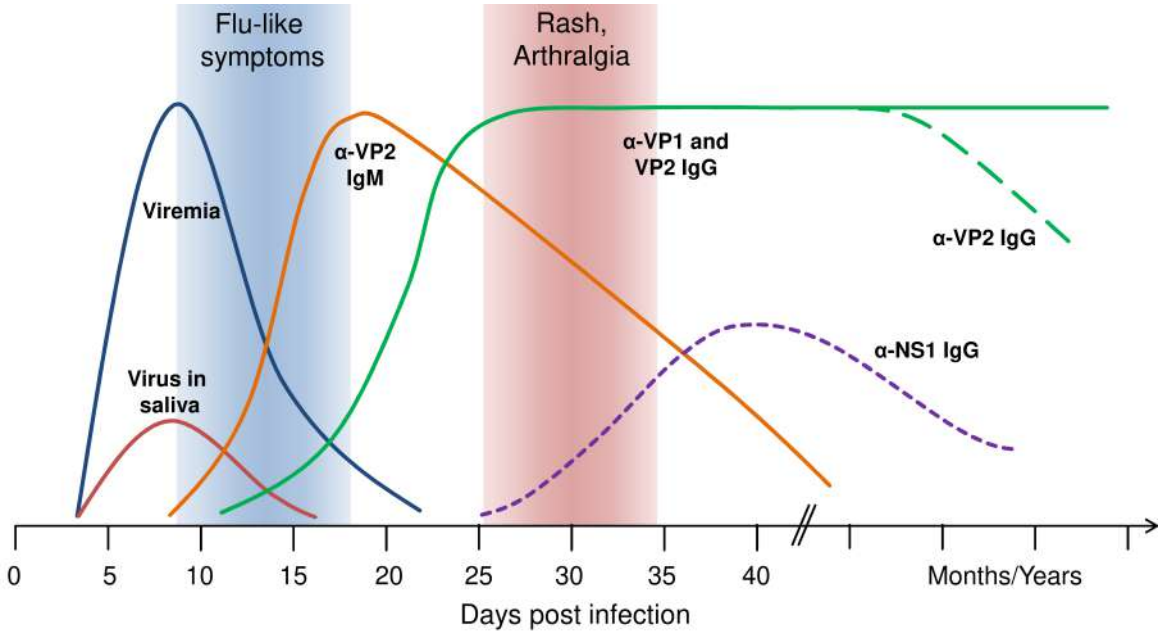

Figure 5: Clinical parameters of B19V infection. Viremia and the presence of the virus in saliva is the first detectable sign of the infection. The production of IgM is followed by IgG [81]. The onset of the main clinical features is denoted by the blue and red areas. Antibodies against NS1 are represented by a dotted line as they are only present in a minority of infections. Antibodies against VP2 slowly decline in favour of the more neutralizing VP1 antibodies.

The main defense against B19V infection is mediated by B cell immunity [73]. Both IgM and IgG antibodies against various viral proteins are produced, mainly targeting the capsid [99][100]. Figure 5 shows the kinetics of antibody production during the infection. IgM antibodies against VP2 epitopes are produced first, leading to decreased viremia. IgM antibodies can persist for some months but will decline eventually [100]. The presence of IgM is an indication of an ongoing or recent infection. IgG production occurs after the first clinical symptoms have abated [101]. They replace the IgM in the humoral immunity and their level remains stationary, indicating permanent immunity.

The VP1u represents the immunodominant part of the capsid, and as such antibodies against this region are indispensable for long-term immunity. In contrast, antibodies against VP2 slowly decay over time after the infection [102]. Accordingly, antibodies that bind the RBD as well as the PLA2 motif of VP1u were shown to have strong neutralizing properties [103][104][105]. The RBD in the VP1u is initially inaccessible to specific antibodies. However, it becomes exposed during the interaction of the virus with receptors on susceptible cells [61]. How the VP1u remains masked until interaction with target cells is not well understood. Other parvoviruses (outside of the Erythroparvovirus

genus) possess a shorter VP1u and their RBDs are located on di erent regions on the capsid surface [106][107][108][109]. Antibodies against the NS1 protein are present in approximately one third of the infections [110][111]. It has been hypothesized that the presence of anti-NS1 antibodies may indicate an ine cient clearance of the virus and may be responsible for the development of chronic arthritis in some patients [110]. However, more recent studies have challenged these ndings and showed that anti-NS1 can also be found in recovered individuals with no chronic infection [112].

Non-neutralizing or poorly neutralizing antibodies may facilitate viral spread through antibody-dependent enhancement (ADE). This mechanism occurs through the interaction of the Fc region of anti-B19V antibodies with Fc receptors expressed in di erent cell types. In cell culture, B19V internalization was enhanced in the presence of speci c antibodies, suggesting that ADE represents an alternative virus uptake mechanism into host cells [113][114][113]. While ADE is involved in the infection of some viruses, such as West Nile virus [115] and Dengue virus [116], it does not seem to lead to productive B19V infection. However, it may explain the persistence of B19V in various tissues from immunocompromised patients.

1.5 Replication cycle of B19V

1.5.1 Binding to cells and internalization

The interaction with attachment factors, receptors, and co-receptors expressed on susceptible cells represents the rst step of the replication cycle of a virus. In the case of B19V, it cannot be discarded that surface molecules, such as globoside or integrins, play a role in stabilizing the interaction or facilitating conformational changes in the viral capsid such as the exposure of the RBD in the VP1u. This is particularly relevant since the RBD is not originally accessible on the native capsid [61][68]. Furthermore, it has been shown that lipid rafts play an important role in the attachment of the virus to the cells [117]. While VP1uR does not seem to be localized to lipid rafts, it is conceivable that the aforementioned molecules, in particular the glycosphingolipid globoside, are enriched in lipid rafts. Following the interaction with the VP1uR, B19V is taken up through clathrin-mediated endocytosis [117].

1.5.2 Intracellular tra cking

Following uptake, the clathrin-coated vesicles carrying the virus uncoat and fuse with early endosomes. B19V spread through the endosomal compartment, eventually reaching the lysosomes [117]. After 10 and 30 min B19V is located in late endosomes and lysosomes respectively [117]. Similar to other parvoviruses, such as MVM, viral escape from the lysosomes does not appear to be possible [117][118], potentially due to low PLA2 activity in a strongly acidic environment [119]. This suggests that B19V escapes from early and/or late endosomes, preventing degradation in lysosomes. The mechanism of virus escape from the endosomal vesicles remains poorly understood. The low pH of the endosomes is required for the progression of the infection, as it leads to the necessary capsid conformational changes that facilitate the translocation of the incoming capsids to the host nucleus where replication takes place [117][120][121][122][123]. Although the PLA2 activity of the VP1u is required for parvoviruses to reach the nucleus [119][124], and has been implicated in breaching the endosomal membrane, the expected endosomal membrane damage has not been observed[117][119][125][126]. After leaving the endosomal compartment, the tra cking steps towards the nucleus are not well understood. Some parvoviruses have been shown to accumulate in a perinuclear region via a microtubule and dynein-dependent transport [127][128][129]. From the perinuclear region, parvoviruses are imported into the nucleus. Viruses associated with the nucleus have their genome partially externalized but still associated with the capsid [129]. With a diameter of roughly 25 nm, the virus is small enough to pass through the nuclear pore complex, which allows the traversal of macromolecules of up to 39 nm [130]. Contrary to many other parvoviruses, B19V does not seem to possess a classical nuclear localization signal (NLS) motif [131][132][133]. However, the presence of a non-classical NLS sequence mediating nuclear import cannot be discarded.

1.5.3 Generation of a transcriptionally active genome

Once in the nucleus, the ssDNA of parvoviruses is transformed into a double-stranded transcription template to generate the viral mRNAs. This is achieved by extension of the free 3'-OH in one of the ITRs by a cellular DNA polymerase, potentially DNA polymerase delta [134][135]. Once the polymerase reaches the 5'-end of the opposite ITR it falls o the viral genome and the two ends are ligated by a still unidenti ed ligase (Figure 6, steps 1-2) [136][137][138]. This double-stranded replicative form (dsRF) is the template for DNA replication as well as for transcription of the viral pre-mRNA [136][139][140]. This form contains the 67 nt long (5214-5280) origin of replication (Ori) [141].

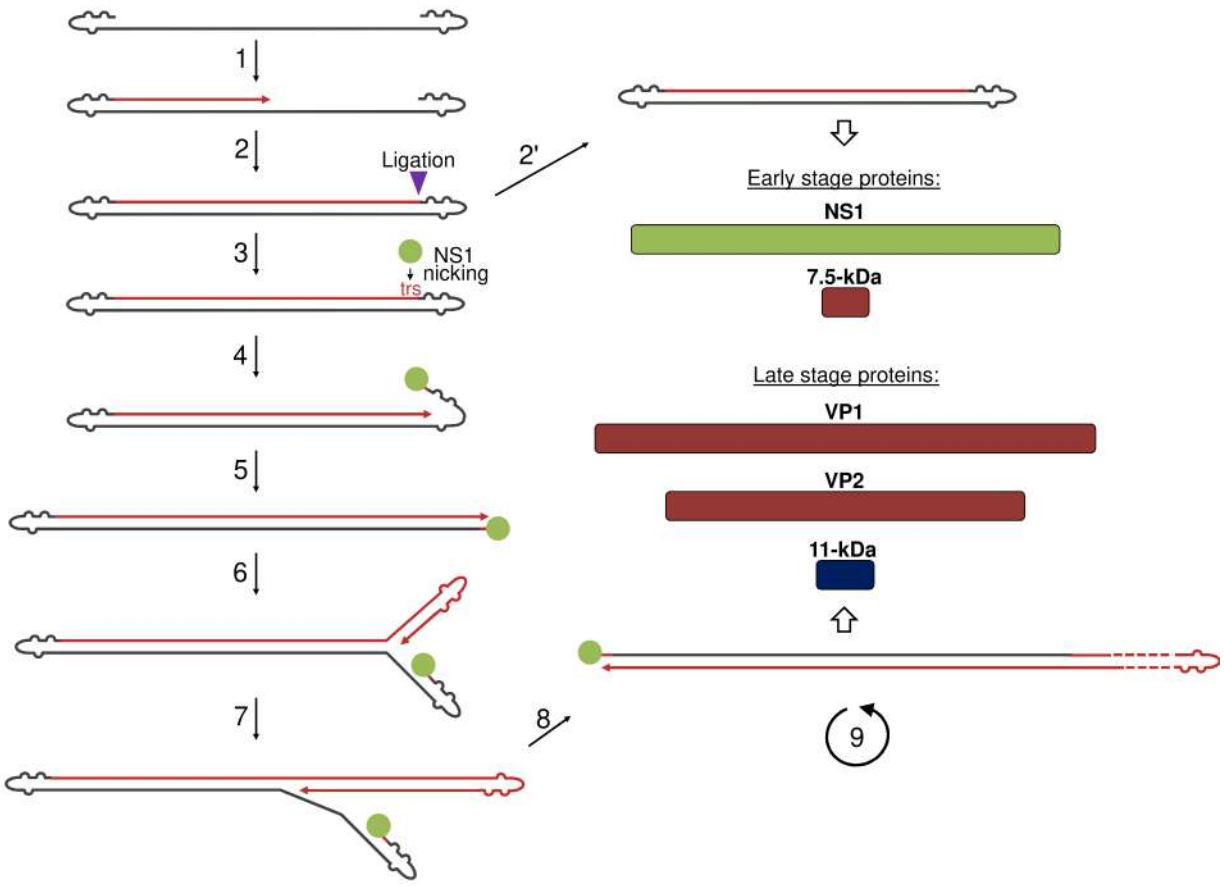

Figure 6: Rolling hairpin model of B19V DNA replication. (1) The elongation occurs from the ITR and newly synthesized DNA is depicted red. (2) Next, a cellular ligase closes the DNA. (3) Expressed NS1 protein nicks the dsRF at the terminal resolution site (trs). (4-5) The elongation continues from the newly generated 3'-OH while the NS1 remains bound to the 5'-end. (6-7) Newly formed ITRs refold and replication continues, creating a concatemeric (doublet) form (8). (9) Replication continues to follow the rolling-hairpin model. NS1 is responsible for the cleavage of the multimeric forms of the DNA to the original single-stranded form to enable packaging. The concatemeric forms are transcriptionally active and generate early- and late-stage viral proteins.

1.5.4 Transcription of early proteins

The dsRF allows the initiation of transcription from the sole promoter at map unit 6. This p6 promoter leads to the transcription of a single pre-mRNA (Figure 6, step 2'). Gene expression is controlled by alternative polyadenylation as well as through di erential splicing.

Polyadenylation can occur at two sites, which are found at proximal [(pA)p] and distal [(pA)d] areas of the genome. This is crucial for the production of viral proteins from the left and right sides of the genome (Figure 7A). The (pA)p readthrough is controlled by replication of the viral genome [142], which allows access to the (pA)d site and expression of the structural proteins and the 11-kDa protein[142]. Readthrough of (pA)p is an important permissive factor and determinant of the tropism of B19V infection.

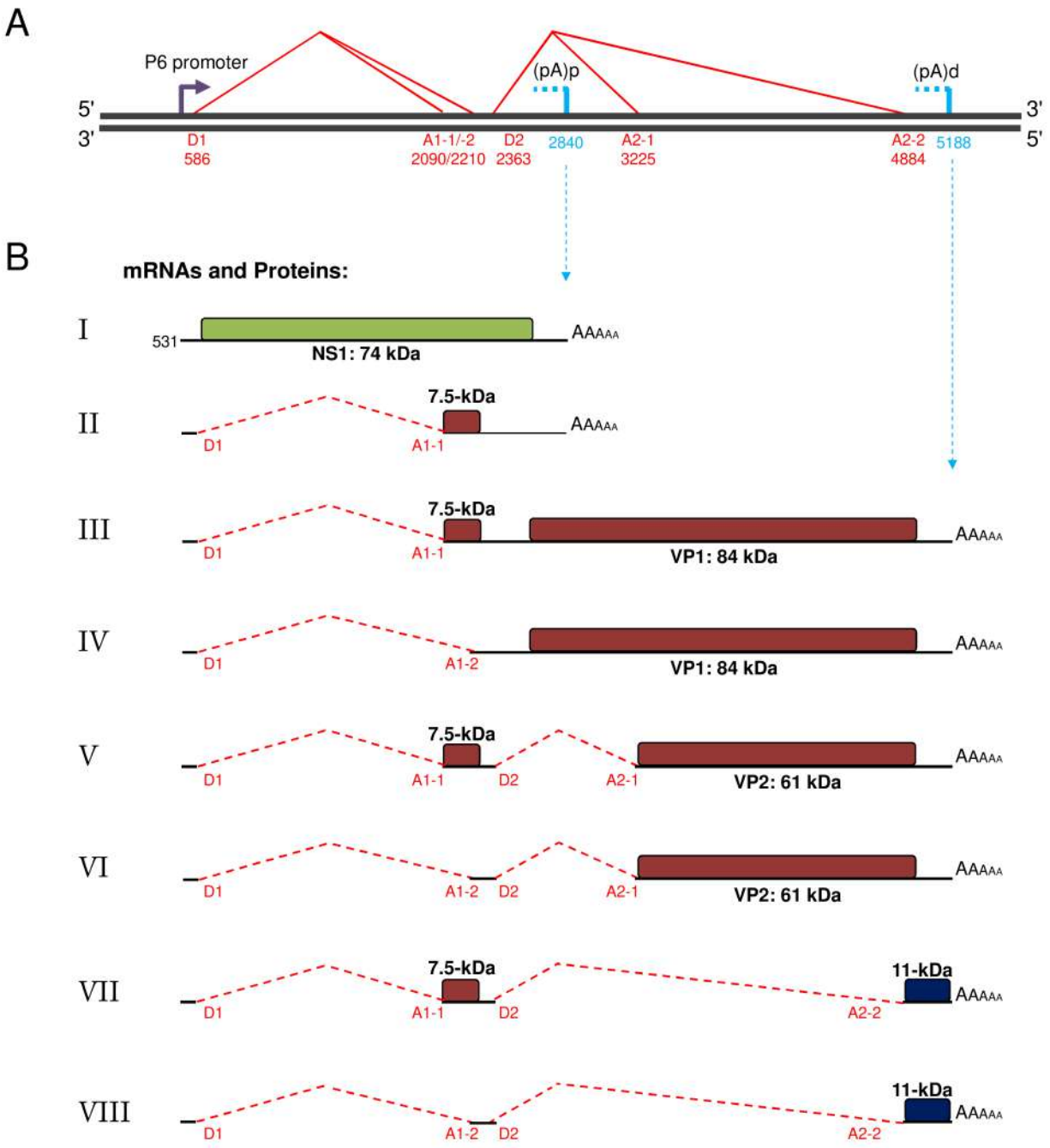

Figure 7: (A) The replicative form of the DNA in an accurately scaled view. Prior to transcription, the genome needs to be converted into a double-stranded form. The p6 promoter drives the expression of precursor mRNAs (pre-mRNA). With the aid of a proximal and distal polyadenylation site [(pA)p/(pA)d] and differential splicing (D1/D2: splice donor sites; A1-1, A1-2, A2-1, A2-2: splice acceptor sites) at least five proteins are produced from a total of three ORFs. (B) Depiction of the most important mRNA transcripts I - VIII. Transcripts not encoding for a protein and those that are polyadenylated at non-conventional sites are not shown [143]. Red dotted lines represent spliced introns while black lines illustrate the exons. The expected proteins are indicated by coloured boxes. NS1 (I) and 7.5-kDa (II) are produced early during the infection, whereas structural proteins (III - VI) and 11-kDa (VII - VIII) are generated later. The 7.5-kDa protein is also produced from bicistronic mRNAs along with all other viral proteins except NS1 (III, V, VII).

Di erential splicing enables the processing of pre-mRNAs to the various mature forms (Figure 7B). The key for this processing is the tightly regulated removal of either the rst (D1 to A1-1 or A1-2) or the second intron (D2 to A2-1 or A2-2) from the pre-mRNA. These narrow regulations are acquired by speci c motifs, such as exon-splicing and intron-splicing enhancer sites [144]. The binding of the cellular U1 spliceosomal RNA to the D2 splice site leads to readthrough of the (pA)p site [145]. Alternative splicing has also been shown to in uence di erential polyadenylation [145].

The transcripts that terminate at (pA)p code for the two non-structural proteins NS1 and 7.5-kDa. NS1 is the rst viral protein expressed during infection and it is the sole protein produced from an unspliced mRNA. It contains multiple NLS and is almost exclusively found in the nucleus [146]. NS1 is a multifunctional protein that is indispensable for the progression of the infection [147]. Besides the NLS, NS1 contains a variety of motifs that are crucial for a successful viral replication cycle. Among other functions, NS1 is necessary for induction of apoptosis, cell cycle arrest [148][149][150] and nicks the viral DNA at the terminal resolution site (trs) during replication [151]. Its helicase activity and ability to transactivate the viral promoter play an important regulatory role in the ampli cation of the genome [150][152]. The function of the 7.5-kDa protein remains unknown. It is produced from mRNA spliced at D1 to A1-1. Interestingly, it is the sole protein that can be produced from mRNAs terminated at (pA)p as well as (pA)d. Thus the 7.5-kDa might play a role both in the early and late stages of infection.

1.5.5 Replication of the viral genome

Contained within the viral Ori are multiple NS1 binding elements (NSBE) as well as a terminal resolution site (trs) [141]. NS1 cleaves the dsRF at the trs, creating a 3'-OH which enables the extension of the DNA through cellular DNA polymerases (Figure 6, steps 3-4). The NS1 remains bound to the 5'-end of the trs, probably through the NSBE present close to the ITR [141][136]. There, the helicase activity of NS1 is thought to be important in opening the dsDNA during replication (see Figure 6, steps 5-6)[151]. As with other parvoviruses, B19V is thought to follow a rolling-hairpin replication mechanism. This leads to the generation of long concatemeric replicative forms, potentially with a length multiple times that of the original genome (Figure 6, steps 7-9). Along with the dsRF, these concatemeric forms are thought to be transcriptionally active and lead to the production of viral proteins. Out of the concatemers, genome ssDNA molecules are created with the help of the NS1 endonuclease activity. Various signalling pathways that in uence the B19V DNA replication, such as DNA damage response, hypoxic signalling, and Epo signalling, are discussed in the following chapter.

1.5.6 Viral signalling pathways

Signalling is the second major form of viral tropism, also called receptor-independent tropism [153]. Receptor-independent tropism restricts replication of the virus after cell entry. For successful infection, a virus requires a suitable intracellular environment with all the necessary factors and signalling pathways for replication. This means that a virus is unable to infect a cell that expresses the entry receptor (susceptibility) but lacks important intracellular factors (permissibility). For B19V, multiple signalling pathways play a complex and interconnected role during viral replication.

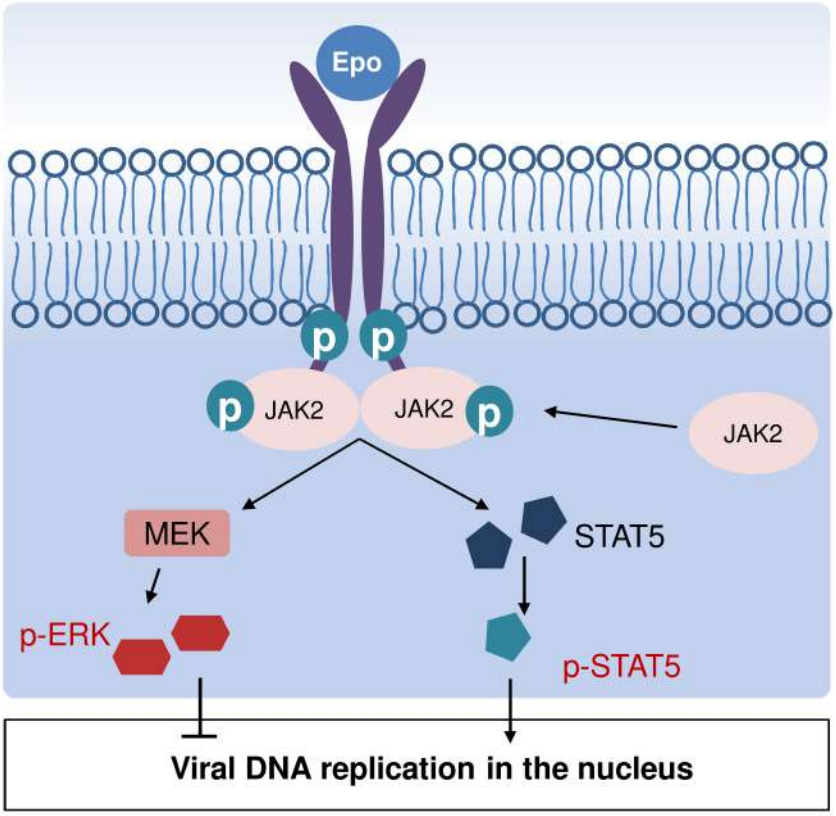

Figure 8: Simplified version of the Epo/EpoR signalling pathway. Upon binding of Epo, Jak2 is recruited, leading to activation of itself and EpoR through phosphorylation. The most important downstream actors for B19V are the MEK/ERK and the STAT5 pathways. The former inhibits B19V replication while the latter promotes it.

Epo signalling: Epo signalling was shown to be a prerequisite for B19V infection, whilst not being required for viral entry [154]. Epo is a glycoprotein that plays an essential role in erythropoiesis. The cellular receptor for Epo, EpoR, is a dimeric transmembrane receptor. Free Epo is secreted from the kidney and can bind the EpoR, leading to dimerization and activation of the receptor [155]. Activation of EpoR leads to the activation of cytosolic Janus kinase 2 (Jak2) which, in turn, phosphorylates itself and the cytoplasmic tail of EpoR (Figure 8). Without Jak2 or phosphorylation of EpoR, B19V is unable to start the infection in the target cell [154]. Three downstream branching pathways are activated through phosphorylation by Jak2: STAT5 (Signal transducer and activator

of transcription 5), MEK/ERK (mitogen-activated kinase/extracellular signal-regulated kinase), and PI3K (phosphoinositide-3 kinase) [155]. These three are crucial for the di erentiation and growth of the EPCs. STAT5 and MEK/ERK directly a ect B19V replication, whereas PI3K is dispensable for B19V infection. Phosphorylated STAT5 (p-STAT5) is able to bind the replicative form of the B19V genome at the Ori, which is crucial for replication of the viral genome [156]. p-STAT5 binding leads to the recruitment of the minichromosome maintenance complex, which promotes the initiation of viral DNA replication [156]. While STAT5 facilitates replication of the viral genome, Epo-mediated MEK/ERK activation has a diminishing e ect on the B19V infection [157].

Hypoxia: The O_2 concentration in the bone marrow is signi cantly lower than that in the blood-stream. The hypoxic conditions promote B19V infection by improving gene expression and replication of the DNA [157]. In cell culture, hypoxia leads to increased amounts of infected cells as well as increasing levels of viable progeny [157]. Hypoxia does not, however, improve the viral entry or traf-cking of the virus. Instead, it a ects the Epo/EpoR signalling pathway by up-regulation of p-STAT5 and down-regulation of phosphorylated ERK (p-ERK).

DNA damage response (DDR): DDR is a defense mechanism of the cell used to repair its genome in case of damaged DNA. It also induces cell cycle arrest to prevent the propagation of defective DNA after heavy DNA damage. DDR is also activated in response to certain viral infections, including B19V [158][159][160]. The genomic composition of B19V with two ITRs divided by a long ssDNA molecule is a prime example of a structure that triggers DDR. Moreover, viral DNA replication leads to the creation of new ITRs and nicked genomes, further provoking activation of DDR [159]. Importantly, the viral infection itself does not lead to signi cant cellular DNA damage [134]. Interestingly, B19V not only induces DDR through replication of its genome but exploits the various signalling pathways in order to promote the infection [161][159]. The three major enzymes that are involved in downstream DDR signalling are all phosphatidylinositol 3-kinase-related kinases, which are activated upon B19V infection: Ataxia-telangiectasia mutated (ATM), ataxia-telangiectasia and Rad3-related (ATR), and DNA-dependent protein kinase catalytic subunit (DNA-PKcs)[162][159]. While ATM is dispensable for the infection, ATR and DNA-PKcs play important roles in B19V replication. Both the activated forms of DNA-PKcs and ATR pathway lead to phosphorylation of downstream e ectors, such as replication protein 32 (RPA32) and H2AX [159]. Both are hallmarks of DDR and co-localize with NS1 inside the nucleus of infected cells [159]. Inhibition of ATR and to a lesser degree of DNA-PKcs leads to reduced e ciency of replication [159]. B19V may also bene t from cellular DDR in other ways. For example, activation of ATR signalling promotes late S-phase arrest in cells, which in turn promotes B19V replication [134].

1.5.7 Late stages of infection

As the viral DNA is replicated in the nucleus, readthrough of the (pA)p site increases, resulting in the generation of mRNA polyadenylated at (pA)d [142]. This allows the expression of the viral structural proteins as well as the non-structural 11-kDa. The viral capsid contains approximately 20 times more VP2 than VP1. In order to maintain a proper ratio between VP1 and VP2, the splicing donor and acceptor sites D2 and A2-1 are strictly regulated (Figure 7)[163]. Translation of the two structural mRNAs gives yield to the monomeric capsid proteins which assemble into trimers while still in the cytoplasm [164][131]. The trimeric capsomers are then transported to the nucleus through a nuclear localization motif that is only accessible in the non-assembled capsid. Once in the nucleus, 20 of those timers form the viral capsid, a process that happens spontaneously due to the thermodynamic favourable symmetrical nature of the virus. The viral DNA is packaged into the capsid through one of the 12 pores present on the ve-fold axis of symmetry, a process that is likely mediated by NS1 [165][166][64]. As with the two structural proteins, expression of the 11-kDa protein also relies on distal polyadenylation. Moreover, the binding of a host cell protein, RBM45, to an intronic splicing enhancer sequence of the viral pre-mRNA facilitates splicing at A2-2 and thus the expression of 11-kDa [167]. This viral protein is found in vast quantities in the cytoplasm of infected cells [168]. It is responsible for inducing apoptosis and also improves the production of structural viral proteins through an unknown mechanism [147]. Moreover, the 11-kDa may inhibit the MEK/ERK pathway, improving the replication of the viral genome [169][170]. As is the case with most non-enveloped viruses, B19V is released from the infected cell through lytic egress [64]. Most probably this is mediated by the activity of 11-kDa and, to a lesser degree, NS1, both inducers of apoptosis[171][172][173].

1.5.8 Limitations of cell culture systems for B19V replication

Almost all the knowledge of the B19V infection stems from cell culture experiments. Infection of human primary EPCs under hypoxia (1 % O_2) is the best method to propagate B19V. However, the method is laborious and expensive and the viral yield remains modest compared to what is observed in natural infections. Various cell lines were shown to support B19V infection, such as the erythroid derived cell lines UT7/Epo [174] MB-02 [175], JK-1 [176], and Ku812Ep6 [177]. In all cases, Epo is required for virus replication and hypoxia increases the infection e ciency [157][178][179]. However, these cell lines do not support the late stages of the infection and the production of infectious progeny is extremely limited or not possible [179]. Improper read-through at (pA)p site leads to high NS1 expression levels but low levels of structural proteins and 11-kDa. While viral capsids can be detected intracellular and in the supernatant, the vast majority is empty, suggesting that packaging of the viral DNA is a rate-limiting step for B19V propagation in cell culture [179]. The currently available

cell lines are therefore only semi-permissive. They are useful to study early steps in the infection, including uptake, tra cking, and initial replication and transcription events, but they do not allow e cient propagation of the virus. This situation hinders basic research on B19V, and certain studies, like mutagenesis, using an infectious clone, are not possible, due to the insu cient progeny mutant produced.

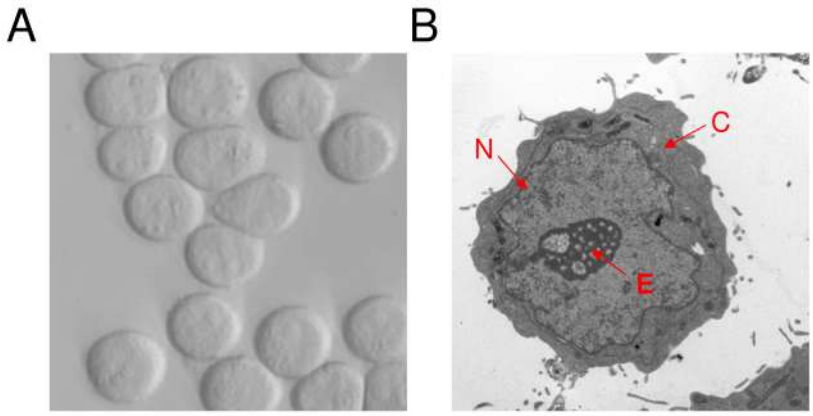

Figure 9: Images of UT7/Epo cells obtained by confocal microscopy (A) or by using a transmission electron microscope (TEM) (B). The cells have a diameter of roughly 15 µm. The TEM image highlights the characteristically large nucleus and comparatively small cytoplasm for these cells. N: nucleus, E: nucleolus, C: cytoplasm.

1.5.9 The conundrum of the B19V route of infection

The exact route of infection for B19V is not well understood. The virus is transmitted via the respiratory route. Droplets from an infected person are taken up through the mouth or the nose and lead to infection and viremia a few days later [73]. The rst interaction of B19V with the host occurs in the airway epithelial cells. It is an open question how the virus interacts with these cells, as the expression of the VP1uR is limited to EPCs in the bone marrow. Moreover, the virus requires Epo for propagation, which is not present in the airway epithelium. It is therefore improbable that the virus has the possibility to replicate in these cells. It is also unlikely that B19V crosses the epithelial barrier through spaces between cells. This is highlighted by the inability of the B19V PLA2 to disturb tight junctions compared to the PLA2 of HBoV, a parvovirus that infects and replicates in the human airway [180]. The mechanism underlying the dissemination of B19V from the infected mother to the fetus also remains unexplained. The mechanism by which the virus crosses the airway epithelium and the placental barrier must follow an as yet undiscovered pathway, involving di erent receptors compared to those involved in the productive infection of EPCs in the bone marrow.

1.6 Globoside

Globoside, also known as P antigen, globotetraosylceramide, Gb4Cer, or Gb4, is a GSL present on the surface of a wide variety of cell types in multiple organisms (see subsection 1.6.1). GSLs are some of the most abundant glycolipids on cell surfaces. They are made out of one or multiple glycans linked to a ceramide core. Globoside consists of a glucose moiety linked to ceramide followed by two galactose moieties and a terminal N-acetylgalactosamine (Figure 10). Interestingly, the oligosaccharides from major glycosphingolipids, such as globoside, can also be found linked to proteins, not just to ceramide [181]. It is estimated that roughly 15 % of the globoside-glycans are present in the form of glycoproteins [181]. How these proteins are modi ed remains unknown.

Globoside is of key relevance for this thesis due to its proposed role as the receptor of parvovirus B19. The current literature concerning the interaction of globoside and B19V is presented in subsection 1.4.2. The following chapters will provide an extensive overview of globoside, i.e., expression pro le, biosynthesis, and function.

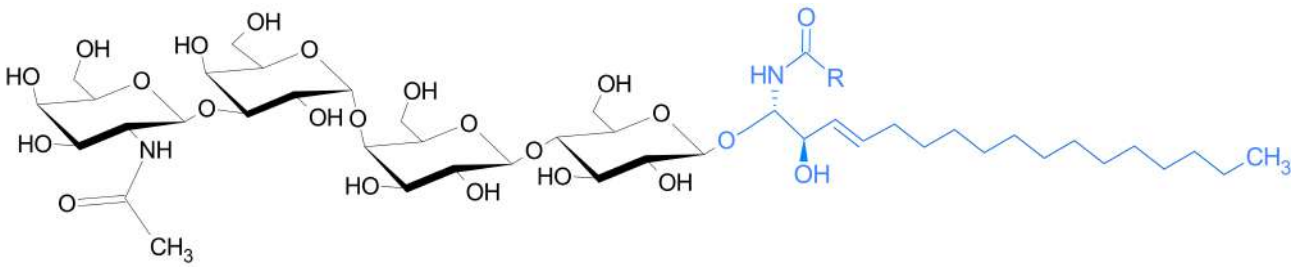

Figure 10: Structural depiction of globoside. It has the chemical composition GalNAcβ1-3Galα1-4Galβ1-4Glc-Cer. The membrane-embedded ceramide (blue) is made out of a sphingosine molecule as well as a fatty acid of variable length (R). The polar headgroup consisting of four sugars extends into the extracellular space.

1.6.1 Expression pro le of globoside

Globoside has been proposed to play a function as the primary receptor of B19V [57]. Individuals without globoside are resistant to the virus, indicating its essential role in the infection [58]. Accordingly, the expression pro le of globoside can facilitate the understanding of the mechanism of virus entry through the respiratory epithelium, dissemination to the bone marrow and the fetus for productive infection, and back to the respiratory tract for transmission.

Globoside is found on a variety of blood cells, including RBCs [182], platelets [183], undi erentiated blast-cells [184][67], erythroblasts [184][67], promyelocytes [67], monocytes [185], macrophages [186], and lymphocytes [187][188]. Moreover, globoside has been found freely in the plasma [189] as well as associated with serum lipoproteins [190]. Globoside is also expressed in various types of tissue, including lung, heart, synovium, liver, kidney, smooth muscles, bowel mucosa [183], and placental

trophoblasts [191]. It is even present on the surface of dental epithelial cells [192]. Interestingly, while globoside is abundantly expressed on human RBCs [182], only trace amounts are found in rabbit RBCs [193]. RBCs from other animals such as tamarin, horse, sheep, guinea-pig, chicken and, turkey also are thought to have a lower globoside content compared to human RBCs, as they are unable to agglutinate in the presence of B19V [194]. The clear lack of globoside has only been reported on a few cells, such as in neutrophils [195] and in the brain tissue [183]. The abundant expression of globoside in the human body stands in direct contrast to the strict tropism of B19V.

1.6.2 Globoside metabolism in the cell

The first step of GSL synthesis begins in the endoplasmic reticulum (ER) where ceramide is synthesized. Figure 11A highlights the entire cycle of globoside biosynthesis. Ceramide is transported to the proximal cis-Golgi apparatus, most probably through COPII vesicles [196][197], where it is glucosylated to form glucosylceramide (GlcCer). As is shown in Figure 11B, this reaction is catalyzed by a glucosyltransferase and occurs at the cytosolic surface of the Golgi apparatus [198]. GlcCer is then transported to the trans-Golgi network (TGN) in a non-vesicular manner mediated by the lipid-transfer protein FAPP2 [199]. A membrane pump, most likely P-Glycoprotein, then flips the GlcCer to the lumen side of the TGN [200][201]. There, GlcCer is galactosylated to form lactosylceramide (LacCer) [202][203]. In the TGN LacCer is then used as a substrate by the Gb3 synthase A4GalT to produce Gb3 [204], which in turn is a substrate for B3GalNT1 to create globoside [199][205]. The expression of globoside is thus controlled by multiple factors, such as the presence of the necessary precursor, the availability of the required sugars, the compartmentalization of enzymes involved in the synthesis as well as the expression of the required glycosyltransferases at a genetic level. The sequential action of the various enzymes involved in their biosynthesis determines the fate of a glycosphingolipid.

Because those biosynthetic pathways are branched, a certain substrate can potentially be used by multiple glycosyltransferases in the same compartment of the Golgi apparatus. This leads to competition between the enzymes for their substrate [206]. To this end, it has been shown that globoside is produced from ceramides that contain long-chain fatty acids (C_{22}:0 and larger), suggesting that the type of ceramide influences the affinity of the transferases [207][208]. After its synthesis, globoside is transported to the plasma membrane, most likely by lipid carrier proteins [209]. Since the ceramide tail of globoside is inserted into the luminal leaflet of the Golgi apparatus, globoside is strongly enriched in the exoplasmic leaflet after transport to the plasma membrane [210][209]. Glycosphingolipids targetted for degradation are transported to the lysosome via early and late endosomes after invagination of the corresponding membrane. There, degradation of globoside takes place with the help of acid hydrolases, which remove terminal sugars in a specific and sequential manner [211][212]. For

short glycosphingolipids with only a few sugar residues, an additional sphingolipid activator protein is required for successful degradation [212]. Ceramide is then further broken down into sphingosine and a fatty acid [213]. The degradation products, including monomeric sugars, leave the lysosomes and can eventually be reused by the cell [212].

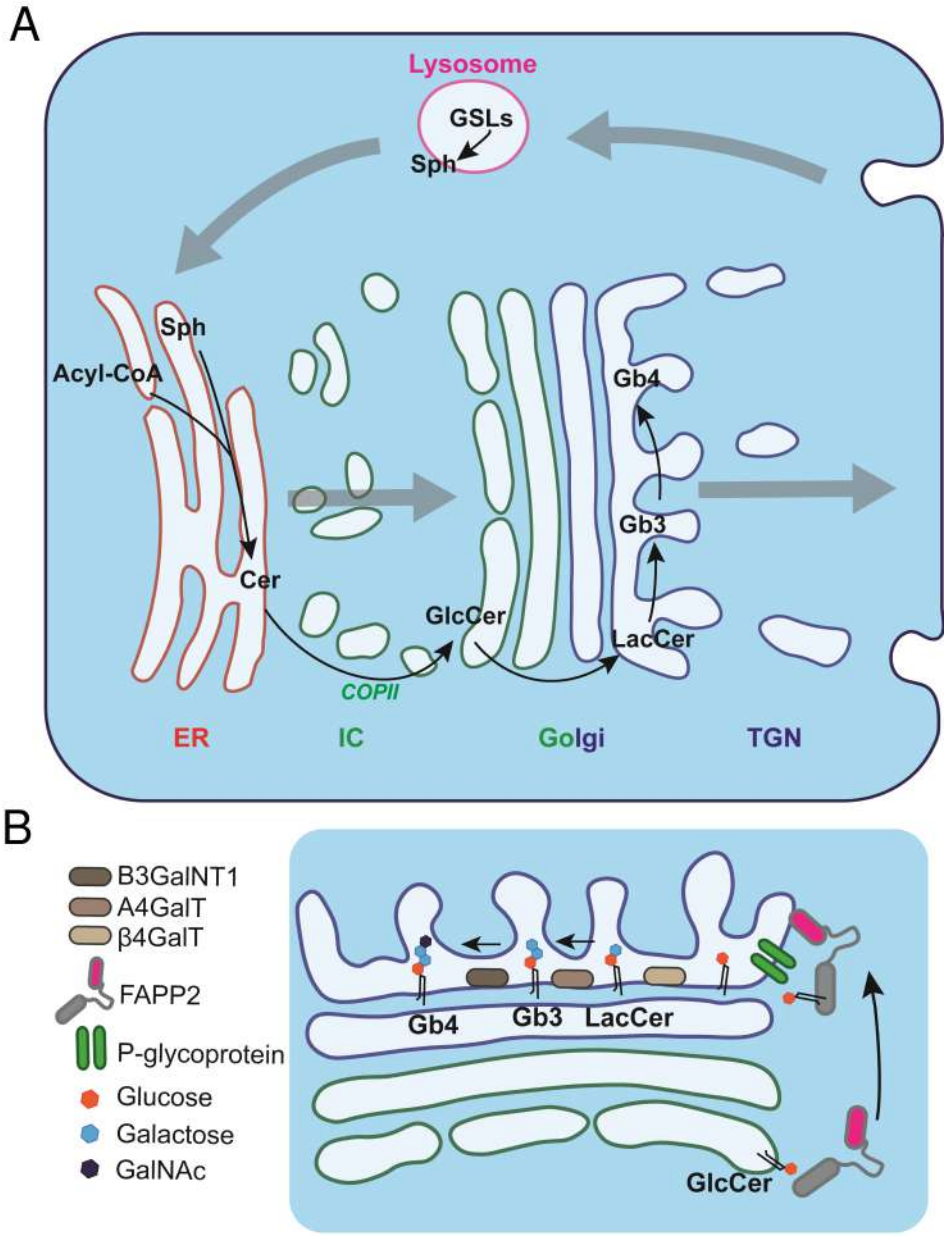

Figure 11: (A) Globoside metabolism cycle in a cell. Synthesis of ceramide starts in the ER out of sphingosine and a fatty acid coupled to acyl-CoA. This is followed by transport to the cis-Golgi. Compartmentalization of glycosyltransferases allows the production of specific glycosphingolipids. From the TGN, globoside is transported to the cell surface where it fulfils various roles (see chapter 1.6.3). Degradation of globoside is a stepwise process that occurs through the acidic environment of the endosomal route. Sph: sphingosine, Cer: ceramide, IC: intermediate compartment. (B) Detailed representation of globoside synthesis out of GlcCer in the Golgi through the sequential action of various enzymes.

1.6.3 The role of globoside in the cell

GSLs can roughly be divided into two functional groups, they can act as signal transducers, playing an important role in cell proliferation and di erentiation, or they can act as receptors for various substrates [214]. Globoside is involved in signalling by interacting directly with EGFR (epidermal growth factor receptor), a receptor tyrosine kinase on the cell membrane [215]. As such, globoside has the ability to phosphorylate EGFR as well as ERK [215], both players of the ERK/MEK pathway. This pathway plays a crucial role in the regulation of cell cycle entry and proliferation [216]. As activation of the MEK/ERK pathway was shown to lead to a lower B19V replication, it seems unlikely that globoside plays a crucial signalling player during B19V infection. Further, globoside promotes the formation of ameloblasts by increasing the di erentiation rate of dental epithelial cells [217]. It has also been proposed that globoside may play a role during early embryogenesis, speci cally for signalling and adhesion, although the speci c mechanisms are undetermined [218][216].

1.6.4 Globoside expression phenotypes

Globoside and the mutations in uencing its expression are fundamental in understanding B19V infection. There are di erent underlying genetic mechanisms that govern the presence or absence of the various GSLs. Globoside is found in practically all individuals, no matter their ethnicities. In individuals with the so-called P_1^k or P_2^k phenotypes (referred to as $P_{1/2}^k$ from now on), the B3GalNT1 gene coding for globoside synthase is non-functional. All the other related glycosyltransferases are una ected, leading to the accumulation of Gb3 [219]. In contrast to this, in individuals with the so-called p phenotype, globoside synthase is active but A4GalT, the enzyme responsible for the synthesis of Gb3, is aberrant, which also leads to the absence of globoside. The p phenotype was found to be extremely rare, around six in a million [220]. The $P_{1/2}^k$ phenotypes are estimated to be even rarer, with an estimated frequency of one per million [219], although both p and $P_{1/2}^k$ phenotypes seem to be more frequent in certain regions of Japan and Sweden compared to the rest of the world [220].

1.6.5 Globoside associated diseases

RBCs of the p phenotype show accumulation of LacCer, whereas the $P_{1/2}^k$ phenotypes have strongly increased levels of Gb3 [207][221]. Both of these phenotypes also show a general increase in ganglioside levels [207][221]. Despite this and the possible e ects of globoside for the cell, discussed in subsection 1.6.3, RBCs from p and $P_{1/2}^k$ individuals appear structurally and functionally normal [207]. Still, it has been shown that the presence of anti-globoside antibodies (present in p and $P_{1/2}^k$ phenotypes) can be the cause for early abortions and miscarriages due to a blood disorder in the fetus [222][223][220]. Next to B19V, other viruses may also be a ected by the presence or absence of globoside. Namely, the

fusion of HIV with its target cells was shown to be a ected by Gb3. Recent experiments have shown that mononuclear blood cells expressing increased amounts of Gb3 showed strong inhibition of HIV infection [219]. This means that individuals with the $P^{k}_{1/2}$ phenotypes, which show an accumulation of Gb3 due to a non-functional globoside synthase, are less susceptible to HIV whereas those with the p phenotype, which completely lack Gb3, are hypersusceptible [219].

1.7 Thesis outline

At the start of my thesis, the foremost aim was to elucidate the role of globoside for B19V infection. Previous results in the literature showed that globoside is the primary cellular receptor of B19V, and it is essential for the infection [67][57]. However, the function of globoside as the B19V receptor remains controversial due to the contradictory data regarding its interaction with the virus and its ubiquitous expression pro le, which does not correlate with the restricted viral tropism.

Elucidating the essential role of globoside could improve our fundamental understanding of B19V. As the project progressed and new data was continuously generated, additional goals could be de ned. Summarized below are the two most central questions that I set out to answer:

1) What is the exact role of globoside in B19V infection?

2) What is the nature of the VP1uR?

Approach:

In an attempt to untangle con icting results from the literature, the generation of a globoside knockout cell line was undertaken. In such a manner we aimed to separate the function of globoside from that of the VP1uR and possible co-receptors. Globoside is not a protein and consequently cannot be directly removed genetically. Instead, the enzyme responsible for its biosynthesis was targeted. Moreover, as cells from individuals without globoside are essentially normal [207], we hypothesized that genetic removal of globoside expression would be possible without a signi cant change in phenotype. The newly developed CRISPR/Cas9 system was therefore chosen to enable speci c and e cient disruption of the B3GalNT1 gene and thus prevent the synthesis of globoside.

In order to uncover the nature of the VP1uR, we aimed to employ proximity-based labeling, a state-of-the-art technique that allows a modifying enzyme to selectively tag proteins with biotin in the vicinity of the receptor-binding site. To this end, recombinant VP1u was fused to horseradish peroxidase (HRP). The binding of the VP1u-HRP construct to the VP1uR enables HRP to label proximal proteins, which are subsequently puri ed with neutravidin beads.

2 Results

Preface

This section will present the key findings of my PhD studies. A large part of the results is presented in the form of two publications. Additional findings that could not yet be finalized into a paper are included as well. Here, I would like to give a brief summary of the results:

In my first publication, Globoside is Dispensable for Parvovirus B19 Entry but Essential at a Postentry Step for Productive Infection , the generation of a globoside knock-out cell line is detailed. Further, we found that globoside deficient cells still allow uptake of the virus but do not permit viral replication.

With the second publication, Human parvovirus B19 interacts with globoside under acidic conditions as an essential step in endocytic trafficking , we went into further detail to elucidate the still nebulous interplay between B19V and globoside. We were able to show that the virus only interacts with globoside under acidic (low pH) conditions, thus proving that no interaction between B19V and globoside occurs in the bloodstream. At the same time, the interaction of B19V with globoside in the acidic endosomal compartments was found to facilitate endosomal escape.

Lastly, in chapter 2.1 a proximity labeling based approach for the identification of the VP1uR is described.

AMERICAN SOCIETY FOR MICROBIOLOGY | Journal of Virology®

VIRUS-CELL INTERACTIONS

Globoside Is Dispensable for Parvovirus B19 Entry but Essential at a Postentry Step for Productive Infection

Jan Bieri,[a] **Carlos Ros**[a]

[a]Department of Chemistry and Biochemistry, University of Bern, Bern, Switzerland

ABSTRACT Globoside (Gb4) is considered the primary receptor of parvovirus B19 (B19V); however, its expression does not correlate well with the attachment and restricted tropism of the virus. The N terminus of VP1 (VP1u) of B19V interacts with an as-yet-unknown receptor required for virus internalization. In contrast to Gb4, the VP1u cognate receptor is expressed exclusively in cells that B19V can internalize. With the aim of clarifying the role of Gb4 as a B19V receptor, we knocked out the gene B3GalNT1 coding for the enzyme globoside synthase in UT7/Epo cells. Consequently, B3GalNT1 transcripts and Gb4 became undetectable in the knockout (KO) cells without affecting cell viability and proliferation. Unexpectedly, virus attachment, internalization, and nuclear targeting were not disturbed in the KO cells. However, NS1 transcription failed, and consequently, genome replication and capsid protein expression were abrogated. The block could be circumvented by transfection with a B19V infectious clone, indicating that Gb4 is not required after the generation of viral double-stranded DNA with resolved inverted terminal repeats. While in wild-type (WT) cells, occupation of the VP1u cognate receptor with recombinant VP1u disturbed virus binding and blocked the infection, antibodies against Gb4 had no significant effect. In a mixed population of WT and KO cells, B19V selectively infected WT cells. This study demonstrates that Gb4 does not have the expected receptor function, as it is dispensable for virus entry; however, it is essential for productive infection, explaining the resistance of the rare individuals lacking Gb4 to B19V infection.

IMPORTANCE Globoside has long been considered the primary receptor of B19V. However, its expression does not correlate well with B19V binding and uptake and cannot explain the pathogenesis or the remarkable narrow tissue tropism of the virus. By using a knockout cell line, we demonstrate that globoside does not have the expected function as a cell surface receptor required for B19V entry, but it has an essential role at a postentry step for productive infection. This finding explains the natural resistance to infection associated with individuals lacking globoside, contributes to a better understanding of B19V restricted tropism, and offers novel strategies for the development of antiviral therapies.

KEYWORDS B3GalNT1, Gb4, P antigen, parvovirus B19, globoside, globoside synthase, receptor, virus entry, virus tropism

Human parvovirus B19 (B19V) is a prominent human pathogen which is typically associated with erythema infectiosum, or fifth disease, a worldwide disease affecting mostly school-aged children (1). B19V infection may cause arthropathies in adults and hydrops fetalis in pregnant women. In individuals with underlying immune or hematologic disorders, B19V may cause severe cytopenia, myocarditis, vasculitis, glomerulonephritis, or encephalitis (2). The 5.6-kb linear single-stranded DNA genome of B19V is encapsidated into a small nonenveloped icosahedral capsid and encodes three nonstructural proteins (NS1, 11 kDa and 7.5 kDa) and two capsid proteins (VP1 and VP2). The capsid consists of 60 structural subunits, of which approximately 95% are

Citation Bieri J, Ros C. 2019. Globoside is dispensable for parvovirus B19 entry but essential at a postentry step for productive infection. J Virol 93:e00972-19. https://doi.org/10.1128/JVI.00972-19.

Editor Rozanne M. Sandri-Goldin, University of California, Irvine

Address correspondence to Carlos Ros, carlos.ros@dcb.unibe.ch.

Received 11 June 2019
Accepted 18 July 2019
Accepted manuscript posted online 24 July 2019
Published 30 September 2019

VP2 (58 kDa) and 5% are VP1 (83 kDa) (3). VP1 is identical to VP2 except for an additional N-terminal region of 227 amino acids, the "VP1 unique region" (VP1u). Although VP2 proteins are the main component of the capsid, VP1u is critical to elicit an efficient immune response (4). The N terminus of VP1u is rich in neutralizing epitopes (5, 6), denoting the critical role of this region in the infection process.

B19V has an exceptionally narrow tissue tropism almost exclusively infecting human erythroid progenitor cells in the bone marrow. During natural infection, B19V can replicate in cells from the erythroid lineage at the BFU-E and CFU-E stages of differentiation, which accounts for the hematological disorders observed during the infection (7). The neutral glycosphingolipid globoside (Gb4), also known as P antigen, is considered the primary cellular receptor of B19V (8). A large body of evidence suggests that B19V recognizes Gb4 and that its expression is important for infection. Gb4 is expressed in various types of cells, but it is particularly abundant in human erythroid progenitor cells in the bone marrow, which are also the natural host cells of the virus (7). B19V exhibits hemagglutinating activity, which can be inhibited by soluble or lipid-associated Gb4 (9, 10). Binding of B19V to Gb4 was demonstrated by thin-layer chromatography (8). Cryo-electron microscopy (cryoEM) image reconstructions suggested that B19V binds Gb4 in the depressions on the 3-fold axes of the capsid (11). Probably the most convincing finding suggesting the essential role of Gb4 in B19V infection is the fact that the rare individuals lacking Gb4 are not susceptible to the infection and, accordingly, have no detectable B19V antibodies (12). The reason for the resistance to B19V infection has been attributed to the lack of the primary receptor required for virus internalization. However, attempts to demonstrate the specific role of Gb4 as the primary receptor required for virus entry into permissive cells have not been undertaken.

The pathogenicity and extreme narrow tropism of B19V do not correlate with the wide-ranging Gb4 expression. It was shown that different expression levels of Gb4 in cells do not correlate with B19V binding to the cells and that its expression is required but not sufficient for productive infection (13). Attempts to demonstrate B19V binding to membrane-associated Gb4 *in vitro* failed. No binding signals above background controls were observed in sensitive assays employing fluorescence-labeled liposomes, radiolabeled B19 protein capsids, surface plasmon resonance, and isothermal titration microcalorimetry (10). In this study, cryoEM image reconstruction at high resolution also failed to confirm B19V binding to Gb4. In another study, binding of B19 virus-like particles (VLPs) to Gb4 in supported lipid bilayers was reported (14). These contradictory results may be explained by a complex interaction in which glycosphingolipid clustering, accessibility, and other plasma membrane molecules may influence the binding to Gb4. Besides Gb4, other glycosphingolipids have been shown to interact with B19V (15).

Although under certain conditions, the interaction of B19V with Gb4 seems undeniable, its role as the primary receptor required for virus entry remains uncertain. Despite Gb4 expression, some cell lines cannot be infected because the virus cannot be internalized, thus suggesting that other receptor molecules are critical for the uptake of the virus into susceptible cells. $\alpha 5\beta 1$ integrin (16) and Ku80 autoantigen (17) have been proposed as potential coreceptors for B19V infection. However, the restricted uptake of B19V does not correspond with their expression profiles. In an earlier study, we showed that VP1u contains a receptor-binding domain (RBD), which mediates the uptake of the virus (18, 19). The receptor that binds the VP1u-RBD has not yet been identified, but its expression profile is far more restricted than that of Gb4, limiting B19V internalization and infection exclusively in cells at erythropoietin-dependent erythroid differentiation stages (20). Although VP1u is not accessible in native capsids, interaction with surface receptors in susceptible cells can render VP1u accessible (21, 22). This process could be partially reproduced by incubation of native capsids with soluble Gb4 (23).

Nevertheless, despite substantial efforts, the unequivocal interplay of B19V with Gb4 in the context of a capsid-receptor interaction required for virus entry has not yet been demonstrated. To clarify the role of Gb4 as the primary virus receptor, the B3GalNT1 gene, coding for globoside synthase, was knocked out. The loss of this enzyme, which

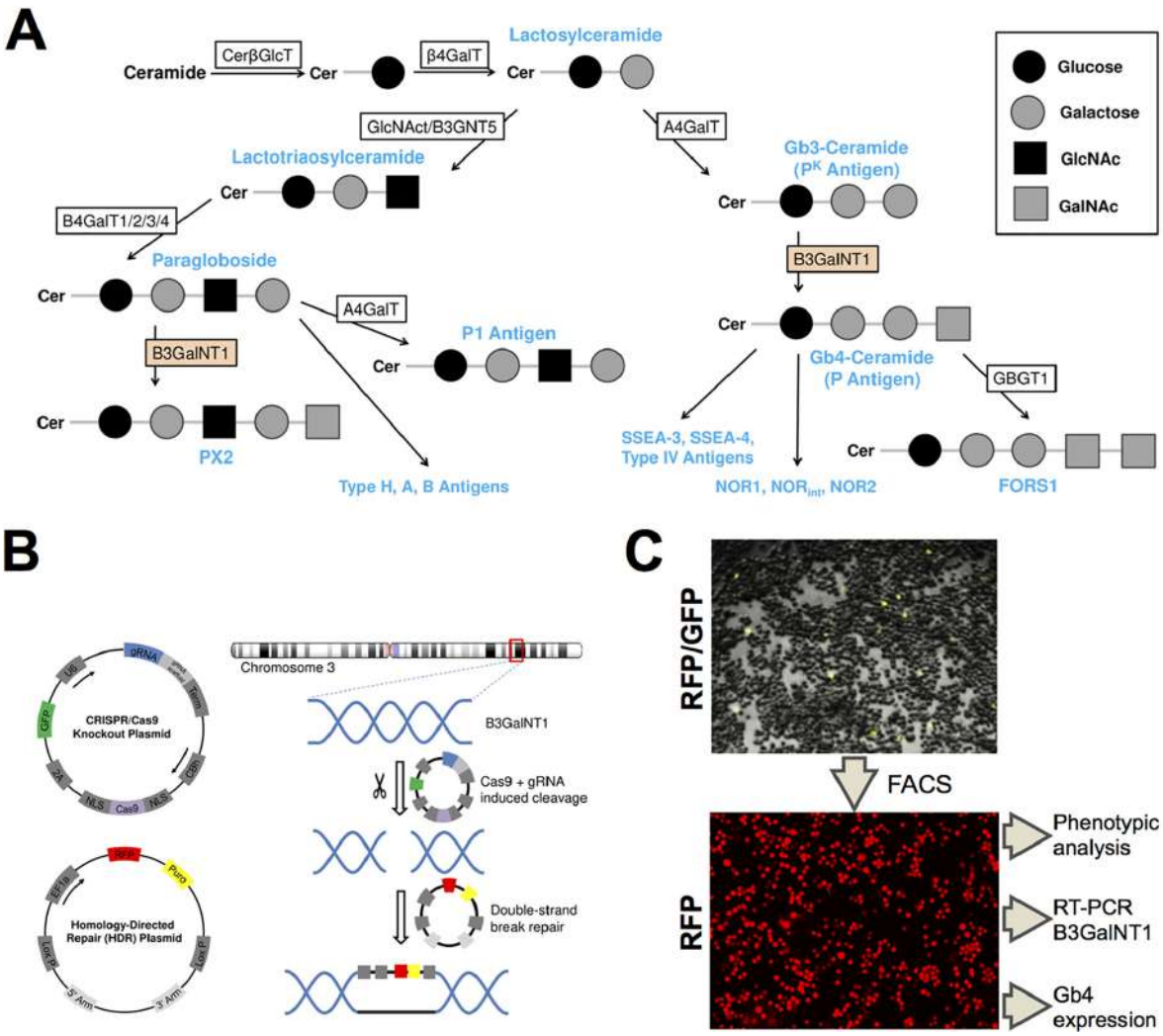

FIG 1 Generation of B3GalNT1 KO UT7/Epo cell line. (A) Schematic depiction of the biosynthetic pathways of the (neo)lacto- and globo-series. Globoside (Gb4-ceramide) is synthesized out of Gb3-ceramide with the help of globoside synthase (B3GalNT1). (B) A set of plasmids was employed to disrupt the B3GalNT1 gene. The CRISPR/Cas9 knockout plasmid was used to generate double-strand breaks at the target site using Cas9 endonuclease. A gRNA specific for the B3GalNT1 gene was used as a guide for Cas9. The homology-directed repair (HDR) plasmid provided homologous 5′ and 3′ arms of the cleavage site and could be used as a template for the double-strand break, leading to the disruption of the gene and introducing a puromycin resistance and RFP marker. (C) Cells cotransfected with the two plasmids showed a yellow fluorescence from the GFP and RFP markers (3 days posttransfection). Cells were sorted in consecutive FACS (13, 42, and 62 days posttransfection) and a single-cell sort to select RFP-expressing cells.

catalyzes the transition of globotriaosylceramide (Gb3) to Gb4 (24), leads to the elimination of Gb4 and downstream glycosphingolipids. The B3GalNT1 knockout (KO) cell line was used to investigate the contribution of Gb4 to virus entry. The results revealed an unexpected essential role of Gb4 at a postentry step.

RESULTS

Generation of B3GalNT1 KO UT7/Epo cell line. To determine the role of Gb4 in B19V infection, we sought to generate a UT7/Epo cell line devoid of Gb4. To this end, the B3GalNT1 gene, coding for globoside synthase, was knocked out. Globoside synthase is responsible for the biosynthesis of Gb4 from its precursor Gb3 (24). The knockout of the B3GalNT1 gene would abolish the synthesis of Gb4 and its downstream glycosphingolipids (Fig. 1A). The strategy of the knockout is depicted in Fig. 1B. UT7/Epo cells were cotransfected with two plasmids, one coding for Cas9 endonuclease and one of three genomic RNAs (gRNAs) targeting the B3GalNT1 gene, and a second plasmid containing homologous arms for homology-directed repair and a cassette con-

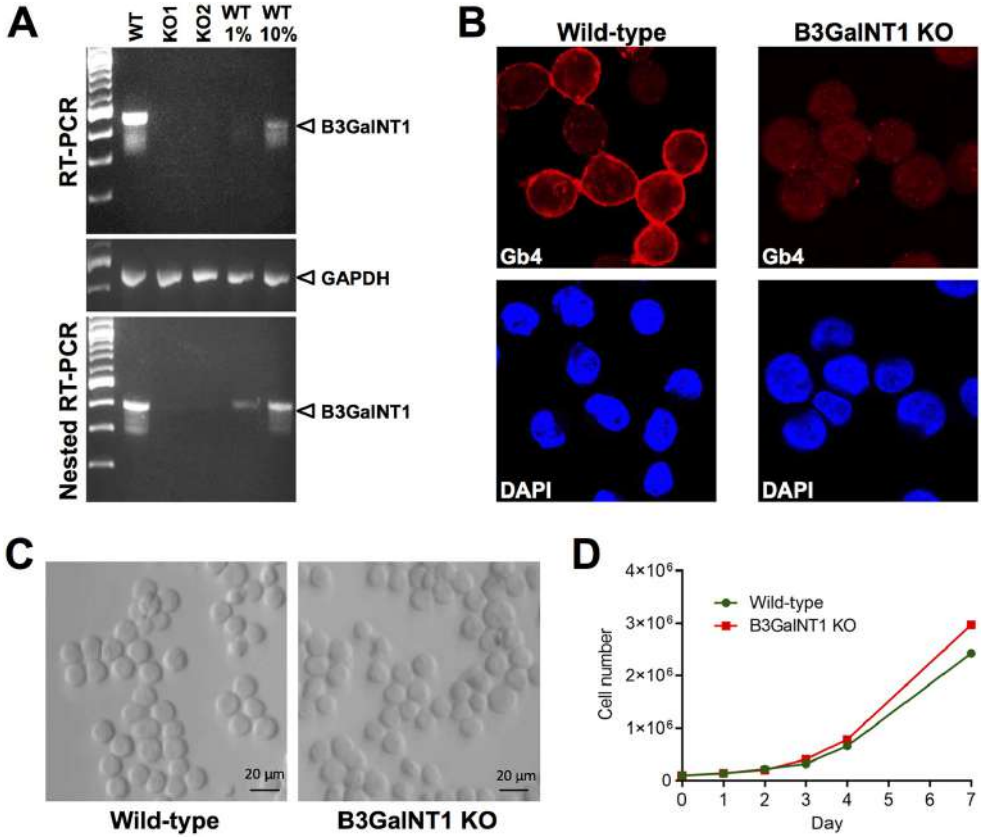

FIG 2 B3GalNT1 KO UT7/Epo cells lack B3GalNT1 transcripts, do not express Gb4, and proliferate normally. (A) Detection of B3GalNT1 mRNA. Total mRNA was isolated from WT cells and from two single cell-derived RFP-expressing clones (KO1 and KO2) and used to detect B3GalNT1 transcripts by RT-qPCR. The amplicons were used in a nested PCR to ensure sufficient sensitivity. Dilutions (1% and 10%) of the WT amplicons were loaded as a reference. GAPDH mRNA was used as a loading control. (B) Detection of Gb4 by immunofluorescence. WT and KO cells were stained with anti-Gb4 antibody, fixed, and visualized by confocal microscopy. Nuclei were stained with 4′,6-diamidino-2-phenylindole (DAPI). (C) Phase-contrast images of WT and KO cells showing no morphological differences. (D) Cell proliferation of WT and KO cells. Cells were incubated at 37°C and counted at the indicated days.

taining red fluorescence protein (RFP) and a puromycin coding sequence. Fluorescence-activated cell sorting (FACS) was used to concentrate RFP-expressing cells by two bulk cell sortings before performing a final single-cell sort (Fig. 1C).

Knockout cells lack B3GalNT1 transcripts, do not express Gb4, and proliferate normally. The presence of B3GalNT1 transcripts was tested in the WT and transfected cells. Total poly(A) mRNA was isolated and used to detect B3GalNT1 mRNA by reverse transcription-PCR (RT-PCR). While in WT cells, an amplicon of the expected size was detected, no detectable signal was observed from two independent single cell-derived RFP-expressing clones. A nested RT-PCR allowed the detection of B3GalNT1 mRNA from 1% of WT cells. Despite the increased sensitivity, B3GalNT1 transcripts remained undetectable in the transfected cells (Fig. 2A). The expression of Gb4 was examined by confocal immunofluorescence microscopy with a specific antibody (25). Gb4 was abundantly expressed in WT cells; however, no specific signal was detectable in the transfected cells (Fig. 2B). A common feature of parvoviruses is their dependence on host cell factors present during cell replication. Hence, it was important to verify that the removal of B3GalNT1 did not alter the replication rate of the cells compared to the WT cells. The two cell types showed no visible morphological differences (Fig. 2C) and exhibited similar growth curves (Fig. 2D).

Gb4 is dispensable for B19V cell attachment and internalization. WT and Gb4 KO UT7/Epo cells were used to compare B19V binding and internalization by confocal immunofluorescence microscopy. KG1a cells were used as controls. These cells derived

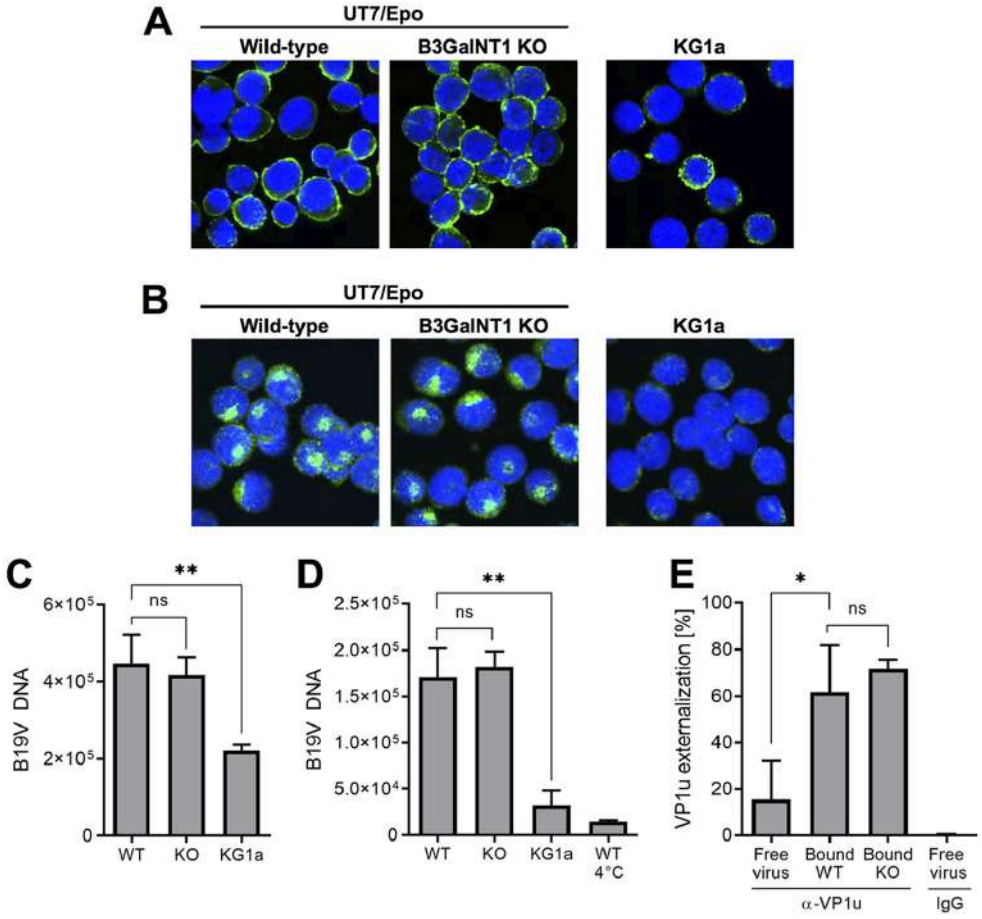

FIG 3 Gb4 is dispensable for B19V cell attachment, internalization, and VP1u exposure. (A) Detection of B19V attachment by immunofluorescence. B19V was incubated with cells at 4°C for 1 h, followed by four washes with cold PBS. Cells were fixed, stained with antibody 860-55D against capsids, and visualized by confocal microscopy. (B) Detection of B19V internalization by immunofluorescence. B19V was incubated with cells at 37°C for 1 h, washed four times with PBS, and trypsinized to remove noninternalized viruses. Cells were fixed, stained with antibody 860-55D, and visualized by confocal microscopy. (C) Quantification of B19V attachment. B19V was incubated with cells at 4°C for 1 h, followed by four washes with cold PBS. The number of virions bound to the cells was quantified by PCR. (D) Quantification of B19V internalization. B19V was incubated with cells at 37°C for 1 h, washed four times with PBS, trypsinized to remove noninternalized viruses, and quantified by PCR. WT cells incubated at 4°C serve as negative controls (no internalization). (E) Quantification of VP1u exposure from free virus or bound to cells. Virions were immunoprecipitated with antibody 860-55D against capsids (total capsids) and a rabbit antibody against the PLA_2 region (α-VP1u), followed by qPCR. Normal rabbit IgG was used as a negative control. *P* values were calculated according to Student's *t* test. *, $P < 0.05$; **, $P < 0.01$; ns, no significant difference.

from bone marrow acute myelogenous leukemia and lack the VP1u cognate receptor required for virus internalization (18). B19V was incubated with the cells for 1 h at 4°C. After several washing steps, the cells were fixed and stained with antibody 860-55D against intact capsids. As shown in Fig. 3A, B19V was able to bind WT and KO cells without noticeable differences. Binding to KG1a cells was less efficient. To verify the capacity of B19V to internalize, the cells were incubated at 37°C for 1 h, trypsinized to remove noninternalized viruses, fixed, and examined by confocal microscopy. Similar to the binding assay, no significant difference was observed in cells with or without Gb4. The virus internalized and displayed the characteristic endocytic distribution (Fig. 3B). As expected, B19V was unable to internalize KG1a cells, which lack the VP1u cognate receptor required for virus uptake. The capacity of B19V to bind and internalize WT and Gb4 KO cells was examined by quantitative PCR (qPCR). B19V was incubated with the cells for 1 h at 4°C for binding or at 37°C for internalization. Cells incubated at 37°C for 1 h were trypsinized to remove noninternalized virus. Cells incubated at 4°C served as controls (no internalization). Total DNA was extracted, and the amount of viral DNA was

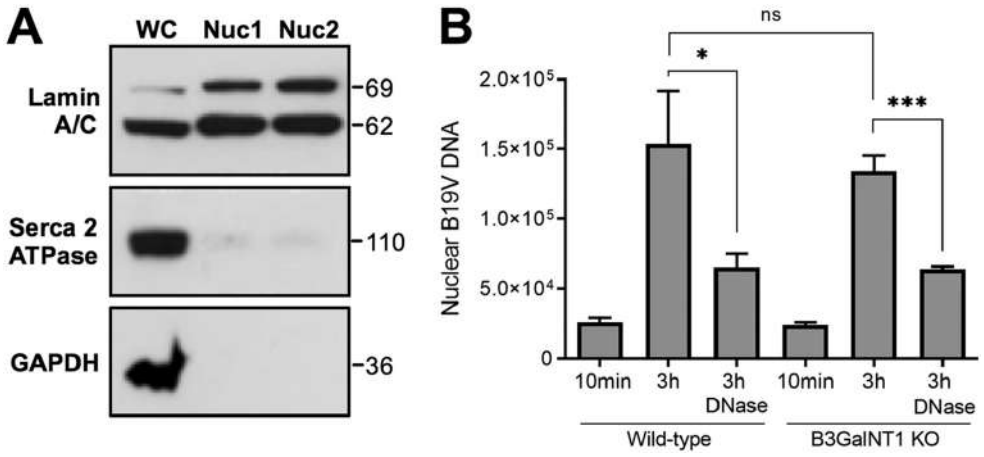

FIG 4 Nuclear targeting and viral DNA accessibility are not disturbed in Gb4 KO cells. (A) Absence of cytoplasmic contamination from two nuclear preparations (Nuc1 and Nuc2). Lamin A/C (nuclear inner membrane), SERCA2 ATPase (endoplasmic reticulum), and GAPDH (cytoplasmic proteins). WC, whole cells. (B) Nuclei from infected cells were isolated at 10 min and 3 h postinfection and were treated or not with DNase I. Total DNA was extracted and the viral DNA was quantified by PCR. *, $P < 0.05$; ***, $P < 0.001$; ns, no significant difference.

quantified by qPCR. Regardless of the presence or absence of Gb4, B19V was able to bind (Fig. 3C) and internalize (Fig. 3D) UT7/Epo cells without significant differences, confirming the results obtained by confocal immunofluorescence microscopy. Similar results were obtained from two independent single cell-derived knockout clones.

Gb4 is dispensable for VP1u externalization. In previous studies, we showed that B19V VP1u is not accessible on the capsid surface but becomes accessible upon interaction with susceptible UT7/Epo cells and erythrocytes at 4°C (21, 22). This conformational change was partially reproduced upon incubation of B19V with soluble Gb4 (23). Later, we demonstrated that this rearrangement is essential to allow the interaction of VP1u with its cognate receptor required for virus internalization (18–20). Since B19V is able to internalize in KO cells, it can be assumed that receptor molecules other than Gb4 can mediate the conformational change. To test this hypothesis, B19V was incubated with the cells at 4°C to allow attachment. After several washing steps and cell lysis, the virions were immunoprecipitated with antibody 860-55D against capsids (total capsids) and an antibody against VP1u, followed by qPCR. While in native free virions VP1u was mostly not accessible, it became largely exposed following attachment to WT or to KO cells without significant differences (Fig. 3E). This result confirms that Gb4 is not required for VP1u exposure and explains the capacity of the virus to internalize KO cells.

The absence of Gb4 does not affect either the accumulation of the incoming B19V in the nuclear fraction or the externalization of the viral DNA. To verify whether the internalized virus is able to follow the infectious route and traffic to the nucleus in the absence of Gb4, nuclei from infected cells were isolated and tested for the presence of B19V DNA. The integrity of the isolated nuclei was judged by light microscopy after trypan blue staining. The purity of the nuclear fraction and the absence of cytoplasmic contamination were verified using antibodies against lamin A/C (nuclear inner membrane marker), glyceraldehyde 3-phosphate dehydrogenase (GAPDH; cytosolic marker), and sarco/endoplasmic reticulum Ca^{2+}-ATPase (SERCA; endoplasmic reticulum marker) (Fig. 4A). Nuclei isolated after 10 min of infection served as negative controls. Viral DNA was quantified from the purified nuclei by qPCR, and the results were normalized by the quantification of the β-actin gene. At 3 h postinfection (pi), similar amounts of viral DNA accumulated in the nuclear fraction from WT and KO cells (Fig. 4B). In a recent study, we showed that a large proportion of B19V particles accumulating in the nuclear fraction of the infected cells have the viral DNA accessible and therefore are sensitive to nuclease digestion (26). As shown in Fig. 4B, the amount

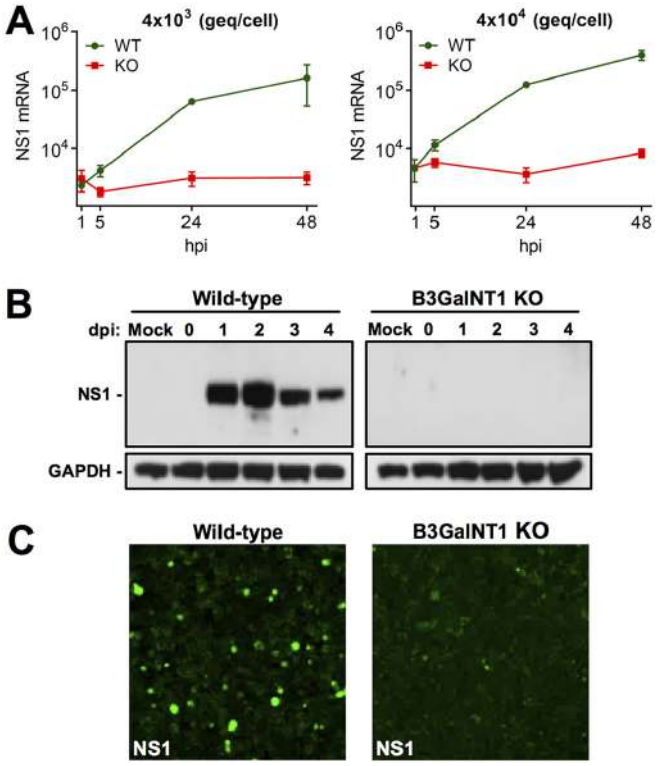

FIG 5 NS1 expression is blocked in Gb4 KO cells. (A) Detection of NS1 transcripts in WT and KO cells. Cells were infected with the indicated genome eqivalents per cell. Total mRNA was extracted at increasing hours postinfection (hpi), and the NS1 mRNA was quantified by RT-qPCR. (B) Detection of NS1 protein by Western blotting at increasing days postinfection (dpi). Cells were infected with 4×10^4 geq/cell. GAPDH was used as a loading control. Mock-infected samples were used as a negative control. (C) Detection of NS1 by immunofluorescence confocal microscopy. Cells were infected with a high dose of B19V (4×10^5 geq/cell). At 4 days postinfection, the cells were fixed and stained with a human NS1 antibody and a goat anti-human Alexa Fluor 488.

of nuclease-sensitive virus was also similar between WT and KO cells. These results indicate that in the Gb4 KO cells, the internalized virus can reach the nuclear fraction and can externalize the DNA with the same efficiency as in wild-type cells.

Gb4 is essential for NS1 expression. In UT7/Epo cells, the expression of NS1 occurs early after nuclear entry (27) and is required for DNA replication and productive infection (28, 29). The presence of NS1 mRNA in WT and KO cells was tested at increasing times pi by an NS1-specific quantitative RT-PCR. While increasing amounts of NS1 transcripts were detected in the WT cells, no NS1 transcripts above the background level were detected in Gb4 KO cells (Fig. 5A). The presence of NS1 proteins was examined by Western blotting with a monoclonal antibody (MAb) against the NS1 protein (30). In WT cells, the NS1 protein was detectable from day 1 pi. However, in KO cells, NS1 proteins remained undetectable up to day 4 pi (Fig. 5B). The absence of NS1 expression in KO cells was further confirmed by immunofluorescence microscopy with the antibody against NS1 (Fig. 5C). Similar results were obtained from two independent single-cell-derived knockout clones.

B19V DNA replication and capsid proteins are not detectable in Gb4 KO cells. Following second-strand synthesis, NS1 is required to initiate and maintain virus replication through a rolling hairpin mechanism, which involves the resolution of the inverted terminal repeats (ITRs) (29). Accordingly, the lack of NS1 in KO cells should prohibit virus replication and subsequent steps of the infection, such as capsid protein expression. To verify the capacity of B19V to replicate, WT and KO cells were infected and at 1 h and 3 days pi, low-molecular-weight DNA was extracted, and B19V DNA species were examined by Southern blotting. Incoming single-stranded DNA (ssDNA) species were detected in both cell types. In infected WT cells, monomer and dimer

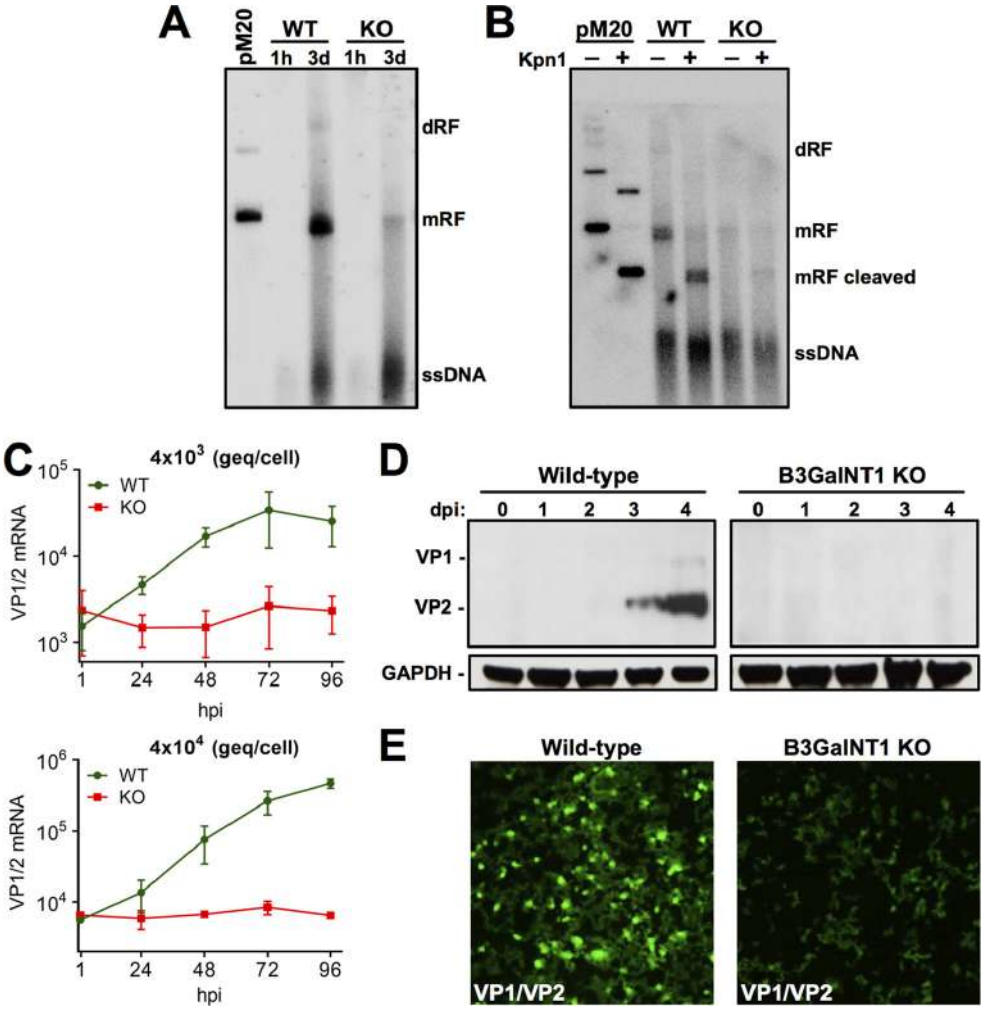

FIG 6 B19V DNA replication and capsid proteins are not detectable in Gb4 KO cells. (A) Southern blot analysis of low-molecular-weight DNA extracted from infected cells at the indicated times postinfection. Linearized pM20 infectious clone was used as a marker. dRF, dimer replicative form; mRF, monomer replicative form. (B) Southern blot analysis of low-molecular-weight DNA extracted from infected cells at 3 days postinfection and digested or not with KpnI. (C) Detection of VP1/VP2 transcripts in WT and KO cells. Cells were infected with the indicated genome equivalents per cell. mRNA was extracted at increasing hours postinfection (hpi), and the VP1/VP2 mRNA was quantified by RT-qPCR. (D) Detection of viral capsid proteins by Western blotting with antibody 3113-81C at increasing days postinfection (dpi). GAPDH was used as a loading control. (E) Detection of viral capsid proteins by immunofluorescence confocal microscopy. Cells were infected with a high dose of B19V (4×10^5 viruses per cell). At 4 days postinfection, the cells were fixed and stained with mouse antibody R9283 and goat anti-mouse Alexa Fluor 488.

replicative forms (mRF and dRF, respectively) were detected, confirming the existence of an active replication process. However, only a small amount of DNA with a molecular weight corresponding to mRF was observed in KO cells, probably corresponding to unprocessed covalently closed double-stranded DNA (dsDNA) or self-hybridized incoming ssDNA of opposite polarity (Fig. 6A). KpnI digestion confirmed the presence of viral dsDNA species in WT and KO cells (Fig. 6B).

The active replication of the viral DNA enhances readthrough of the proximal poly(A) and the polyadenylation of transcripts at the distal poly(A), which encode for the capsid proteins (31). Therefore, the absence of NS1 and virus replication in the KO cells should prohibit the generation of transcripts encoding structural proteins. As expected and regardless of the quantities of virions used, capsid protein mRNA was undetectable in KO cells (Fig. 6C). While capsid proteins accumulated at increasing days pi in WT cells, no detectable proteins were observed in KO cells (Fig. 6D). The lack of capsid protein expression was further confirmed by immunofluorescence microscopy with an antibody against viral structural proteins (Fig. 6E).

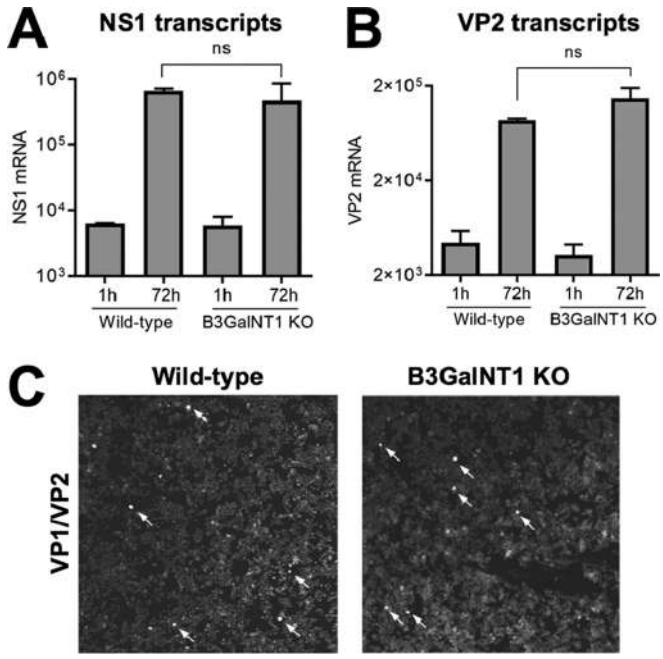

FIG 7 Transfection with a B19V infectious clone can circumvent the Gb4 block. Transfection of WT and KO cells with pM20. (A and B) mRNA was extracted 1 h or 72 h posttransfection and quantified by RT-qPCR with primers for NS1 mRNA (A) or VP1/VP2 mRNA (B). (C) At 3 days posttransfection, cells were fixed and stained with antibody R9283 against viral capsid proteins. Arrows indicate cells with positive staining. ns, no significant difference.

Transfection with a B19V infectious clone can circumvent the Gb4 block. Transfection with a B19V infectious clone was performed to evaluate the permissiveness of KO cells to B19V infection when the full-length dsDNA with resolved ITRs is directly transferred to the nucleus by nucleofection. The B19V infectious clone was digested with SalI to release the full-length genomes and used to transfect WT and KO cells using a Nucleofector device. As shown in Fig. 7A and B, similar amounts of NS1 and VP1/2 mRNAs were detected in the two cell types. At 4 days posttransfection, the cells were examined by immunofluorescence microscopy with an antibody against viral capsid proteins. Although the efficiency of transfection is typically low in UT7/Epo cells, similar amounts of positively transfected cells were observed in the two cell types (Fig. 7C). This result demonstrates that Gb4 is dispensable for B19V infection when viral dsDNA with resolved ITRs are already present in the nucleus.

Interaction of B19V with the VP1u cognate receptor but not with Gb4 is essential for virus internalization. Although B19V does not require Gb4 for cell attachment, uptake, and nuclear targeting, a transient interaction with Gb4 at the plasma membrane may still be important for the infection at a postentry step. In order to test this hypothesis, WT cells were incubated with the antibody against Gb4, and subsequently, B19V was added at 4°C to allow virus attachment. In parallel, cells were preincubated with a ΔC128 recombinant VP1u (recVP1u) construct, to block the interaction of B19V with the VP1u cognate receptor, which is required for virus uptake (18). ΔC128 lacks the C-terminal 128 amino acids of VP1u and has an intact receptor-binding domain (RBD). As a control, cells were incubated with a truncated ΔN29 recVP1u construct. This construct lacks the N-terminal 29 amino acids of VP1u, which disable the RBD. The expression and purification of the VP1u constructs have been described elsewhere (18). While the antibody against Gb4 had no effect on virus binding (Fig. 8A), approximately 50% binding inhibition was observed in the presence of the ΔC128 recVP1u (Fig. 8B). Similar cell-binding inhibition was observed when the cells were incubated with ΔC128 recVP1u and the Gb4 antibody together (Fig. 8C). Cells incubated with the truncated ΔN29 recVP1u or normal chicken IgY had no effect on virus binding.

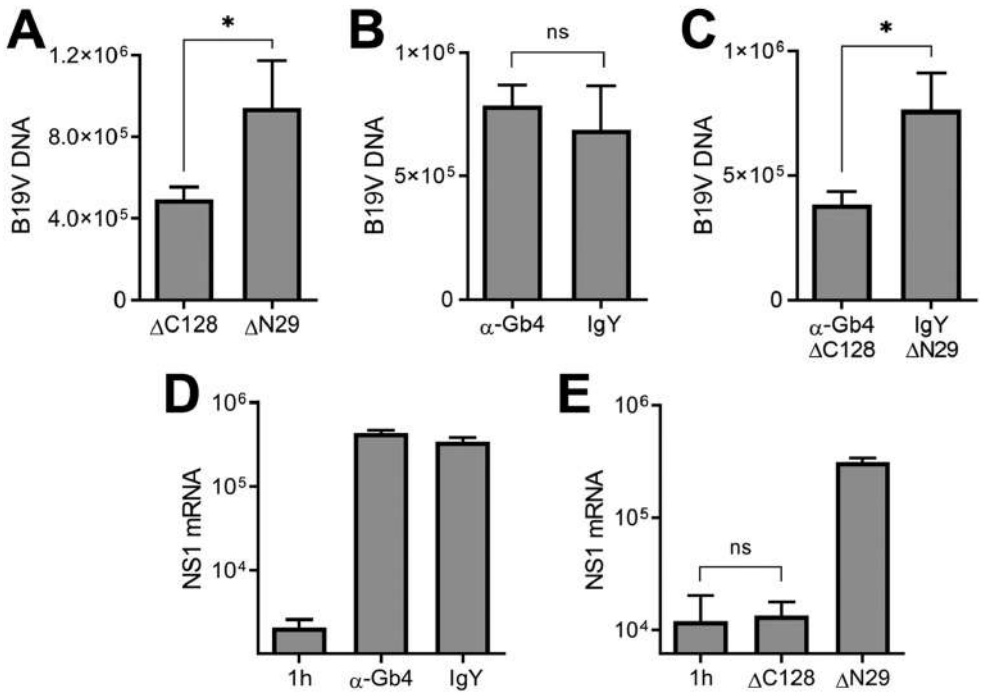

FIG 8 Effect of recVP1u and Gb4 antibody in virus binding and NS1 expression in wild-type cells. (A to C) Quantification of B19V binding to wild-type cells in the presence of chicken anti-Gb4 (A), recVP1u (ΔC128 mutant; 70 ng) (B), or both (C). (D and E) NS1 mRNA expression was quantified 24 h postinfection in the presence of anti-Gb4 (D) or recVP1u (ΔC128 mutant; 70 ng) (E). NS1 mRNA was quantified after 1 h as background control. Normal chicken IgY and truncated recVP1 (ΔN29 mutant; 70 ng), lacking the receptor-binding domain, were used as controls. *, $P < 0.05$; ns, no significant difference.

We next analyzed the effect of the Gb4 antibody and the ΔC128 recVP1u on B19V NS1 expression. The presence of the antibody did not affect NS1 expression (Fig. 8D). In sharp contrast, in the presence of the ΔC128 recVP1u, NS1 expression was completely inhibited. As a control, cells incubated with the truncated ΔN29 recVP1u or normal chicken IgY had no effect on the infection (Fig. 8E).

B19V selectively infects WT cells in a mixed population of WT and KO cells. In earlier studies, we showed that not all B19V bound to UT7/Epo cells at 4°C can internalize the cells after raising the temperature to 37°C. Instead, some viruses detach from the cells. The detached viruses have VP1u exposed, remain infectious, and are able to bind cells more efficiently than are viruses exposed for the first time to the cells (23). The numbers of bound viruses becoming detached from WT or KO cells were similar (Fig. 9A). We then sought to test whether the virus detached from the Gb4-expressing cells gains the ability to infect cells without Gb4. To this end, WT and KO cells were mixed (1:1) and incubated with a high dose of B19V (4×10^5 genome equivalents [geq]/cell) at 37°C. This approach was also intended to explore a possible complementing effect of Gb4 via juxtacrine signaling. As shown in Fig. 9B, a large proportion of WT cells became infected, as judged by the expression of viral capsid proteins. However, none of the KO cells, which are recognized by the expression of red fluorescent protein, were productively infected. The fact that viruses exposed to Gb4-expressing cells remain unable to infect KO cells further confirms that the interaction with Gb4 at the plasma membrane, if occurring, is not critical for infection.

DISCUSSION

The cell receptor of a virus plays a central role in the infection, as it represents a major determinant of the host range, tissue tropism, and viral pathogenesis. The glycosphingolipid globoside or P antigen (Gb4) has long been considered the primary cell receptor of B19V (8). Individuals with a rare mutation in the B3GalNT1 gene do not express Gb4 and are naturally resistant to the infection (12). However, the role of Gb4

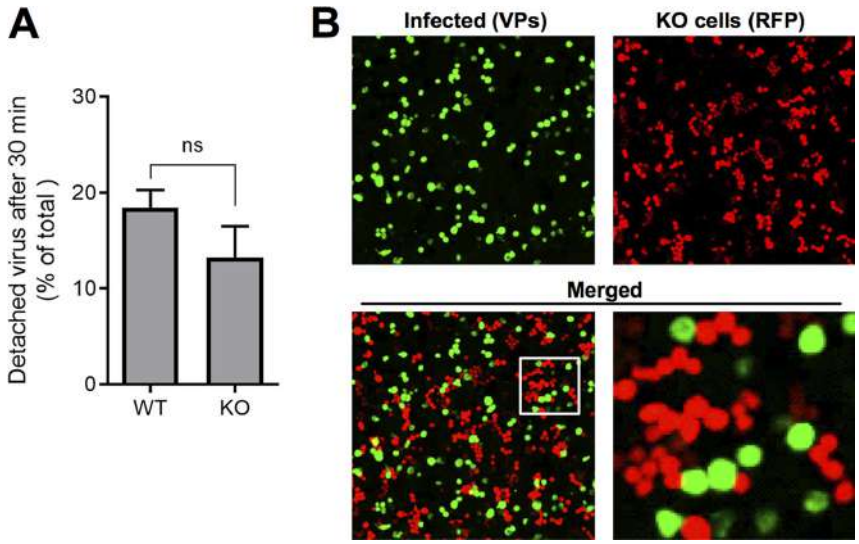

FIG 9 B19V selectively infects WT cells in a mixed population of WT and KO cells. (A) Detachment of B19V from WT and KO cells. B19V was incubated with the cells at 4°C. Following five washes to remove unbound virus, the cells were transferred to 37°C to allow internalization and detachment. At 0 min (background control) and 30 min, the cells were pelleted. The numbers of viruses bound to the cells and in the supernatant (detached) were quantified by PCR. (B) B19V infection in a mixed population of UT7/Epo WT and KO cells. WT and KO cells were mixed (1:1) and infected with a high dose of B19V (4×10^5 viruses per cell). At 4 days postinfection, the cells were washed, fixed in 4% formaldehyde to preserve the RFP signal, and stained with a mouse antibody R9283 and a goat anti-mouse Alexa Fluor 488. KO cells are recognized by the expression of RFP. ns, no significant difference.

as a B19V receptor remains controversial, as its expression does not correlate well with virus attachment, internalization, or the remarkable narrow tissue tropism of B19V. To clarify the role of Gb4 and to explore its function as the primary receptor of B19V, the B3GalNT1 gene, coding for globoside synthase, was knocked out in UT7/Epo cells, leading to the elimination of Gb4 and downstream glycosphingolipids (24). The glycosphingolipid PX2, which is also generated by globoside synthase (32), would also be lost in the B3GalNT1 KO cells. Systematic and quantitative analyses of the progression of B19V infection in WT and KO cells revealed that Gb4 does not have the expected function as a cell surface receptor required for B19V entry. Instead, Gb4 has an essential role at a postentry step for the expression of the incoming viral genomes and productive infection.

Although Gb4 is dispensable for virus entry, the interaction of B19V with Gb4 cannot be excluded. There is solid experimental evidence that the interaction may occur under certain conditions. For example, the interaction should be possible on the surface of erythrocytes since soluble Gb4 can inhibit B19V-mediated hemagglutination (9, 10). In an earlier study, we observed that incubation of B19V with erythrocytes or with UT7/Epo cells triggered conformational changes in the capsid leading to VP1u externalization (21, 22). This conformational change could be partially mimicked by incubation of capsids with soluble Gb4 (23). Since VP1u also became exposed following attachment to KO cells (Fig. 3E), other structures besides Gb4 should be recognized by B19V at the plasma membrane, which can trigger VP1u exposure. In this respect, it has been suggested that B19V recognizes several glycosphingolipids (15). A stable interaction of B19V with Gb4 could not be demonstrated in a systematic study using various sensitive assays (10). In another study, the interaction of B19 virus-like particles with Gb4 was documented (14). These apparently contradictory results may reflect the existence of an interaction exclusively under specific conditions, such as receptor clustering, the surrounding molecular environment, or structural conformations. However, the fact that B19V may recognize Gb4 under certain conditions should not imply that the interaction occurs at the plasma membrane of host cells and in the context of a virus-receptor interaction required for entry.

Glycosphingolipids are mainly associated with the plasma membrane; however, they are also found in intracellular compartments. Gb4 has been found associated with secretory granules (33) and intermediate filaments (34, 35). Accordingly, the relevant interaction with Gb4 may not occur at the plasma membrane but after virus entry. In line with this concept, we could not block virus attachment and the infection by targeting plasma membrane Gb4 with specific antibodies. The specificity of the Gb4 antibody used in this study has been thoroughly documented in previous publications (25) and further confirmed in our experiments where no signal was visible in KO cells (Fig. 2B). In sharp contrast to the Gb4 antibody, masking the VP1u cognate receptor with recVP1u disturbed the binding of the virus and completely abrogated the infection (Fig. 8). Furthermore, in a cell mixture containing equal amounts of WT and KO cells, B19V infected exclusively the cells expressing Gb4 (Fig. 9). Of note, Gb4 is a relatively small molecule, and its accessibility at the plasma membrane can be compromised by surrounding molecules. Pretreatment of cells with pronase or neuraminidase has been shown to significantly increase the accessibility of the cryptic Gb4 to antibodies (33).

Although B19V capsids may interact with Gb4 intracellularly, the essential role of Gb4 may not be related to direct physical interaction with incoming B19V capsids. Instead, the glycosphingolipid may provide a permissive intracellular environment for B19V replication. Erythropoietin (EPO) signaling is not required for virus entry and nuclear targeting, but it is essential for virus DNA replication (36). Similar to EPO, Gb4 may also promote signal transduction required for B19V infection. Clustered glycosphingolipids at the cell surface membrane interact with functional membrane proteins, such as integrins, growth factor receptors, and tetraspanins. Gb4 is involved in a variety of cellular processes, including cell adhesion, growth, motility, and cell differentiation (37, 38). Gb4 was found to promote activation of extracellular signal-related kinase (ERK), to induce the enhanced activity of specific transcription factors, and to accelerate cell differentiation (39–41). Accordingly, Gb4 may provide the required intracellular conditions for the expression of the incoming genomes.

Our data suggest that Gb4 is essential at a postentry step between nuclear entry and before the generation of dsDNA with resolved ITRs. Accumulation of the incoming capsids in the nuclear fraction and the accessibility of their DNA were similar in WT and KO cells, suggesting that Gb4 is not required for these steps. However, it cannot be excluded that Gb4 is required for the translocation of the perinuclear cytosolic capsids into the nucleus. Following virus entry into the host nucleus, the incoming ssDNA genome is converted to the double-stranded monomer replicative form (mRF), which serves as the template for virus replication and transcription. In KO cells, dsDNA corresponding in size to mRF was barely detectable in KO cells, and the dimer RF (dRF) typically observed during active DNA replication was not observed (Fig. 6A and B). The presence of viral dsDNA in KO cells suggests that Gb4 is not essential for second-strand synthesis from the incoming ssDNA genomes. However, in the absence of Gb4, the mRF remains transcriptionally inactive (Fig. 6C to E). Without NS1, the viral DNA cannot be processed further at the terminal resolution sites to initiate active DNA replication by the rolling hairpin mechanism, explaining the lack of virus replication and protein expression in the KO cells. It cannot be excluded, however, that all or a proportion of dsDNA species observed in KO cells originate from hybridized incoming ssDNA of opposite polarity. Introduction of full-length viral dsDNA with resolved ITRs by transfection can circumvent the block (Fig. 7), suggesting that Gb4 is required at a postentry step between nuclear entry and the generation of full-length viral dsDNA.

In summary, this study reveals that Gb4 does not have the expected receptor function in B19V infection, as it is dispensable for virus entry and trafficking. However, Gb4 is required at a postentry step for productive infection, either through direct interaction with incoming viruses or by means of signal transduction. The failure of B19V to infect productively Gb4 KO cells, even at a very high multiplicity of infection or in the presence of WT cells, explains the natural resistance of the rare individuals lacking Gb4 to B19V infection. Further studies will aim to investigate the postentry step

that is defective in Gb4 KO cells, and the information obtained will provide novel opportunities for the development of selective antiviral therapies.

MATERIALS AND METHODS

Cells and viruses. The human megakaryoblastoid UT7/Epo cells were maintained in Eagle's minimal essential medium (MEM) containing 5% fetal calf serum (FCS) and 2 U/ml recombinant erythropoietin (EPO). The KG1a human erythroleukemia cells were cultured in Iscove's modified Dulbecco's medium (IMDM) containing 10% FCS. B19V-infected plasma (4×10^9 genome equivalents [geq]/μl) was obtained from a donation center (CSL Behring AG, Charlotte, NC). The plasma IgGs were removed by using HiTrap protein G high-performance (HP) columns (GE Healthcare, Chicago, IL).

Antibodies. The human monoclonal antibody (MAb) 860-55D was purchased from Mikrogen (Neuried, Germany). The antibody recognizes a conformational epitope and does not react with disassembled capsid proteins (30). The human MAb against NS1 (24) was kindly provided by G. Gallinella. The mouse antibodies 3113-81C (United States Biological, Boston, MA) and R9283 (Merck, Burlington, MA) were used in Western blotting and immunofluorescence analyses, respectively. The antibody against the viral PLA_2 region was obtained as previously described (22). The polyclonal chicken anti-Gb4 IgY antibody JM07/164-4 was kindly provided by J. Müthing. The preparation and specificity of the antibody against Gb4 have been reported in previous publications (25). Rabbit anti-GAPDH and mouse anti-SERCA were purchased from Abcam (Cambridge, MA). Rabbit anti-lamin A/C was purchased from Cell Signaling Technologies (Danvers, MA).

Generation of B3GalNT1 knockout UT7/Epo cells. One day prior to transfection, 2×10^6 UT7/Epo cells were seeded in a 6-well plate with 3 ml MEM containing 5% FCS and 2 U/ml EPO. A plasmid to generate a double-strand break in the target gene (β-1,3-Gal-T3 CRISPR/Cas9 KO green fluorescence protein [GFP]) and a plasmid for homology-directed repair (β-1,3-Gal-T3 HDR RFP) (Santa Cruz Biotechnology, TX) were used for transfection using Lipofectamine 3000 (Invitrogen, CA), according to the manufacturer's instructions. Doubly transfected cells were sorted by FACS (FACSAria; BD Biosciences, NJ). Serial bulk cell sorting was performed to isolate and concentrate RFP-expressing cells, followed by a final single-cell sorting.

Analysis of B3GalNT1 KO cells. mRNA was isolated using the Dynabeads mRNA Direct kit (Invitrogen, CA), according to the manufacturer's instructions. For detection of the B3GalNT1 mRNA, the Luna Universal one-step reverse transcription-quantitative PCR (RT-qPCR) kit (New England BioLabs, Ipswich, MA) was used. The forward primer was 5′-CTCCTGAGTTTCTTTGTGATGTGG-3′, and the reverse primer was 5′-CATTACGTACTTGGCATTGGGG-3′. The nested-PCR forward primer was 5′-CCCCACTACAATGTGATAGA ACGC-3′, and the reverse primer was 5′-GGCAAAACTCAGTTACCCACC-3′. For the detection of Gb4, cells were incubated in phosphate-buffered saline (PBS) containing 2% bovine serum albumin at 4°C for 20 min. Subsequently, the cells were resuspended in 50 μl PBS containing 2% goat serum and incubated with the chicken antibody against Gb4 (0.5 μl) at 4°C for 1 h. After several washing steps with ice-cold PBS, the cells were fixed with methanol-acetone (1:1) at −20°C for 4 min, blocked with 10% goat serum in PBS, and incubated with a polyclonal antibody against chicken IgY Alexa Fluor 594 (Abcam). The proliferation rates of wild-type and transfected cells were examined. For each measurement, 10^5 cells were harvested, resuspended in fresh medium, and seeded in a 12-well plate. At different time points, cells were counted using a Moxi Z automated cell counter (Orflo Technologies, Ketchum, ID).

Virus binding and internalization. Cells (3×10^5) were resuspended in 50 μl MEM without FCS. For binding, B19V was added (10^4 virions per cell) and incubated at 4°C for 1 h. For internalization, the samples were incubated at 37°C for 1 h, washed 4 times with PBS at 4°C, and trypsinized at 37°C for 4 min to remove noninternalized viruses. Subsequently, the samples were examined by confocal immunofluorescence microscopy and by qPCR. Cells were fixed with methanol-acetone (1:1) at −20°C for 4 min, blocked with 10% goat serum in PBS, and incubated with antibody 860-55D against capsids. Anti-human IgG Alexa Fluor 488 (Invitrogen, Carlsbad, CA) was used as the secondary antibody. For qPCR, DNA was extracted using the DNeasy blood and tissue kit (Qiagen, Hilden, Germany), according to the manufacturer's instructions, and used for qPCR using iTaq polymerase (iTaq Universal SYBR green supermix; Bio-Rad, CA) with the following primers: forward, 5′-GGGCAGCCATTTTAAGTGTTT-3′; and reverse, 5′-CC AGGAAAAAGCAGCCCAG-3′.

Nuclear targeting. Cells (6×10^5) were resuspended in 100 μl MEM and incubated with B19V (10^4 virions per cell) at 4°C for 1 h to allow virus binding. After three washes with PBS, the cells were resuspended in 500 μl MEM containing 5% FCS and 2 U/ml EPO and incubated at 37°C. After 3 h, cells were pelleted and washed thrice with PBS, and the nuclei were extracted using the Nuclei EZ Prep kit (Sigma-Aldrich, MO), as previously described (26). Trypan blue staining was used to evaluate the integrity of the isolated nuclei. The absence of cytoplasmic contamination was examined with antibodies against lamin A/C (nuclear inner membrane), SERCA (endoplasmic reticulum), and GAPDH (cytoplasmic proteins). Total DNA was extracted from the isolated nuclei, and B19V DNA was quantified as specified above.

NS1 and capsid protein expression. The expression of the incoming viral genome in infected WT and KO cells was examined. NS1 and VP1/VP2 mRNA were detected by quantitative RT-PCR and proteins by Western blotting and immunofluorescence. UT7/Epo WT and KO cells were incubated with B19V for up to 4 days. The cells were washed four times with PBS, and mRNA was extracted as described above. For the detection of NS1 mRNA, the following primers were used: forward primer, 5′-GGGGCAGCATGT GTTAA-3′; and reverse primer, 5′-AGTGTTCCAGTATATGGCATGG-3′. For the detection of VP1/VP2 mRNA, the following primers were used: forward primer, 5′-CATGCACACCTACTTTCCCAA-3′; and reverse primer, 5′-GGAGGATGGGGTTTGCATCA-3′. The presence of NS1 and VP1/VP2 proteins was analyzed by Western blotting and by immunofluorescence using specific antibodies. For immunofluorescence, cells were fixed

with methanol-acetone (1:1), blocked with 10% goat serum in PBS, and incubated with the antibody against NS1 or viral structural proteins. Secondary antibodies with conjugated Alexa Fluor 488 (Invitrogen) were used against the primary antibodies. The samples were visualized using confocal microscopy (Zeiss LSM 880).

Southern blot. Cells were infected with B19V (4×10^4 virions per cell), harvested at 1 h or 3 days postinfection, washed with PBS, resuspended in 50 μl Tris-buffered saline (TBS), and lysed with 750 μl lysis buffer (10 mM Tris [pH 8], 10 mM EDTA, 0.6% SDS, and 200 μg proteinase K per ml) at room temperature (RT) for 1 h. NaCl (200 μl, 1 M final concentration) was added and incubated overnight at 4°C. The samples were then spun at 16,000 $\times$ *g* for 30 min to pellet precipitated chromosomal DNA. Total DNA was extracted from the supernatant and quantified as specified above. The viral DNA species were separated on a 0.8% agarose gel, depurinated, denatured, and neutralized before being transferred onto a positively charged nylon membrane (Amersham Hybond-N+; GE Healthcare) by capillary transfer using 20$\times$ saline-sodium citrate (SSC) buffer. The DNA was fixed to the membrane by baking. The membrane was incubated for 2 h in hybridization buffer (7% [wt/vol] SDS, 0.125 M sodium phosphate buffer [pH 7.2], 0.25 M NaCl, 1 mM EDTA, 45% [vol/vol] formamide) at 42°C. DNA was detected by overnight hybridization with a ^{32}P-labeled probe of 944 nucleotides (nt) (B19V J35 isolate, nt 773 to 1716). The membrane was washed four times at 42°C with 2$\times$ SSC and 0.1% SDS for 5 min and twice with 0.1$\times$ SSC and 0.1% SDS for 30 min before detection with a phosphorimager (Typhoon FLA 9500; GE Healthcare).

Transfection. The B19V infectious clone pM20 (0.5 μg) (42) was digested with SalI to release the full-length genome from the plasmid backbone. The linearized genome was transfected into the cells (10^5) using Lipofectamine 3000 reagent (Invitrogen), as described above. B19V NS1 and capsid protein mRNAs were examined 3 days posttransfection by RT-qPCR, and capsid proteins were analyzed by immunofluorescence microscopy, as specified above.

Quantification of VP1u exposure from free and cell-bound virus. Virus binding to UT7/Epo WT or KO cells was carried out at 4°C (2×10^4 viruses per cell) for 1 h. Cells were washed 4$\times$ with 1% bovine serum albumin in PBS (PBSA 1%) and once with PBS. Cells were lysed in lysis buffer (1% NP40, 150 mM NaCl, 50 mM Tris-HCl [pH 8], 5 mM EDTA), and the cell debris was removed by centrifugation at 10,000 $\times$ *g* for 10 min at 4°C. The supernatant was transferred to a new tube and incubated with antibody 860-55D against the viral capsid (total capsids) or with an antibody against the PLA_2-region (α-VP1u) at 4°C for 1 h. Protein G Plus-agarose (20 μl; Santa Cruz Biotechnology) was added and incubated overnight at 4°C. The beads were washed 4$\times$ with PBSA 1% and once with PBS, followed by DNA extraction and qPCR.

ACKNOWLEDGMENTS

This study was supported by a grant from the Swiss National Science Foundation (SNSF grant 31003A_179384 to J.B.).

We are grateful to J. Müthing (University of Münster, Germany) for providing the antibody against globoside and to G. Gallinella (University of Bologna, Italy) for providing the antibody against NS1.

REFERENCES

1. Young NS, Brown KE. 2004. Parvovirus B19. N Engl J Med 350:586–597. https://doi.org/10.1056/NEJMra030840.
2. Servey JT, Reamy BV, Hodge J. 2007. Clinical presentations of parvovirus B19 infection. Am Fam Physician 75:373–376.
3. Cotmore SF, McKie VC, Anderson LJ, Astell CR, Tattersall P. 1986. Identification of the major structural and nonstructural proteins encoded by human parvovirus B19 and mapping of their genes by prokaryotic expression of isolated genomic fragments. J Virol 60:548–557.
4. Zuffi E, Manaresi E, Gallinella G, Gentilomi GA, Venturoli S, Zerbini M, Musiani M. 2001. Identification of an immunodominant peptide in the parvovirus B19 VP1 unique region able to elicit a long-lasting immune response in humans. Viral Immunol 14:151–158. https://doi.org/10.1089/088282401750234529.
5. Anderson S, Momoeda M, Kawase M, Kajigaya S, Young NS. 1995. Peptides derived from the unique region of B19 parvovirus minor capsid protein elicit neutralizing antibodies in rabbits. Virology 206:626–632. https://doi.org/10.1016/S0042-6822(95)80079-4.
6. Saikawa T, Anderson S, Momoeda M, Kajigaya S, Young NS. 1993. Neutralizing linear epitopes of B19 parvovirus cluster in the VP1 unique and VP1-VP2 junction regions. J Virol 67:3004–3009.
7. Takahashi T, Ozawa K, Takahashi K, Asano S, Takaku F. 1990. Susceptibility of human erythropoietic cells to B19 parvovirus in vitro increases with differentiation. Blood 75:603–610.
8. Brown KE, Anderson SM, Young NS. 1993. Erythrocyte P antigen: cellular receptor for B19 parvovirus. Science 262:114–117. https://doi.org/10.1126/science.8211117.
9. Brown KE, Cohen BJ. 1992. Haemagglutination by parvovirus B19. J Gen Virol 73:2147–2149. https://doi.org/10.1099/0022-1317-73-8-2147.
10. Kaufmann B, Baxa U, Chipman PR, Rossmann MG, Modrow S, Seckler R. 2005. Parvovirus B19 does not bind to membrane-associated globoside in vitro. Virology 332:189–198. https://doi.org/10.1016/j.virol.2004.11.037.
11. Chipman PR, Agbandje-McKenna M, Kajigaya S, Brown KE, Young NS, Baker TS, Rossmann MG. 1996. Cryo-electron microscopy studies of empty capsids of human parvovirus B19 complexed with its cellular receptor. Proc Natl Acad Sci U S A 93:7502–7506. https://doi.org/10.1073/pnas.93.15.7502.
12. Brown KE, Hibbs JR, Gallinella G, Anderson SM, Lehman ED, McCarthy P, Young NS. 1994. Resistance to parvovirus B19 infection due to lack of virus receptor (erythrocyte P antigen). N Engl J Med 330:1192–1196. https://doi.org/10.1056/NEJM199404283301704.
13. Weigel-Kelley KA, Yoder MC, Srivastava A. 2001. Recombinant human parvovirus B19 vectors: erythrocyte P antigen is necessary but not sufficient for successful transduction of human hematopoietic cells. J Virol 75:4110–4116. https://doi.org/10.1128/JVI.75.9.4110-4116.2001.
14. Nasir W, Nilsson J, Olofsson S, Bally M, Rydell GE. 2014. Parvovirus B19 VLP recognizes globoside in supported lipid bilayers. Virology 456-457:364–369. https://doi.org/10.1016/j.virol.2014.04.004.
15. Cooling LL, Koerner TA, Naides SJ. 1995. Multiple glycosphingolipids determine the tissue tropism of parvovirus B19. J Infect Dis 172:1198–1205. https://doi.org/10.1093/infdis/172.5.1198.
16. Weigel-Kelley KA, Yoder MC, Srivastava A. 2003. Alpha5beta1 integrin as a cellular coreceptor for human parvovirus B19: requirement of func-

tional activation of beta1 integrin for viral entry. Blood 102:3927–3933. https://doi.org/10.1182/blood-2003-05-1522.
17. Munakata Y, Saito-Ito T, Kumura-Ishii K, Huang J, Kodera T, Ishii T, Hirabayashi Y, Koyanagi Y, Sasaki T. 2005. Ku80 autoantigen as a cellular coreceptor for human parvovirus B19 infection. Blood 106:3449–3456. https://doi.org/10.1182/blood-2005-02-0536.
18. Leisi R, Ruprecht N, Kempf C, Ros C. 2013. Parvovirus B19 uptake is a highly selective process controlled by VP1u, a novel determinant of viral tropism. J Virol 87:13161–13167. https://doi.org/10.1128/JVI.02548-13.
19. Leisi R, Di Tommaso C, Kempf C, Ros C. 2016. The receptor-binding domain in the VP1u region of parvovirus B19. Viruses 8:61. https://doi.org/10.3390/v8030061.
20. Leisi R, Von Nordheim M, Ros C, Kempf C. 2016. The VP1u receptor restricts parvovirus B19 uptake to permissive erythroid cells. Viruses 8:265. https://doi.org/10.3390/v8100265.
21. Ros C, Gerber M, Kempf C. 2006. Conformational changes in the VP1-unique region of native human parvovirus B19 lead to exposure of internal sequences that play a role in virus neutralization and infectivity. J Virol 80:12017–12024. https://doi.org/10.1128/JVI.01435-06.
22. Bönsch C, Kempf C, Ros C. 2008. Interaction of parvovirus B19 with human erythrocytes alters virus structure and cell membrane integrity. J Virol 82:11784–11791. https://doi.org/10.1128/JVI.01399-08.
23. Bönsch C, Zuercher C, Lieby P, Kempf C, Ros C. 2010. The globoside receptor triggers structural changes in the B19 virus capsid that facilitate virus internalization. J Virol 84:11737–11746. https://doi.org/10.1128/JVI.01143-10.
24. Chien JL, Williams T, Basu S. 1973. Biosynthesis of a globoside-type glycosphingolipid by a -N-acetylgalactosaminyltransferase from embryonic chicken brain. J Biol Chem 248:1778–1785.
25. Legros N, Dusny S, Humpf HU, Pohlentz G, Karch H, Müthing J. 2017. Shiga toxin glycosphingolipid receptors and their lipid membrane ensemble in primary human blood-brain barrier endothelial cells. Glycobiology 27:99–109. https://doi.org/10.1093/glycob/cww090.
26. Caliaro O, Marti A, Ruprecht N, Leisi R, Subramanian S, Hafenstein S, Ros C. 2019. Parvovirus B19 uncoating occurs in the cytoplasm without capsid disassembly and it is facilitated by depletion of capsid-associated divalent cations. Viruses 11:430. https://doi.org/10.3390/v11050430.
27. Wolfisberg R, Ruprecht N, Kempf C, Ros C. 2013. Impaired genome encapsidation restricts the in vitro propagation of human parvovirus B19. J Virol Methods 193:215–225. https://doi.org/10.1016/j.jviromet.2013.06.003.
28. Zhi N, Mills IP, Lu J, Wong S, Filippone C, Brown KE. 2006. Molecular and functional analyses of a human parvovirus B19 infectious clone demonstrates essential roles for NS1, VP1, and the 11-kilodalton protein in virus replication and infectivity. J Virol 80:5941–5950. https://doi.org/10.1128/JVI.02430-05.
29. Ganaie SS, Qiu J. 2018. Recent advances in replication and infection of human parvovirus B19. Front Cell Infect Microbiol 8:166. https://doi.org/10.3389/fcimb.2018.00166.
30. Gigler A, Dorsch S, Hemauer A, Williams C, Kim S, Young NS, Zolla-Pazner S, Wolf H, Gorny MK, Modrow S. 1999. Generation of neutralizing human monoclonal antibodies against parvovirus B19 proteins. J Virol 73:1974–1979.
31. Guan W, Cheng F, Yoto Y, Kleiboeker S, Wong S, Zhi N, Pintel DJ, Qiu J. 2008. Block to the production of full-length B19 virus transcripts by internal polyadenylation is overcome by replication of the viral genome. J Virol 82:9951–9963. https://doi.org/10.1128/JVI.01162-08.
32. Westman JS, Benktander J, Storry JR, Peyrard T, Hult AK, Hellberg Å, Teneberg S, Olsson ML. 2015. Identification of the molecular and genetic basis of PX2, a glycosphingolipid blood group antigen lacking on globoside-deficient erythrocytes. J Biol Chem 290:18505–18518. https://doi.org/10.1074/jbc.M115.655308.
33. Katz HR, Austen KF. 1986. Plasma membrane and intracellular expression of globotetraosylceramide (globoside) in mouse bone marrow-derived mast cells. J Immunol 136:3819–3824.
34. Gillard BK, Heath JP, Thurmon LT, Marcus DM. 1991. Association of glycosphingolipids with intermediate filaments of human umbilical vein endothelial cells. Exp Cell Res 192:433–444. https://doi.org/10.1016/0014-4827(91)90062-y.
35. Gillard BK, Thurmon LT, Marcus DM. 1992. Association of glycosphingolipids with intermediate filaments of mesenchymal, epithelial, glial, and muscle cells. Cell Motil Cytoskeleton 21:255–271. https://doi.org/10.1002/cm.970210402.
36. Chen AY, Guan W, Lou S, Liu Z, Kleiboeker S, Qiu J. 2010. Role of erythropoietin receptor signaling in parvovirus B19 replication in human erythroid progenitor cells. J Virol 84:12385–12396. https://doi.org/10.1128/JVI.01229-10.
37. Kojima N, Hakomori S. 1991. Synergistic effect of two cell recognition systems: glycosphingolipid-glycosphingolipid interaction and integrin receptor interaction with pericellular matrix protein. Glycobiology 1:623–630. https://doi.org/10.1093/glycob/1.6.623.
38. D'Angelo G, Capasso S, Sticco L, Russo D. 2013. Glycosphingolipids: synthesis and functions. FEBS J 280:6338–6353. https://doi.org/10.1111/febs.12559.
39. Song Y, Withers DA, Hakomori S. 1998. Globoside-dependent adhesion of human embryonal carcinoma cells, based on carbohydrate-carbohydrate interaction, initiates signal transduction and induces enhanced activity of transcription factors AP1 and CREB. J Biol Chem 273:2517–2525. https://doi.org/10.1074/jbc.273.5.2517.
40. Park SY, Kwak CY, Shayman JA, Kim JH. 2012. Globoside promotes activation of ERK by interaction with the epidermal growth factor receptor. Biochim Biophys Acta 1820:1141–1148. https://doi.org/10.1016/j.bbagen.2012.04.008.
41. Nakamura T, Chiba Y, Naruse M, Saito K, Harada H, Fukumoto S. 2016. Globoside accelerates the differentiation of dental epithelial cells into ameloblasts. Int J Oral Sci 8:205–212. https://doi.org/10.1038/ijos.2016.35.
42. Zhi N, Zádori Z, Brown KE, Tijssen P. 2004. Construction and sequencing of an infectious clone of the human parvovirus B19. Virology 318:142–152. https://doi.org/10.1016/j.virol.2003.09.011.

PLOS PATHOGENS

RESEARCH ARTICLE

Human parvovirus B19 interacts with globoside under acidic conditions as an essential step in endocytic trafficking

Jan Bieri, Remo Leisi, Cornelia Bircher, Carlos Ros*

Department of Chemistry, Biochemistry and Pharmaceutical Sciences, University of Bern, Bern, Switzerland

* carlos.ros@dcb.unibe.ch

OPEN ACCESS

Citation: Bieri J, Leisi R, Bircher C, Ros C (2021) Human parvovirus B19 interacts with globoside under acidic conditions as an essential step in endocytic trafficking. PLoS Pathog 17(4): e1009434. https://doi.org/10.1371/journal.ppat.1009434

Editor: Patrick Hearing, Stony Brook University, UNITED STATES

Received: February 26, 2021

Accepted: April 12, 2021

Published: April 20, 2021

Peer Review History: PLOS recognizes the benefits of transparency in the peer review process; therefore, we enable the publication of all of the content of peer review and author responses alongside final, published articles. The editorial history of this article is available here: https://doi.org/10.1371/journal.ppat.1009434

Data Availability Statement: All relevant data are within the manuscript and its Supporting information files.

Abstract

The glycosphingolipid (GSL) globoside (Gb4) is essential for parvovirus B19 (B19V) infection. Historically considered the cellular receptor of B19V, the role of Gb4 and its interaction with B19V are controversial. In this study, we applied artificial viral particles, genetically modified cells, and specific competitors to address the interplay between the virus and the GSL. Our findings demonstrate that Gb4 is not involved in the binding or internalization process of the virus into permissive erythroid cells, a function that corresponds to the VP1u cognate receptor. However, Gb4 is essential at a post-internalization step before the delivery of the single-stranded viral DNA into the nucleus. In susceptible erythroid Gb4 knockout cells, incoming viruses were arrested in the endosomal compartment, showing no cytoplasmic spreading of capsids as observed in Gb4-expressing cells. Hemagglutination and binding assays revealed that pH acts as a switch to modulate the affinity between the virus and the GSL. Capsids interact with Gb4 exclusively under acidic conditions and dissociate at neutral pH. Inducing a specific Gb4-mediated attachment to permissive erythroid cells by acidification of the extracellular environment led to a non-infectious uptake of the virus, indicating that low pH-mediated binding to the GSL initiates active membrane processes resulting in vesicle formation. In summary, this study provides mechanistic insight into the interaction of B19V with Gb4. The strict pH-dependent binding to the ubiquitously expressed GSL prevents the redirection of the virus to nonpermissive tissues while promoting the interaction in acidic intracellular compartments as an essential step in infectious endocytic trafficking.

Author summary

The neutral glycosphingolipid globoside (Gb4) has been historically considered the cellular receptor of B19V, however, its wide expression profile does not correlate well with the restricted tropism of the virus. Here, we show that Gb4 is essential for the infection at a step following virus uptake and before the delivery of the viral ssDNA into the nucleus. B19V interacts with Gb4 exclusively under acidic conditions, prohibiting the interaction on the plasma membrane and promoting it inside the acidic endosomal compartments, which are engaged by the virus and the GSL after internalization. In the absence of Gb4,

Funding: This study was supported by a grant from the Swiss National Science Foundation (grant 31003A_179384 to J.B.). www.snf.ch. The funders had no role in study design, data collection and analysis, decision to publish, or preparation of the manuscript.

Competing interests: The authors have declared that no competing interests exist.

incoming viruses are retained in the endocytic compartment and the infection is aborted. This study reveals the mechanism of the interaction between the virus and the glycosphingolipid and redefines the role of Gb4 as an essential intracellular partner required for infectious entry.

Introduction

Parvovirus B19 (B19V) is a human pathogen discovered in 1974 [1]. The virus causes infections worldwide that vary in severity depending on the age as well as the immunologic and hematologic status of the host [2,3]. In healthy children, B19V causes a mild disease named *erythema infectiosum* or fifth disease [4]. The virus can occasionally lead to more severe complications, such as arthropathies in adults [5], *hydrops fetalis* in pregnant women [6] and chronic red cell aplasia in patients with underlying hemolytic anemia [7,8]. The linear single-stranded DNA genome of 5.6-kb in length is encapsidated within a small, non-enveloped, icosahedral particle consisting of 60 structural proteins, VP1 and VP2 [9]. These proteins share the same sequence except for an additional amino-terminal VP1 unique region (VP1u) of 227 amino acids. VP1u harbors strong neutralizing epitopes and is crucial to elicit an efficient immune response against the virus [10]. The two most relevant domains in the VP1u is a receptor binding domain (RBD) required for virus uptake into host cells [11] and a phospholipase A2 (PLA_2) domain required for the infection [12–15], presumably to promote endosomal escape [16].

B19V is transmitted primarily via the respiratory route [5]. From the respiratory epithelium, the virus particles access the bloodstream by an unknown mechanism. A striking feature of B19V is its marked tropism for erythroid progenitor cells (EPCs) in the bone marrow [17–19]. The lytic replication of the virus in this cell population accounts for the hematological disorders typically associated with the infection. The distribution of specific cellular receptors in concert with essential intracellular factors explains the remarkable narrow tropism of B19V [19–22].

Historically, the neutral glycosphingolipid (GSL) globoside (Gb4) or P antigen has been considered the primary cellular receptor of B19V [23]. Gb4 is expressed in target EPCs and the virus exhibits hemagglutinating activity, which can be inhibited by soluble or lipid-associated Gb4 [24,25]. The rare persons lacking Gb4 (p phenotype) are naturally resistant to the infection and their erythrocytes cannot be hemagglutinated by the virus [26]. Despite the solid evidence, the role of Gb4 as the cellular receptor of B19V has been increasingly questioned. The restricted tropism of B19V [17–19] does not align well with the wide expression profile of Gb4 [27,28]. Gb4 is the most abundant neutral GSL expressed on the membranes of human red blood cells (RBCs) [29,30], which cannot be productively infected. Moreover, the degree of virus attachment to cells does not correspond with the expression levels of Gb4, and although the presence of Gb4 was shown to be essential for the infection, it was not enough for productive infection [31].

The fact that the virus cannot internalize certain cells despite the expression of Gb4, suggests that other receptor molecules must be required for the uptake of the virus into susceptible cells. In line with this assumption, we showed that VP1u is required for virus uptake and identified a functional RBD at the most amino-terminal part of the protein, which mediates virus uptake independently of the rest of the capsid [11,19,32]. Different from Gb4, the expression profile of the VP1u cognate receptor (VP1uR) corresponds to the narrow tropism of B19V, limiting virus internalization and infection exclusively in cells at erythropoietin-dependent

erythroid differentiation stages [19,33]. Although VP1u is not accessible in native capsids, interaction with surface receptors on susceptible cells renders VP1u accessible [34,35]. This process could be partially reproduced by incubation of native capsids with soluble Gb4 [36], suggesting that the neutral GSL may assist the uptake process. However, in a recent study, we showed that in susceptible erythroid cells expressing VP1uR and lacking Gb4, VP1u becomes exposed and the virus is internalized, highlighting the irrelevance of Gb4 in this process. However, Gb4 was found to be essential for the internalized virus to initiate the infection [37].

It remains unclear whether B19V requires Gb4 as a host cell binding partner, or indirectly as a signaling molecule or cellular component required for the infection. The hemagglutination of human erythrocytes by B19V [24], which express large quantities of Gb4 [29,30], and the hemagglutination inhibition in the presence of soluble Gb4 [25], strongly indicate that B19V interacts with Gb4. However, attempts to confirm the interaction have not yet been conclusive. The binding of B19 virus-like particles (VLPs) to Gb4 in supported lipid bilayers has been reported [38], and the complex has been observed by cryoEM image reconstruction [39]. However, other studies using a higher resolution cryoEM failed to confirm the interaction [25]. In the same study, no binding signals above background controls were detected in various highly sensitive assays employing fluorescence-labeled liposomes, radiolabeled B19 capsids, surface plasmon resonance, and isothermal titration microcalorimetry [25]. These inconsistent observations suggest that either the interaction between B19V and Gb4 does not occur or requires specific conditions that have not yet been identified.

In this study, we have addressed the interplay between B19V and Gb4, the conditions required for the interaction, and the infection step where the GSL is essential. To this end, the hemagglutinating activity and adsorption capacity of native virions and virus-like particles (VLPs) to Gb4 expressed on human erythrocytes and erythroleukemia cells were examined under different experimental conditions. The role of Gb4 was investigated by following the infection of native virus and engineered capsids, differing in their capacity to interact with Gb4, in wild-type and Gb4 knockout erythroid cells. The study confirms the binding of B19V to Gb4, identifies the strict conditions modulating the interaction and redefines the essential role of the GSL at a post-internalization step for the infectious trafficking of the incoming virus.

Results

Gb4 is essential at a post-internalization step and before the delivery of the viral genome into the nucleus for replication

In an earlier study, we established a Gb4 knockout (KO) UT7/Epo cell line and demonstrated that Gb4 is essential for productive infection, but it is not required for virus attachment and internalization, which is mediated by the VP1u cognate receptors (VP1uR) [32,37]. Here, we used a recombinant VP1u construct (S1A and S1B Fig) to demonstrate that VP1uR expression is not altered in Gb4 KO cells. The expression of VP1uR in cells was sufficient to trigger virus attachment and uptake, however, in the absence of Gb4, the intracellular capsids failed to initiate the infection (Fig 1A and S2 Fig). In sharp contrast, blocking VP1uR by pre-incubation of cells with recombinant VP1u abolished attachment and internalization (Fig 1B).

To test the capacity of VP1uR to mediate virus internalization without the involvement of Gb4 or any other additional receptor(s) or attachment factor(s), recombinant VP1u subunits were chemically coupled to bacteriophage MS2 capsids, as previously described with some modifications [19] (S1C and S1D Fig). The engineered capsids were incubated with wild-type (WT) or with Gb4 KO UT7/Epo cells for 1h at 4˚C for virus attachment or at 37˚C for virus internalization. Regardless of the presence or absence of Gb4, the VP1u decorated particles

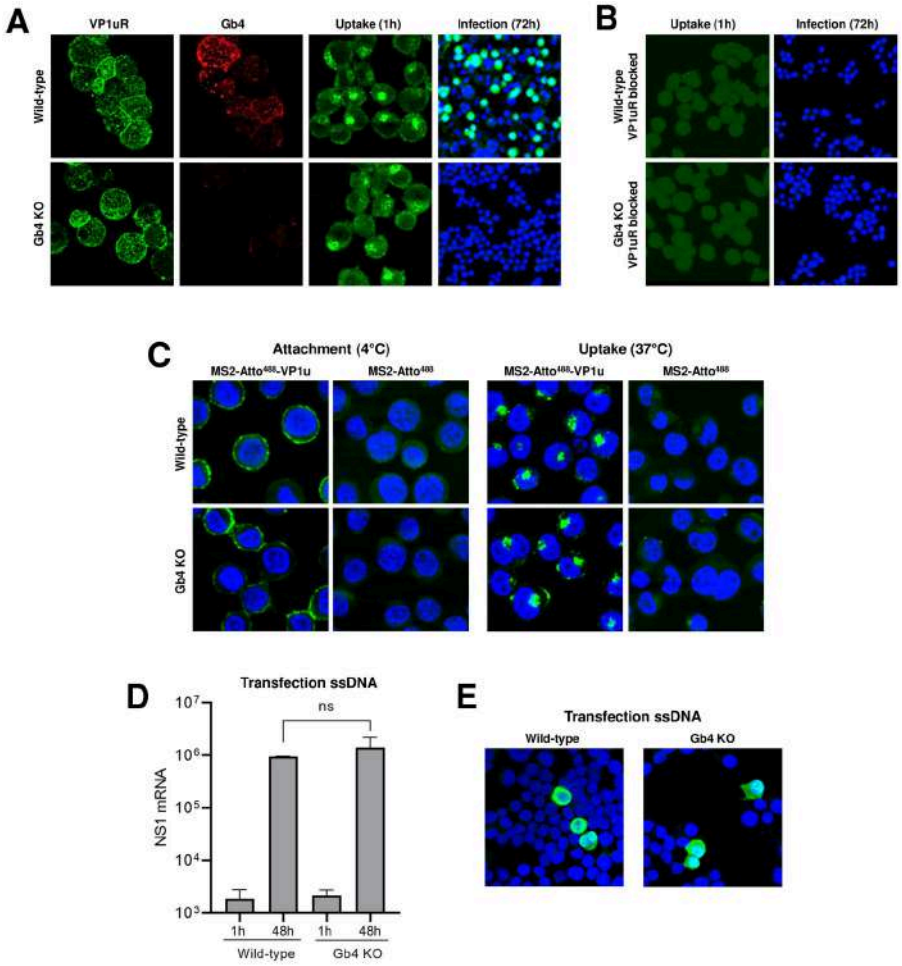

Fig 1. Gb4 is essential at a post-internalization step and before the delivery of the viral genome into the nucleus for replication. (A) Detection of VP1u cognate receptor (VP1uR) and Gb4 in UT7/Epo wild-type (WT) and Gb4 knockout (KO) cells by immunofluorescence (IF). Cells were incubated with either recombinant VP1u labelled with anti-FLAG antibody or anti-Gb4 antibody, washed, fixed and stained with secondary antibodies for confocal microscopy. B19V uptake (1h at 37˚C) was detected with the antibody 860-55D against intact capsids, while progeny virus (72h at 37˚C) was detected with the antibody 3113-81C against viral capsid proteins. (B) B19V uptake (1h) and infection (72h) in cells pre-incubated with recombinant VP1u (VP1u ΔC126) (S1 Fig) for 30 min at 4˚C to block the VP1uR. (C) Attachment (1h at 4˚C) and uptake (1h at 37˚C) of fluorescently labelled (Atto 488) MS2 bacteriophage capsids with conjugated recombinant VP1u ΔC126 from B19V (MS2-Atto^{488}-VP1u) (S1 Fig). As a control, unconjugated fluorescently labelled MS2 bacteriophage capsids were used (MS2-Atto^{488}). Nuclei were stained with DAPI. (D) NS1 mRNA quantification by RT-qPCR after transfection of genomic ssDNA (1h and 48h) in WT and Gb4 KO cells. The results are presented as the mean ± SD of three independent experiments. ns, not significant. (E) Detection of capsid protein expression (3113-81C; green) after transfection of genomic ssDNA (48h) in WT and Gb4 KO cells.

https://doi.org/10.1371/journal.ppat.1009434.g001

were able to bind and internalize into the cells without detectable differences (Fig 1C). This result indicates that virus uptake is activated by the interaction of VP1u with VP1uR, without the contribution of other capsid regions.

To better define the step of the infection where Gb4 is required, the viral ssDNA genome was extracted from native virions and directly introduced into the cells by transfection. This approach allows bypassing the cytoplasmic trafficking steps but not the second-strand synthesis, which is the first step in viral DNA replication. As shown in Fig 1D, a similar amount of

NS1 mRNAs was detected in transfected WT and Gb4 KO cells. The capacity of B19V to infect Gb4 KO cells following transfection was further confirmed by immunofluorescence microscopy with an antibody against viral capsid proteins (Fig 1E). These results together indicate that Gb4 is not required for virus attachment and uptake, but instead plays an essential role at an intracellular trafficking step before the delivery of the viral genome into the nucleus for replication.

In the absence of Gb4, internalized B19V is arrested in the endosomal compartment

Following interaction with VP1uR, B19V is internalized by clathrin-mediated endocytosis and rapidly spreads throughout the early-late endosomes and lysosomes [32,40]. Thereafter, capsids move progressively from the endo-lysosomal compartment, which typically appears as a dense perinuclear signal, to a more dispersed spatial arrangement with limited or no co-localization with endo-lysosomal markers [40]. To further circumscribe the trafficking step where Gb4 is required, we followed the intracellular progression of the virus in the presence (WT cells) or absence of Gb4 (Gb4 KO cells) by immunofluorescence microscopy with antibodies targeting B19V capsids (860-55D) and endo-lysosomal markers (M6PR and Lamp1). The results revealed a striking difference depending on the presence or absence of Gb4. As expected, at 30 min post-infection (pi), B19V co-localized with late endosomes and lysosomes in WT and Gb4 KO cells. At 3h pi, co-localization of incoming viruses with endo-lysosomal markers decreased in WT cells and their clustered spatial distribution changed to a more scattered arrangement. In contrast, in cells lacking Gb4, the internalized virus did not show the same progression and remained associated with the endo-lysosomal markers, showing no cytoplasmic spreading of capsids as observed in Gb4-expressing cells (Fig 2A). The distinct endocytic progression of incoming capsids in presence or absence of Gb4 was further confirmed by quantitative analysis of intracellular fluorescent foci per cell (Fig 2B and S3 Fig).

This observation suggests a role of the GSL in the infectious endocytic trafficking of B19V. To further corroborate this assumption, we compared the endocytic trafficking of native B19V and MS2-VP1u particles. Similar to B19V, MS2-VP1u can internalize into the host cell through VP1uR interaction, however, these artificial capsids lack potential interaction sites harbored in the B19 capsid structure, such as a putative Gb4 binding site. Besides, MS2-VP1u lacks the PLA_2 domain, which is required for endosomal escape [16,41] (S1A Fig). Accordingly, following uptake these particles remained steadily associated with endo-lysosomal markers (S4 Fig). WT and Gb4 KO cells were infected with B19V for 30 min at 37˚C to allow virus internalization followed by incubation with MS2-VP1u for an additional 1h at 37˚C. At 3h pi, the cells were examined by confocal immunofluorescence microscopy. In WT cells, B19V and MS2-VP1u had a different distribution with limited co-localization. B19V appeared more scattered, while MS2-VP1u exhibited the characteristic endo-lysosomal distribution. In cells lacking Gb4, both B19V and MS2-VP1u displayed the same intracellular distribution with a strong co-localization (Fig 2C). The scattered signal observed at 3h pi in WT cells did not co-localize with early-late endosomes (EEA1, M6PR), lysosomes (Lamp1), recycling endosomes (Rab11), Golgi apparatus (Giantin) or trans-Golgi network (TGN46), however, it co-localized partially with the cis-Golgi marker GM130 (Fig 2D).

B19V interacts with soluble and membrane-associated Gb4 in a pH-dependent manner

Various studies conducted to investigate the binding of B19V with Gb4 generated contradictory results, which was attributed to the rigorous conditions required for the interaction

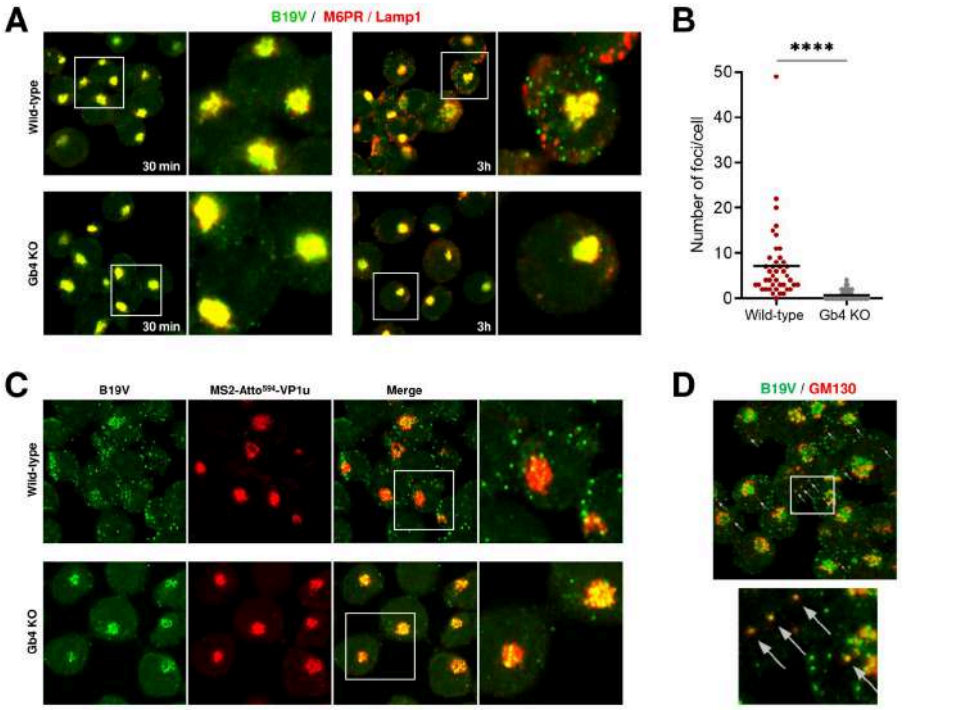

Fig 2. In the absence of Gb4, internalized B19V is arrested in the endosomal compartment. (A) Co-localization of incoming B19V capsids (860-55D; green) with endo-lysosomal markers (M6PR and Lamp1; red) in UT7/Epo WT and Gb4 KO cells at 30 min and 3h pi. (B) Quantitative analysis of scattered cytoplasmic foci (B19V capsid signal) not colocalizing with endocytic markers at 3h pi (S3 Fig). Unpaired Students t-test with Welch's correction (not assuming same SD) was used for statistical comparison. ****, $p<0.0001$. (C) Co-localization of incoming B19V capsids (860-55D; green) with MS2-Atto^{594}-VP1u in UT7/Epo WT and Gb4 KO cells at 3h pi. (D) Co-localization of B19V capsids (860-55D; green) with a cis-Golgi marker (GM130; red) in WT cells at 3h pi.

https://doi.org/10.1371/journal.ppat.1009434.g002

[23,25,38]. The endosomal retention of incoming capsids in cells lacking Gb4 suggests a possible interaction inside acidic endosomes, which are engaged by both the virus and the GSL shortly after internalization [40,42]. To test this hypothesis, the interaction with Gb4 expressed on human red blood cells (RBCs) was examined under characteristic acidic endosomal conditions. Interestingly, hemagglutination by B19V is routinely performed at low pH because it enhances the reaction [24,43], however, the underlying mechanism has not been elucidated. Inspired by this phenomenon, the hemagglutinating activity and the binding capacity of the virus to RBCs were quantitatively analyzed under a wide range of pH conditions. As shown in Fig 3A, hemagglutination of RBCs by B19V occurs exclusively under acidic conditions (pH $<$ 6.4). In contrast, hemagglutination with equal amounts of minute virus of mice (MVM), a parvovirus that binds sialic acid on erythrocytes, is not influenced by pH. Increasing the number of B19 virions did not influence the results (Fig 3B). Accordingly, the low pH-dependent hemagglutination of RBCs by B19V is due to the intrinsic nature of the interaction between the virus and Gb4. As a control, the visualization of RBCs at neutral or acidic conditions by scanning electron microscopy did not reveal detectable differences in cell integrity (S5 Fig).

To confirm that the hemagglutination is caused by the interaction of the virus with Gb4, the binding of B19V to RBCs was quantified in the presence of soluble Gb4. Globotriaosylceramide (Gb3), which is the precursor of Gb4 was used as a control. Compared to pH 7.4, a sharp increase ($>$ 2 log10) in the binding of B19V to RBCs was observed at pH 6.3. While the

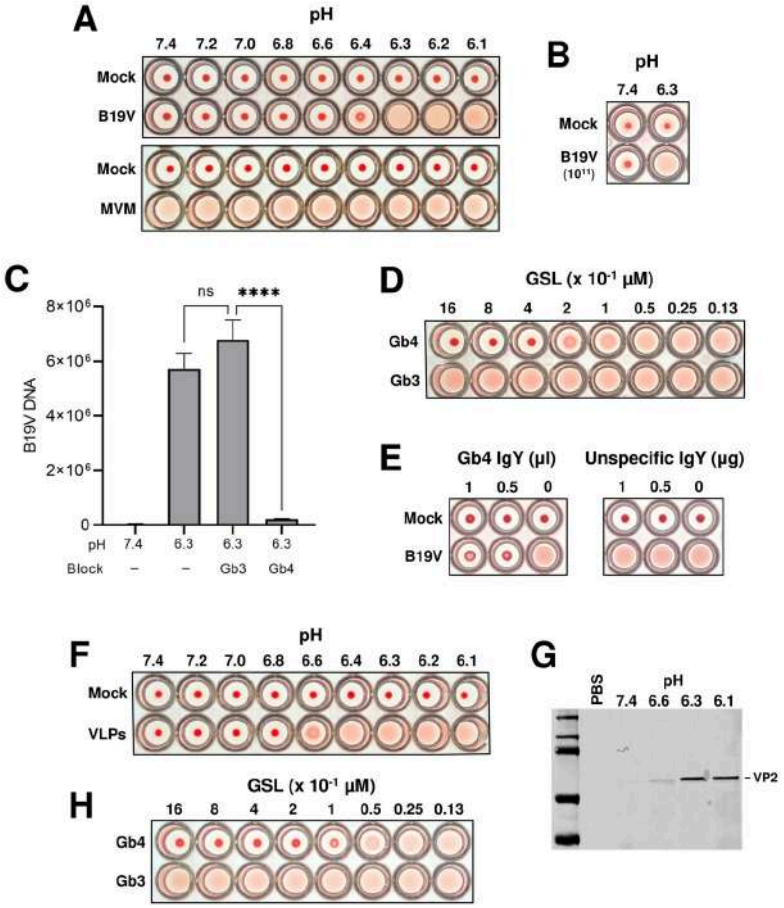

Fig 3. B19V interacts with soluble and membrane Gb4 in a pH-dependent manner. (A) Hemagglutination of human RBCs (0.5% in 100 µl PiBS) by B19V or MVM ($5x10^9$) at different pH values. (B) Hemagglutination of RBCs with a 20-fold increase of B19V particles at pH 7.4 and 6.3. (C) Quantitative analysis of B19V binding to RBCs at pH 7.4 and 6.3 in the presence or absence of GSLs (Gb3 or Gb4). Virus ($5x10^9$) was incubated directly with RBCs (0.5% in 100 µl PiBS) at the indicated pH or pre-blocked with $5x10^{14}$ molecules (Gb3 or Gb4) for 1h at pH 6.3 prior to incubation with RBCs. After 1h at room temperature, the erythrocytes were washed four times with the corresponding buffer and the viral DNA was extracted and quantified. The results are presented as the mean ± SD of three independent experiments. ****, $p<0.0001$; ns, not significant. (D) Hemagglutination inhibition test in the presence or absence of different amount (0.013–1.6 µM) of GSLs (Gb3 or Gb4) at pH 6.3. (E) Hemagglutination inhibition test in the presence of anti-Gb4 or non-specific IgY antibodies at pH 6.3 (antibodies were incubated with RBCs 1h before adding the virus). (F) Hemagglutination of RBCs (0.5% in 100 µl PiBS) by VLPs ($5x10^9$) at different pH values. (G) Detection of VLPs bound to RBCs at different pH values by Western blot using antibody 3113-81C. (H) Hemagglutination inhibition test in the presence or absence of different amount (0.013–1.6 µM) of Gb3 or Gb4 at pH 6.3.

https://doi.org/10.1371/journal.ppat.1009434.g003

presence of soluble Gb3 did not prevent the interaction, a significant inhibition of the binding was observed in the presence of soluble Gb4 (Fig 3C). Confirming this observation, Gb4 (> 0.2–0.4 µM) but not Gb3 inhibited hemagglutination of RBCs in a dose-dependent manner (Fig 3D). Likewise, hemagglutination was inhibited in the presence of a specific antibody against Gb4 (Fig 3E).

To verify that binding to Gb4 is exclusively due to a pH-mediated capsid rearrangement, the interaction was also tested with B19 virus-like particles (VLPs) consisting of VP2 (VP2-only particles). Recombinant baculoviruses that express VP2-only VLPs were prepared using the Bac-to-Bac system. The purity of the VP2 particles was verified by SDS-PAGE and

their integrity was examined by electron microscopy and by dot blot with an antibody against intact capsids (S6 Fig). Similar to the plasma-derived B19V, hemagglutination of erythrocytes by VLPs was also pH-dependent (Fig 3F). A minor shift in the pH required for hemagglutination between VLPs (6.4 full, 6.6 partial) and B19V (6.3 full, 6.4 partial) was observed. Since the accurate quantification of B19V by PCR is not possible for VLPs, this minor variation might be explained by differences in the number of particles applied. The pH-dependent binding of VLPs to erythrocytes was examined by Western blot with an antibody against VP2. The binding at the different pH values correlated well with the HA (Fig 3G). Similar to native B19V, hemagglutination by VLPs was inhibited in a dose-dependent manner by Gb4 but not by Gb3 (Fig 3H). Together, these results demonstrate that B19V does not bind to Gb4 expressed on cellular membranes, which are typically exposed to neutral pH conditions. The interaction occurs exclusively under acidic conditions and is mediated by the VP2 region of the capsid.

Different to the extracellular environment, the early endosomal compartment provides optimal conditions for Gb4 interaction

B19V binding to Gb4 expressed on human erythrocytes was tested at various pH conditions and quantified by qPCR. The results revealed a progressive increase in affinity at decreasing pH values, reaching a maximum at pH 6.0 (Fig 4A), which corresponds to the average pH measured in early endosomes [44,45]. At neutral pH, the binding affinity decreased more than 3 logs to background levels, confirming that B19V does not recognize Gb4 expressed on the plasma membrane.

Parvovirus capsid proteins are fine-tuned to rearrange in response to pH conditions, but also to other cellular cues encountered during entry. Besides the low pH, early endosomes are characterized by a depleted Ca^{2+} environment [46,47]. Divalent cations have been shown to play important roles in the capsid stability of parvoviruses and their depletion can trigger structural rearrangements and alter capsid integrity [48–50]. The influence of divalent cations in the interaction was examined at pH 6.3, which is close to the hemagglutination threshold and therefore more sensitive to affinity fluctuations between the virus and the GSL. Neither the sequestration of Ca^{2+} by EGTA or Mg^{2+} by EDTA nor their addition influenced the low pH-dependent hemagglutination activity of B19V. The HA was also undisturbed in a complex solution, such as cell culture media (MEM, minimal essential medium) (Fig 4B). Low pH-

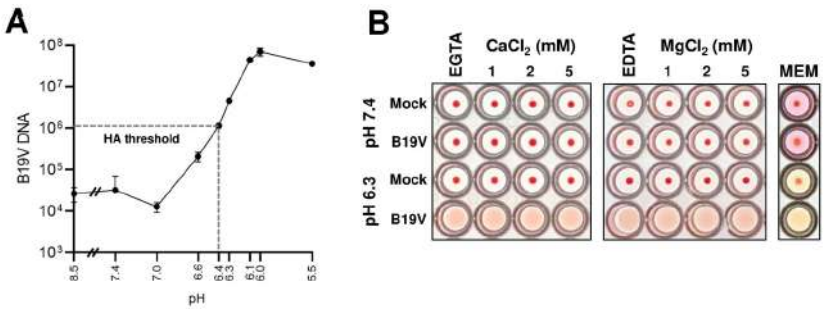

Fig 4. Determination of the optimal conditions required for B19V and Gb4 interaction. (A) Determination of the optimal pH for B19V binding to Gb4. RBCs (0.5% in 100 μl PiBS) were incubated with B19V ($5x10^9$) at pH values ranging from 8.5 to 5.5. After 1h, cells were washed in the corresponding buffer, and viral DNA was extracted and quantified by qPCR. (B) Hemagglutination at neutral (7.4) or acidic (6.3) pH was carried out in the presence of divalent cations (Ca^{2+} or Mg^{2+}), chelating agents (5 mM EGTA or EDTA) or in minimal essential medium (MEM). B19V was incubated with the different buffers for 1h before incubation with the erythrocytes. HA, hemagglutination assay.

https://doi.org/10.1371/journal.ppat.1009434.g004

mediated binding of B19V to Gb4 was also independent of the temperature (S7 Fig). These results indicate that contrary to the extracellular milieu, the conditions found in the early endosomal compartment are optimal for the interaction between incoming viruses and Gb4.

pH acts as a switch to regulate the affinity between B19V and Gb4

The interaction of viruses with cellular partners is highly dynamic and influenced by the different environmental conditions encountered during the process of entry, resulting in affinity fluctuations. These affinity changes are finely tuned to promote binding or dissociation with the target molecules. During entry, B19V is initially exposed to the acidic conditions of the endosomal compartment, followed by the neutral pH of the cytosol, where the dissociation from the GSL would facilitate the virus targeting to the nucleus. To investigate pH-dependent changes in binding affinity, the dissociation of B19V from Gb4 expressed on human erythrocytes was examined by adjusting the pH from 6.3 to 7.4. As shown in Fig 5A, more than 95% of the particles bound to Gb4 on erythrocyte membranes at pH 6.3 dissociated when the pH was restored to 7.4. Moreover, preincubation of viruses or RBCs separately at pH 6.3 did not allow hemagglutination at neutral pH (S8 Fig). Additionally, the reversibility of the interaction was tested by direct visualization of the hemagglutination reaction with VLPs. Under light microscopy, the erythrocytes appeared dispersed at pH 7.4 and formed large clusters at pH 6.3, conforming with the HA. The erythrocyte clusters were not detected when the acidic pH was neutralized (Fig 5B), indicating that binding of VLPs to Gb4 is also reversible.

Although the interaction is reversible, binding of B19V to Gb4 may trigger irreversible capsid conformational changes that prepare the virus for subsequent infection steps or even render the incoming capsids independent of Gb4. To test this hypothesis, viruses bound to Gb4 at low pH were released by exposure to neutral pH and used to infect WT and Gb4 KO cells. The previous interaction of the virus with Gb4 on the surface of RBCs at low pH changed neither their capacity to infect WT cells nor their inability to infect Gb4 KO cells (Fig 5C). These results together reveal that pH acts as a regulatory switch, modulating the affinity between the virus and the GSL.

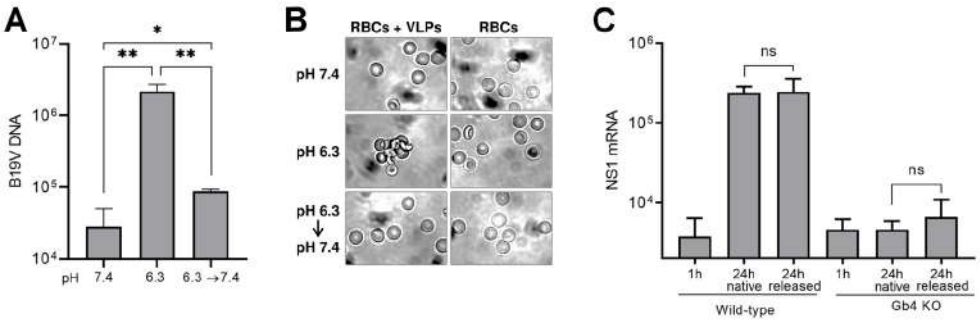

Fig 5. pH acts as an affinity switch to regulate binding and dissociation between B19V and Gb4. (A) B19V (510^9) was incubated with RBCs (0.5% in 100 μl PiBS) for 1h at pH 7.4 or 6.3. The cell suspensions were washed twice with a buffer of the same pH, except for one sample incubated at pH 6.3 and washed at pH 7.4. RBCs were incubated 30 additional minutes in the washing buffer at room temperature, washed twice, and viral DNA was extracted and quantified by qPCR. The results are presented as the mean ± SD of three independent experiments. *, $p<0.05$; **, $p<0.01$. (B) Visualization of the hemagglutination reaction by VLPs. RBCs were incubated with VLPs (510^9) at pH 7.4 or 6.3 for 1h at room temperature. Prior to visualization by phase contrast microscopy, the samples were diluted with a buffer of the same pH or neutralized to pH 7.4. (C) Infectivity of Gb4-dissociated virus. Viruses bound to RBCs at pH 6.3 and dissociated at pH 7.4 were quantified by qPCR. Equal amounts of native and Gb4-dissociated virus were added to UT7/Epo WT or Gb4 KO cells. After 1h or 24h, cells were washed four times and NS1 mRNA was extracted and quantified by RT-qPCR. The results are presented as the mean ± SD of three independent experiments. ns, not significant.

https://doi.org/10.1371/journal.ppat.1009434.g005

Low pH-mediated interaction of B19V with Gb4 initiates active membrane processes

Multivalent interactions of certain ligands, such as toxins, lectins and viruses with GSLs have been shown to change membrane properties resulting in membrane invaginations and vesicle formation [51–58]. The multimeric configuration of the B19V capsid and the small size of Gb4 would favor multivalent interactions with the GSL and the subsequent changes in membrane properties. To examine the capacity of B19V binding to Gb4 to initiate active membrane processes, we sought to induce the interaction of the virus with Gb4 expressed on UT7/Epo cells. Even though Gb4 is expressed abundantly on the plasma membrane of UT7/Epo cells, the neutral pH conditions at the cell surface prohibit the interaction. To force the binding to the GSL, WT and Gb4 KO cells were incubated with the virus at pH 6.3 for 1h at 37˚C. In WT cells, a 92-fold average increase in virus attachment was observed at acidic compared to neutral pH. In sharp contrast, the pH conditions had no significant effect on virus attachment in Gb4 KO cells, confirming that Gb4 is responsible for the pH-dependent binding enhancement in WT cells (Fig 6A). Virus attachment was also analyzed under VP1uR blocking conditions. To this end, WT and KO cells were either incubated with functional (ΔC126) or non-functional (ΔN29, lacking the RBD) recombinant VP1u (S1A Fig). Subsequently, the cells were incubated with B19V at 37˚C for 1h at pH 7.4 or 6.3. As expected, when VP1uR was not blocked, WT and KO cells exhibited a comparable virus binding at pH 7.4, whereas at pH 6.3 virus binding was substantially increased only in WT cells. Under VP1uR blocking conditions, virus attachment was inhibited, except for WT cells at pH 6.3, which represents viruses bound exclusively to Gb4 (Fig 6B).

We next analyzed the capacity of B19V bound to Gb4 to trigger membrane processes resulting in virus uptake. To this end, WT cells were preincubated with recombinant VP1u ΔC126 to block VP1uR. Subsequently, the virus was incubated with the cells at pH 6.3 for 1h at 4˚C to allow attachment to Gb4 or 37˚C to allow attachment and uptake. After the incubation, the cells were washed with PBS pH 7.4 to detach non-internalized capsids. While most of the viral particles were removed from cells incubated at 4˚C, cells incubated at 37˚C displayed a strong intracellular accumulation of capsids (Fig 6C).

To examine the capacity of the Gb4-mediated uptake to initiate the infection, viruses were incubated with cells under VP1uR-blocking conditions at pH 6.3 to allow binding to Gb4. Subsequently, NS1 mRNA was quantified after 24h by qPCR and the presence of progeny capsids was examined after 72h by immunofluorescence. Although there was a modest increase of NS1 mRNA mediated by Gb4 entry (Fig 6D), no capsid proteins were produced after three days (Fig 6E). Expectedly, Gb4-mediated uptake did not result in infection, since the interaction with extracellular Gb4 was induced under conditions that are not expected to occur during the natural infection. However, this experimental approach demonstrated that binding of B19V to Gb4 can stimulate active membrane processes similar to those observed with other ligands interacting with GSLs.

VLPs consisting of VP2, lack the entire VP1. Without the VP1u, these particles are unable to recognize the VP1uR and thus cannot be internalized into permissive cells [32,36]. These capsids are particularly useful because they allow the study of Gb4 interaction in a more specific way without the interference of the VP1uR.

The pH-dependent interaction of VLPs with WT and Gb4 KO UT7/Epo cells was examined by Western blot with an antibody against VP2. The results showed a low pH-dependent interaction with Gb4 exclusively in WT cells (Fig 7A). This result was corroborated by immunofluorescence microscopy with an antibody against intact capsids (Fig 7B).

We next tested the capacity of VLPs bound to Gb4 to internalize into UT7/Epo cells. Cells were incubated with VLPs at pH 6.3 at 4˚C or 37˚C. After 1h, the cells were washed, fixed and

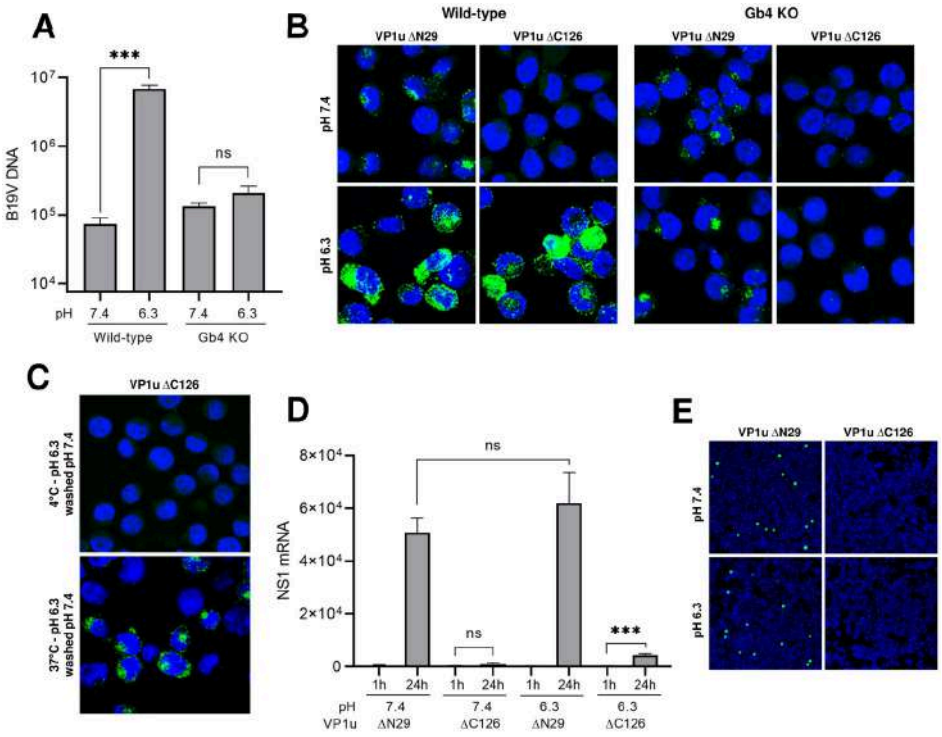

Fig 6. Low pH-mediated interaction of B19V with Gb4 initiates active membrane processes. (A) Quantification of B19V attachment to UT7/Epo WT and Gb4 KO cells at neutral and acidic pH. Cells were infected with B19V (10^4 geq/cell) at 37˚C for 1h followed by four washes. DNA was extracted and quantified by qPCR. The results are presented as the mean ± SD of three independent experiments. $^{***}p<0.001$; ns, not significant. (B) Detection of B19V capsids (860-55D) in UT7/Epo WT and Gb4 KO cells under neutral or acidic pH by IF. Cells were incubated for 30 min with functional (ΔC126) to block the VP1uR or non-functional (ΔN29) recombinant VP1u, as a control (S1 Fig) at 4˚C. Subsequently, B19V (510^4 geq/cell) was added for 1h at 37˚C. (C) Gb4-mediated uptake of native B19V. Cells were preincubated with functional VP1u ΔC126 for 1h at 4˚C prior to infection to block the VP1uR followed by incubation with B19V at 4˚C or 37˚C for 1h at pH 6.3. Non-internalized virus was removed by a washing step at neutral pH. Internalized viruses were detected by IF with antibody 860-55D against capsids. (D) Infectivity assay at neutral and acidic pH. WT cells were incubated for 30 min at 4˚C with functional recombinant VP1u (ΔC126) to block the VP1uR or non-functional (ΔN29), as a control. Subsequently, B19V (510^4 geq/cell) was added for 1h at 37˚C in a buffer with the indicated pH. Cells were washed after 1h or further incubated for 24h at 37˚C. NS1 mRNA was extracted and quantified by RT-qPCR. The results are presented as the mean ± SD of three independent experiments. ns, not significant. (E) Alternatively, 72h post-infection, capsid protein expression was examined by IF with antibody 3113-81C.

https://doi.org/10.1371/journal.ppat.1009434.g006

examined by confocal immunofluorescence microscopy. Pictures taken from the top and the middle sections revealed the presence of internalized capsids in cells incubated at 37˚C, but not at 4˚C (Fig 7C). Alternatively, following 1h incubation at 4˚C or 37˚C, cells were washed with PBS pH 7.4 to detach non-internalized capsids. While most of the viral particles were removed from cells incubated at 4˚C, cells incubated at 37˚C displayed a strong intracellular signal (Fig 7D). Collectively, these results confirm that the low pH-mediated interaction of B19V with Gb4 is mediated by the VP2 region and induces changes in membrane properties resulting in vesicle formation.

Erythrocytes do not play a significant role as viral decoy targets during B19V infection

B19V can establish high-titer viremia during the acute phase of the infection. Gb4 is the most abundant neutral GSL expressed on RBCs [29,30]. Since RBCs cannot be infected by viruses,

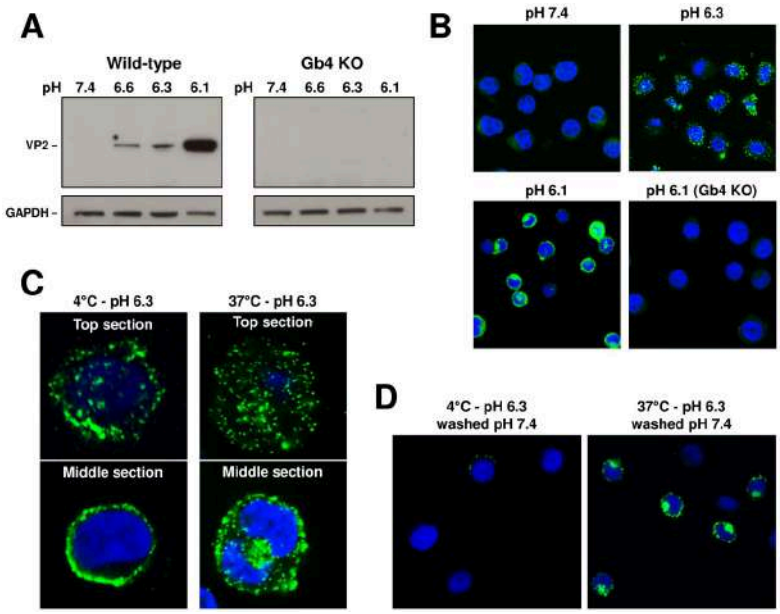

Fig 7. pH-mediated interaction of VP2-only particles with Gb4 triggers the uptake process independently of the VP1uR. (A) Detection of VLPs bound to WT and Gb4 KO UT7/Epo cells at different pH values by Western blot using antibody 3113-81C. VLPs (10^{10}) were incubated with cells ($3x10^5$) at the indicated pH values for 1h at 37˚C. GAPDH expression was used as a loading control. (B) Detection of VLPs (860-55D) in UT7/Epo WT and Gb4 KO cells under neutral or acidic pH by IF. (C) Gb4-mediated uptake of VLPs. Top and middle sections of cells incubated with VLPs at 4˚C or 37˚C for 1h at pH 6.3. (D) Gb4-mediated uptake of VLPs. Cells were incubated with VLPs at 4˚C or 37˚C for 1h at pH 6.3. Non-internalized virus was removed by a washing step at neutral pH. Internalized particles were detected by IF with antibody 860-55D against capsids.

https://doi.org/10.1371/journal.ppat.1009434.g007

binding of B19V to Gb4 expressed on erythrocytes would trap the virus and hinder the infection. The interaction of B19V with RBCs was tested in the natural environment of the blood. To this end, B19V was spiked into fresh blood samples (pH 7.4) without B19V-specific antibodies. After incubation for 1h, the erythrocytes were separated from the plasma by centrifugation and washed at neutral pH. As shown in Fig 8A, B19V was consistently found in the plasma fraction in three distinct blood samples. The absence of significant B19V binding to RBCs was further confirmed by immunofluorescence microscopy with an antibody against intact capsids. As expected, decreasing the pH to 6.3 triggered a substantial binding of the virus to RBCs (Fig 8B). Besides the neutral pH of the blood, an unknown component(s) of the plasma has been shown to inhibit the hemagglutination activity of B19V [24]. Consistent with this observation, the binding efficiency of B19V to RBCs increased approximately 10-fold when no blood plasma components were present (Fig 8C). Since the conditions for the interaction with Gb4 are largely suboptimal in the blood, we conclude that despite the abundant expression of Gb4, the erythrocytes do not play a significant role as viral decoy targets during B19V viremia.

Discussion

B19V has a marked tropism for erythroid progenitor cells (EPCs) in the bone marrow [17–19]. The narrow tropism of B19V is mediated by multiple factors highly restricted to the Epo-dependent erythroid differentiation stages [21,59–64]. A virus demanding such strict conditions for replication would also require a selective receptor exclusively expressed in the target cells. This strategy would allow the virus to avoid nonpermissive cells, which have the potential

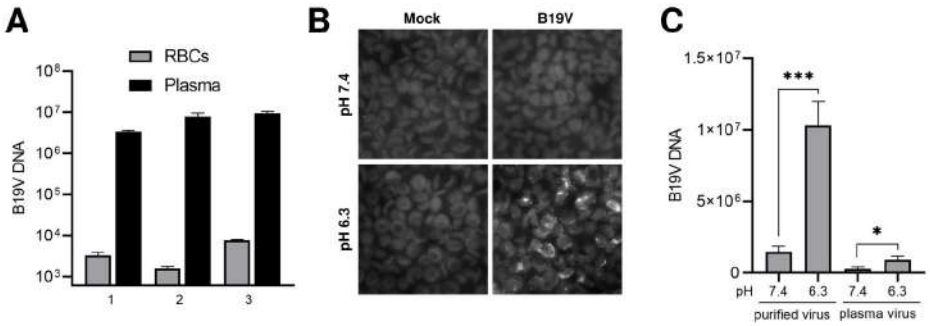

Fig 8. Erythrocytes do not play a significant role as viral decoy targets during B19V viremia. (A) Freshly collected blood samples (with EDTA as anticoagulant) and tested negative for antibodies against B19V, were spiked with B19V (10^9 virions) and incubated for 1h at 37˚C. The plasma and the RBC fractions were separated by centrifugation, the RBCs were washed with PBS (pH 7.4) and the viral DNA was extracted from both fractions and quantified by qPCR. (B) Detection of B19V in the RBC fraction by IF with an antibody against intact capsids (860-55D). (C) A component (s) in human plasma inhibits binding of B19V to RBCs. RBCs (0.5% in 100 μl PiBS) were incubated at pH 7.4 or 6.3 with B19V ($5x10^9$) directly from an infected plasma sample or after purification by iodixanol density gradient centrifugation. After 1h at room temperature, the erythrocytes were washed four times with the corresponding buffer and viral DNA was extracted and quantified. The results are presented as the mean ± SD of three independent experiments. *, $p<0.05$; ***, $p<0.001$.

https://doi.org/10.1371/journal.ppat.1009434.g008

to hamper the infection by diverting viruses away from target tissues. The neutral glycosphingolipid (GSL) globoside (Gb4) has been historically considered the primary cellular receptor of B19V [23,26]. However, Gb4 is not the receptor that would be expected for a virus with the remarkable restricted tropism of B19V. Gb4 is expressed in a multitude of cell types that are not permissive to the infection [27,28], and is the major neutral GSL of RBCs, which cannot support viral infections [29,30]. Accordingly, the interaction between the virus and the GSL either does not occur or requires strict conditions.

In an earlier study, we identified a functional RBD in the VP1u region of B19V, which mediates virus attachment and uptake in EPCs through interaction with a yet unidentified receptor, referred to as VP1uR [11,32]. In contrast to the ubiquitous expression of Gb4, VP1uR expression is restricted to EPCs, which are the only cells that B19V can productively infect [19,32]. In a follow-up study, we showed that B19V was able to attach and internalize cells expressing VP1uR but lacking Gb4. However, in the absence of Gb4, the internalized virus was unable to initiate the infection [37]. These findings together reveal that VP1uR is the cellular receptor of B19V responsible for the restricted virus uptake in permissive erythroid cells, whereas Gb4 is an essential factor required at a post-internalization step.

In this study, the mechanism of the interaction of B19V with Gb4 and the step of the infection where the GSL is required were investigated. We confirmed that the genetic removal of the gene encoding for Gb4 in UT7/Epo cells does not disturb the expression and function of the VP1uR, and consequently, the uptake of B19V is also not affected (Fig 1A–1C). However, Gb4 is required after virus internalization and before the delivery of the ssDNA into the nucleus for replication (Fig 1D and 1E). It has been previously shown that during the first hour following B19V uptake in UT7/Epo cells, the incoming capsids colocalize with endo-lysosomal markers, appearing as a dense perinuclear signal. Subsequently, the virus signal becomes more scattered and colocalization with endocytic markers decreases gradually [40]. As shown in Fig 2A, 30 min post-internalization in WT and Gb4 KO cells, the virus signal colocalizes intensively with endo-lysosomal markers. As expected, 3h pi in WT cells, capsid signal becomes more scattered and less co-localized with endo-lysosomal markers. In contrast, in cells lacking Gb4, the virus signal does not progress and remains associated with endosomal

markers, suggesting a role of Gb4 in the infectious endocytic trafficking of B19V. Furthermore, in Gb4 KO cells, B19V behaves like artificial MS2-VP1u capsids, which are unable to escape from endosomes (Fig 2B and S3 Fig).

The finding that pH acts as a switch to modulate the affinity between B19V and Gb4 has major implications in the virus tropism, infection and spread. Under neutral conditions, which are characteristic of the extracellular milieu, B19V does not interact with the ubiquitously expressed Gb4. This strategy prevents the redirection of the virus to nonpermissive tissues facilitating the selective targeting of the EPCs in the bone marrow. We and others observed a strong association of B19V to RBCs in viremic blood samples [35,65]. The blood sample used in our studies was acidic due to anaerobic glycolysis, a process that occurs naturally during blood storage [66]. In the study of Chehadeh et al., the RBCs were washed in acidic PBS and stored in Alsever's solution, which is an acidic solution (pH 6.1) routinely used as an anticoagulant and preservative. In other studies, when B19V was spiked into a fresh blood sample to mimic viremia, the virus was mostly associated with the plasma fraction and those found in the RBC fraction were easily removed by a washing step. [67]. This result was confirmed in our studies, where no significant binding to RBCs was observed when B19V was spiked into fresh blood samples with an experimentally verified neutral pH (Fig 8A and 8B). Besides a suboptimal pH for Gb4 binding, blood plasma contains an inhibitor(s) that interferes with hemagglutination (Fig 8C) [24]. Our results revealed that during B19V viremia, the fairly constant neutral pH of the blood and the presence of an inhibitor(s) hinder the stable binding of the virus to Gb4 on RBCs, which would otherwise divert the virus with an overwhelming amount of decoy targets and thereby hamper the infection.

The acidic pH conditions required for the interaction exclude the binding to Gb4 expressed on the plasma membrane, which is typically exposed to neutral pH conditions. However, Gb4 is also found in intracellular compartments. GSLs are continuously internalized from the cell surface by clathrin-dependent and independent mechanisms in invaginated vesicles. These vesicles fuse with early endosomes, resulting in the glycan component of the GSL facing the vesicle lumen [42,68]. From early endosomes, GSLs can be recycled back to the plasma membrane, transported to the Golgi apparatus or to late endosomes and finally lysosomes where they undergo terminal degradation by specific lysosomal enzymes [42,69–71]. Although B19V is internalized via clathrin-dependent endocytosis [40], and Gb4 is mostly internalized via clathrin-independent endocytosis [42], both reach the early endosomes. The acidic luminal pH in early endosomes around 6.0 and the depleted Ca^{2+} levels coincide with the optimal conditions required for the interaction with Gb4 (Fig 4). Accordingly, incoming B19V can potentially interact with Gb4 inside early endosomes as an essential step in the infectious trafficking. In line with this assumption, the absence of Gb4 resulted in endosomal retention of the incoming capsids (Fig 2).

Multivalent interactions of certain ligands, such as bacterial toxins, lectins and viruses, with GSLs trigger membrane curvature and invaginations that ultimately result in vesicle formation [51–58]. In our studies, the interaction under acidic conditions of B19V and VLPs with Gb4 in the exoplasmic membrane leaflet resulted in virus uptake (Figs 6C, 7C and 7D), suggesting that similar active membrane processes are induced by the multivalent binding of the capsid with Gb4 molecules. Further research will aim to characterize changes in membrane properties mediated by the interaction of the virus with GSL-enriched areas of the endosomal membrane and the influence of additional intracellular factors in the interplay between B19V and Gb4.

In summary, this study provides mechanistic insight into the interaction of B19V with Gb4 and its essential role as an intracellular interacting partner required for infectious trafficking. The finding that pH acts as an affinity switch to modulate the interaction between the virus and the GSL contributes to a better understanding of B19V restricted tropism, infection and

spread. In the future, studies will aim at elucidating the precise function of Gb4 in B19V endocytic trafficking, which will deepen our understanding of membrane dynamics induced by the interaction of viruses with GSLs and inspire novel strategies interfering with the early steps of the infection.

Materials and methods

Cells and viruses

The human megakaryoblastoid cells UT7/Epo were cultured in Eagle's minimal essential medium (MEM) containing 5% fetal calf serum (FCS) along with 2 U/ml recombinant erythropoietin (Epo). Whole blood samples from anonymous donors were washed three times with PBS. Packed red blood cells (RBCs) were resuspended in an equal volume of Alsever's solution (4.2 g/l NaCl, 8 g/l sodium citrate, 0.55 g/l citric acid, 20.5 g/l dextrose) and stored at 4˚C. ExpiSf9 cells for recombinant baculovirus production were cultured at 27˚C and 125 rpm in ExpiSf CD Medium (Thermo Fisher Scientific, Waltham, MA). B19V-infected plasma sample was obtained from a donation center (CSL Behring AG, Charlotte, NC) and virus concentration ($3x10^9$ geq/μl) was determined by qPCR. B19V was concentrated by ultracentrifugation through a 20% sucrose cushion and further purified by iodixanol density gradient ultracentrifugation, as previously described [50]. Plaque-purified MVM was obtained from ATCC (VR-1346).

Antibodies

The human monoclonal antibody 860-55D against intact capsids was purchased from Mikrogen (Neuried, Germany). The monoclonal mouse antibody 3113-81C (US Biological, Boston, MA) was used for the detection of viral proteins by Western blot as well as for the detection of progeny virus by immunofluorescence. A polyclonal chicken anti-Gb4 IgY antibody was a gift from J. Müthing (University of Münster). Antibodies against late endosomes (M6PR, ab2733), lysosomes (Lamp1, ab25630), cis-Golgi (GM130, ab52649) and GAPDH (ab9485) were obtained from abcam (Cambridge, UK). A rat anti-FLAG monoclonal antibody (200474) was purchased from Agilent (Santa Clara, CA). MS2 capsid proteins were detected with a polyclonal rabbit antibody (ABE76-I, Merck Millipore, France).

Generation of MS2-VP1u bioconjugate

Fluorescent MS2 VLPs bioconjugated to B19V VP1u were produced as previously described [19]. Briefly, MS2 coat protein or truncated VP1u (ΔC126/ΔN29) proteins were expressed in *E. coli* BL21(DE3) cells for 4h at 37˚C. Assembled MS2 capsids in cell lysate were purified by ultracentrifugation through a sucrose cushion. Recombinant VP1u was purified twice with nickel nitrilotriacetic acid (Ni-NTA) agarose. Chemical crosslinking between MS2 VLPs and truncated VP1u proteins was carried out in two steps. First, surface lysines on MS2 capsids were modified with fluorescent dyes (NHS-Atto488 or NHS-Atto633) and the heterobifunctional maleimide-PEG24-N-hydroxysuccinimide ester crosslinker (Thermo Fisher Scientific). Second, purified fluorescent maleimide-activated MS2 capsids were incubated with reduced VP1u proteins to achieve bioconjugation. After quenching of the reaction, MS2-VP1u constructs were pelleted by ultracentrifugation.

Production and purification of B19 virus-like particles

Recombinant B19 virus-like particles (VLPs) consisting of VP2 were produced using the ExpiSf Expression System Starter Kit (Thermo Fisher Scientific) following the manufacturer's

instructions. Briefly, the B19 VP2 gene was cloned into a pFastBac1 plasmid and used to create recombinant bacmids, which were transfected into ExpiSf9 cells to generate recombinant baculovirus. This virus was able to express VP2 particles by infection of ExpiSf9 cells at a multiplicity of infection of 5. Infected ExpiSf9 cells were lysed 72h pi and the assembled B19 VP2 particles were purified by ultracentrifugation through a sucrose cushion followed by a separation on a sucrose gradient. Positive fractions were identified by dot blot and exchanged into a storage buffer (20 mM Tris-HCl, [pH 7.8], 10 mM NaCl, 2 mM $MgCl_2$) using desalting columns. Quantification of VP2 particles was determined by absorbance at A280 with NanoDrop (NanoDrop2000, Thermo Fisher Scientific), as well as by comparison to a reference B19V sample on a dot blot.

Immunofluorescence

For surface staining, UT7/Epo cells were incubated at 4˚C with anti-Gb4 antibody or with anti-FLAG-tag labelled recombinant VP1u prior to fixation. UT7/Epo cells were fixed with a mixture of methanol and acetone (1:1) at -20˚C for 4 min. RBCs were fixed with 1% glutaraldehyde at room temperature for 10 min. Fixed cells were blocked with 10% goat-serum prior to staining with antibodies. Bound primary antibodies were detected with secondary antibodies with conjugated Alexa Fluor dyes and analyzed using confocal microscopy (LSM 880, Zeiss, Germany).

Virus binding and internalization

For each experiment, either UT7/Epo cells ($3x10^5$) or alternatively a 0.5% RBC suspension were prepared in 100 μl PiBS (20 mM piperazine-N,N′-bis[2-ethanesulfonic acid], 123 mM NaCl, 2.5 mM KCl) of varying pH or PBS. B19V was added to UT7/Epo cells (10^4 geq/cell for PCR analysis, $5x10^4$ geq/cell for immunofluorescence analysis) or to RBCs ($5x10^9$) and incubated at 4˚C or 37˚C for 1h. Cells were washed 4 times at room temperature. Subsequently, the samples were prepared for immunofluorescence analysis or qPCR. For qPCR, B19V DNA was isolated by the DNeasy Blood & Tissue Kit (Qiagen, Hilden, Germany) according to the manufacturer's protocol. The following primers were used, forward primer: 5'-GGGGCAGCATGT GTTAA-3'; reverse: 5'- AGTGTTCCAGTATATGGCATGG-3'.

Transfection

B19V DNA was isolated and quantified as described earlier. The viral DNA was transfected into UT7/Epo cells ($2x10^5$) seeded one day prior using lipofectamine 3000 reagent (Invitrogen) according to the manufacturer's instructions. B19V NS1 mRNA and viral capsid proteins were analyzed 2 days post infection using immunofluorescence as described above or RT-qPCR. Viral mRNA transcripts were isolated using the Dynabeads mRNA DIRECT Kit (Invitrogen) according to the proposed protocol. Identical primers as indicated above were employed.

NS1 mRNA and capsid protein expression

Infection of UT7/Epo cells was examined by quantification of viral NS1 mRNA and by immunofluorescence staining of viral proteins. Cells were washed four times 1h after virus binding and incubated in medium for up to three days. The cells were harvested and washed four times with PBS. For immunofluorescence analysis the cells were fixed as described above and stained with a monoclonal mouse antibody against the viral capsid proteins followed by staining with a goat anti-mouse IgG Alexa Fluor 488 (Invitrogen). Viral mRNA was extracted and analyzed as described for transfected cells.

Hemagglutination assay

RBCs were washed 3 times and brought to a concentration of 1% in PiBS. Glycosphingolipids (Gb3 [Globotriaosylceramide] and Gb4, Matreya LLC, PA) were dissolved in DMSO (5 mg/ml and 25 mg/ml respectively) and diluted to the desired concentration immediately before use. When applicable, B19V or VP2 particles ($5x10^9$) were incubated for 30 min in 50 μl of the indicated buffers along with Gb3/Gb4 prior to hemagglutination experiments. 50 μl 1% RBC solution were then added to each well and incubated for 1h at room temperature.

Western blot analysis of VP2 particles binding

A total of 10^{10} VP2 particles were added to either a 0.5% RBC solution or to $3x10^5$ UT7/Epo cells in 100 μl PiBS of varying pH. The cell suspension was incubated for 1h at 37 ˚C. The cells were subsequently washed three times and resuspended in 2x Laemmli buffer containing 0.1M dithiothreitol. Samples were boiled and resolved on a 10% SDS-PAGE and transferred to a PVDF membrane. The membrane was blocked overnight at 4˚C using 5% milk in TBS-T. Viral proteins were detected using the same mouse antibody described above followed by far-red fluorescent based detection using an 680RD goat anti-Mouse IgG secondary antibody (LI-COR Biosciences, Lincoln, NE) in the case of RBCs or with chemiluminescent detection using an HRP-conjugate for the UT7/Epo cells.

Cell cycle analysis

UT7/Epo cells ($1.5x10^5$) were seeded in 1 ml MEM in a 12-well plate and infected with B19V containing plasma (40'000 geq per cell) or mock infected. Cells were harvested 3 days post infection and washed with PBS containing 1% albumin (PBSA), resuspended in 300 μl PBSA and fixed by dropwise addition of 700 μl ethanol cooled to -20˚C. Tubes were carefully inverted five times stored at 4˚C for 1h. The cells were pelleted and washed twice with PBSA. Cells were incubated with 100 μg RNase A for 30 min at 37˚C and stained with 1 μg 4′,6-diamidino-2-phenylindole (DAPI). Cells were sorted on a Cytoflex flow cytometer (Beckman Coulter) and analyzed using FCS express 7 (De Novo Software).

Analysis

Data analysis was performed using GraphPad Prism *and* presented as the mean of three independent experiments ± standard deviation (SD). Differences in the binding of B19V to Gb4, NS1 mRNA synthesis, and cell cycle arrest at the G2/M-phase, were evaluated by Student's t-test. A P value less than 0.05 was considered statistically significant.

Supporting information

S1 Fig. B19V VP1u constructs and engineered MS2 particles. (A) Schematic depiction of the functional (ΔC126) and non-functional (ΔN29) recombinant VP1u constructs. (B) SDS-PAGE of purified recombinant VP1u constructs under reducing conditions. (C) Schematic depiction of an MS2 particle showing Atto fluorophores and VP1u constructs incorporated on the capsid surface. (D) Crosslinking between recombinant MS2 capsid proteins and VP1u constructs was verified by Western blot using an anti-MS2 antibody.
(TIF)

S2 Fig. B19V induces cell cycle arrest in WT but not in Gb4 KO UT7/Epo cells. Cells were fixed 3d pi and cellular DNA was stained with DAPI. Cell cycle progression was analyzed using flow cytometry. The results are presented as the mean ± SD of three independent

experiments. **, $p<0.01$; ns, not significant.
(TIF)

S3 Fig. Quantitative analysis of intracellular fluorescent foci per cell. Cells exhibiting perinuclear cluster of endosomes in focus (encircled by a dotted line) were selected for analysis. Distinct, clearly visible fluorescent spots (B19V capsids; green) not colocalizing with endocytic markers (red) were counted.
(TIF)

S4 Fig. Internalized MS2-VP1u particles remain sequestered inside the endosomes. UT7/Epo cells ($3x10^5$) were incubated with 2 μl Atto 488-labeled MS2-VP1u at 4˚C for 1h, washed and further incubated at 37˚C for 30 min and 3h. Cells were fixed and labeled with antibodies against late endosomes (M6PR) and lysosomes (Lamp1) and visualized under confocal microscopy.
(TIF)

S5 Fig. RBCs integrity is not compromised by exposure to mild acidic conditions. Scanning electron microscopy of RBCs exposed to pH 7.4 or 6.3 for 2h. RBCs were fixed with 1% glutaraldehyde, dehydrated by subsequent treatment with increasing concentrations of ethanol. Specimen were mounted and analyzed on a scanning electron microscope (Zeiss) with a 100'000-fold magnification. Bar, 10 μm.
(TIF)

S6 Fig. Purity and integrity of B19 VLPs. (A) Capsid protein purity of VLPs (VP2-only particles) was verified by SDS-PAGE. Capsid integrity was analyzed by electron microscopy (B), and by dot blot hybridization with an antibody against intact capsids (860-55D) (C). Bar; 100 μm.
(TIF)

S7 Fig. Effect of temperature on the low pH-mediated interaction of B19V with Gb4. RBCs (0.5% in 100 μl PiBS) were incubated with B19V ($5x10^9$) at pH 7.4 or 6.3 at different temperatures for 1h. The cells were subsequently washed at room temperature or at 4˚C and viral DNA was extracted and quantified by qPCR.
(TIF)

S8 Fig. Preincubation of viruses or RBCs separately at acid pH does not support hemagglutination at neutral pH. B19V ($5x10^9$) and RBCs (0.5% in 100 μl PiBS) were incubated separately at acidic pH for 1h. Subsequently, the HA was performed at neutral (7.4) of acidic (6.3) pH. HA, hemagglutination assay.
(TIF)

Acknowledgments

We are grateful to Beatrice Frey for the assistance with the transmission electron microscope.

Author Contributions

Conceptualization: Jan Bieri, Remo Leisi, Carlos Ros.

Data curation: Jan Bieri, Carlos Ros.

Formal analysis: Jan Bieri, Remo Leisi, Carlos Ros.

Funding acquisition: Carlos Ros.

Investigation: Jan Bieri, Carlos Ros.

Methodology: Jan Bieri, Remo Leisi, Cornelia Bircher, Carlos Ros.

Project administration: Carlos Ros.

Resources: Carlos Ros.

Supervision: Carlos Ros.

Writing – original draft: Jan Bieri, Carlos Ros.

Writing – review & editing: Jan Bieri, Remo Leisi, Cornelia Bircher, Carlos Ros.

References

1. Cossart YE, Cant B, Field AM, Widdows D. Parvovirus-Like Particles in Human Sera. Lancet. 1975; 305: 72–73. https://doi.org/10.1016/s0140-6736(75)91074-0 PMID: 46024
2. Qiu J, Söderlund-Venermo M, Young NS. Human Parvoviruses. Clin Microbiol Rev. 2017; 30: 43 LP–113. https://doi.org/10.1128/CMR.00040-16 PMID: 27806994
3. Servey JT, Reamy B V., Hodge J. Clinical presentations of parvovirus B19 infection. Am Fam Physician. 2007; 75. PMID: 17304869
4. Anderson MJ, Jones SE, Fisher-Hoch SP, Lewis E, Hall SM, Bartlett CLR, et al. Human parvovirus, the cause of erythema infectiosum (Fifth disease)? The Lancet. 1983. https://doi.org/10.1016/s0140-6736(83)92152-9 PMID: 6134148
5. Anderson MJ, Higgins PG, Davis LR, Willman JS, Jones SE, Kidd IM, et al. Experimental parvoviral infection in humans. J Infect Dis. 1985. https://doi.org/10.1093/infdis/152.2.257 PMID: 2993431
6. Bonvicini F, Bua G, Gallinella G. Parvovirus B19 infection in pregnancy—awareness and opportunities. Curr Opin Virol. 2017; 27: 8–14. https://doi.org/10.1016/j.coviro.2017.10.003 PMID: 29096233
7. Chorba T, Coccia P, Holman RC, Tattersall P, Anderson LJ, Sudman J, et al. The role of parvovirus b19 in aplastic crisis and erythema infectiosum (Fifth disease). J Infect Dis. 1986. https://doi.org/10.1093/infdis/154.3.383 PMID: 3016109
8. Saarinen UM, Chorba TL, Tattersall P. Human parvovirus B-19-induced epidemic acute red cell aplasia in patients with hereditary hemolytic anemia. Blood. 1986. https://doi.org/10.1182/blood.v67.5.1411.1411 PMID: 3008891
9. Cotmore SF, McKie VC, Anderson LJ, Astell CR, Tattersall P. Identification of the major structural and nonstructural proteins encoded by human parvovirus B19 and mapping of their genes by procaryotic expression of isolated genomic fragments. J Virol. 1986. https://doi.org/10.1128/JVI.60.2.548-557.1986 PMID: 3021988
10. Anderson S, Momoeda M, Kawase M, Kajigaya S, Young NS. Peptides derived from the unique region of B19 parvovirus minor capsid protein elicitneutralizing antibodies in rabbits. Virology. 1995. https://doi.org/10.1016/s0042-6822(95)80079-4 PMID: 7530397
11. Leisi R, Di Tommaso C, Kempf C, Ros C. The receptor-binding domain in the VP1u region of parvovirus B19. Viruses. 2016. https://doi.org/10.3390/v8030061 PMID: 26927158
12. Zádori Z, Szelei J, Lacoste MC, Li Y, Gariépy S, Raymond P, et al. A Viral Phospholipase A2 Is Required for Parvovirus Infectivity. Dev Cell. 2001; 1: 291–302. https://doi.org/10.1016/s1534-5807(01)00031-4 PMID: 11702787
13. Dorsch S, Liebisch G, Kaufmann B, von Landenberg P, Hoffmann JH, Drobnik W, et al. The VP1 Unique Region of Parvovirus B19 and Its Constituent Phospholipase A2-Like Activity. J Virol. 2002; 76: 2014–2018. https://doi.org/10.1128/jvi.76.4.2014-2018.2002 PMID: 11799199
14. Canaan S, Zádori Z, Ghomashchi F, Bollinger J, Sadilek M, Moreau ME, et al. Interfacial Enzymology of Parvovirus Phospholipases A2. J Biol Chem. 2004; 279: 14502–14508. https://doi.org/10.1074/jbc.M312630200 PMID: 14726513
15. Deng X, Dong Y, Yi Q, Huang Y, Zhao D, Yang Y, et al. The Determinants for the Enzyme Activity of Human Parvovirus B19 Phospholipase A2 (PLA2) and Its Influence on Cultured Cells. PLoS One. 2013; 8. https://doi.org/10.1371/journal.pone.0061440 PMID: 23596524
16. Farr GA, Zhang LG, Tattersall P. Parvoviral virions deploy a capsid-tethered lipolytic enzyme to breach the endosomal membrane during cell entry. Proc Natl Acad Sci U S A. 2005; 102: 17148–17153. https://doi.org/10.1073/pnas.0508477102 PMID: 16284249

17. Ozawa K, Kurtzman G, Young N, Shimizu A, Honjo T. Replication of the B19 Parvovirus in Human Bone Marrow Cell Cultures. Science. 2016; 233: 883–886. https://doi.org/10.1126/science.3738514 PMID: 3738514

18. Takahashi T, Ozawa K, Takahashi K, Asano S, Takaku F. Susceptibility of human erythropoietic cells to B19 parvovirus in vitro increases with differentiation. Blood. 1990; 75: 603–10. https://doi.org/10.1182/blood.V75.3.603.603 PMID: 2404522

19. Leisi R, Von Nordheim M, Ros C, Kempf C. The VP1u receptor restricts parvovirus B19 uptake to permissive erythroid cells. Viruses. 2016. https://doi.org/10.3390/v8100265 PMID: 27690083

20. Wong S, Zhi N, Filippone C, Keyvanfar K, Kajigaya S, Brown KE, et al. Ex Vivo-Generated CD36+ Erythroid Progenitors Are Highly Permissive to Human Parvovirus B19 Replication. J Virol. 2008; 82: 2470–2476. https://doi.org/10.1128/JVI.02247-07 PMID: 18160440

21. Chen AY, Guan W, Lou S, Liu Z, Kleiboeker S, Qiu J. Role of Erythropoietin Receptor Signaling in Parvovirus B19 Replication in Human Erythroid Progenitor Cells. J Virol. 2010; 84: 12385–12396. https://doi.org/10.1128/JVI.01229-10 PMID: 20861249

22. Bua G, Manaresi E, Bonvicini F, Gallinella G. Parvovirus B19 Replication and Expression in Differentiating Erythroid Progenitor Cells. PLoS One. 2016; 11: 1–19. https://doi.org/10.1371/journal.pone.0148547 PMID: 26845771

23. Brown KE, Anderson SM, Young NS. Erythrocyte P antigen: Cellular receptor for B19 parvovirus. Science (80-). 1993. https://doi.org/10.1126/science.8211117 PMID: 8211117

24. Brown KE, Cohen BJ. Haemagglutination by parvovirus B19. J Gen Virol. 1992. https://doi.org/10.1099/0022-1317-73-8-2147 PMID: 1645153

25. Kaufmann B, Baxa U, Chipman PR, Rossmann MG, Modrow S, Seckler R. Parvovirus B19 does not bind to membrane-associated globoside in vitro. Virology. 2005. https://doi.org/10.1016/j.virol.2004.11.037 PMID: 15661151

26. Brown KE, Hibbs JR, Gallinella G, Anderson SM, Lehman ED, Mccarthy P, et al. Resistance to parvovirus B19 infection due to lack of virus receptor (erythrocyte P antigen). N Engl J Med. 1994. https://doi.org/10.1056/NEJM199404283301704 PMID: 8139629

27. Bailly P, Bouhours JF. P blood group and related antigens. Cartron J.P., Rouger P. (Eds.), Molecular Basis of Major Human Blood Group Antigens, Plenum Press, New York (1995), pp. 299–329.

28. Cooling LLW, Koerner TAW, Naides SJ. Multiple glycosphingolipids determine the tissuetropism of parvovirus b19. J Infect Dis. 1995; 172: 1198–1205. https://doi.org/10.1093/infdis/172.5.1198 PMID: 7594654

29. Naiki M, Marcus DM. Human erythrocyte P and Pk blood group antigens: Identification as glycosphingolipids. Biochem Biophys Res Commun. 1974; 60: 1105–1111. https://doi.org/10.1016/0006-291x(74)90426-4 PMID: 4429565

30. Fletcher KS, Bremer EG, Schwarting GA. P blood group regulation of glycosphingolipid levels in human erythrocytes. J Biol Chem. 1979; 254: 11196–11198. PMID: 500637

31. Weigel-Kelley KA, Yoder MC, Srivastava A. Recombinant Human Parvovirus B19 Vectors: Erythrocyte P Antigen Is Necessary but Not Sufficient for Successful Transduction of Human Hematopoietic Cells. J Virol. 2001. https://doi.org/10.1128/jvi.75.9.4110-4116.2001

32. Leisi R, Ruprecht N, Kempf C, Ros C. Parvovirus B19 Uptake Is a Highly Selective Process Controlled by VP1u, a Novel Determinant of Viral Tropism. J Virol. 2013. https://doi.org/10.1128/JVI.02548-13 PMID: 24067971

33. Leisi R, Von Nordheim M, Kempf C, Ros C. Specific targeting of proerythroblasts and erythroleukemic cells by the VP1u region of parvovirus B19. Bioconjug Chem. 2015; 26: 1923–1930. https://doi.org/10.1021/acs.bioconjchem.5b00321 PMID: 26240997

34. Ros C, Gerber M, Kempf C. Conformational changes in the VP1-unique region of native human parvovirus B19 lead to exposure of internal sequences that play a role in virus neutralization and infectivity. J Virol. 2006; 80. https://doi.org/10.1128/JVI.01435-06 PMID: 17020940

35. Bönsch C, Kempf C, Ros C. Interaction of Parvovirus B19 with Human Erythrocytes Alters Virus Structure and Cell Membrane Integrity. J Virol. 2008; 82: 11784–11791. https://doi.org/10.1128/JVI.01399-08 PMID: 18815302

36. Bönsch C, Zuercher C, Lieby P, Kempf C, Ros C. The Globoside Receptor Triggers Structural Changes in the B19 Virus Capsid That Facilitate Virus Internalization. J Virol. 2010; 84: 11737–11746. https://doi.org/10.1128/JVI.01143-10 PMID: 20826697

37. Bieri J, Ros C. Globoside Is Dispensable for Parvovirus B19 Entry but Essential at a Postentry Step for Productive Infection. J Virol. 2019. https://doi.org/10.1128/jvi.00972-19 PMID: 31341051

38. Nasir W, Nilsson J, Olofsson S, Bally M, Rydell GE. Parvovirus B19 VLP recognizes globoside in supported lipid bilayers. Virology. 2014. https://doi.org/10.1016/j.virol.2014.04.004 PMID: 24889255

39. Chipman PR, Agbandje-Mckenna M, Kajigaya S, Brown KE, Young NS, Baker TS, et al. Cryo-electron microscopy studies of empty capsids of human parvovirus B19 complexed with its cellular receptor. Proc Natl Acad Sci U S A. 1996; 93: 7502–7506. https://doi.org/10.1073/pnas.93.15.7502 PMID: 8755503

40. Quattrocchi S, Ruprecht N, Bonsch C, Bieli S, Zurcher C, Boller K, et al. Characterization of the Early Steps of Human Parvovirus B19 Infection. J Virol. 2012; 86: 9274–9284. https://doi.org/10.1128/JVI.01004-12 PMID: 22718826

41. Stahnke S, Lux K, Uhrig S, Kreppel F, Hösel M, Coutelle O, et al. Intrinsic phospholipase A2 activity of adeno-associated virus is involved in endosomal escape of incoming particles. Virology. 2011; 409: 77–83. https://doi.org/10.1016/j.virol.2010.09.025 PMID: 20974479

42. Puri V, Watanabe R, Singh RD, Dominguez M, Brown JC, Wheatley CL, et al. Clathrin-dependent and -independent internalization of plasma membrane sphingolipids initiates two Golgi targeting pathways. J Cell Biol. 2001; 154: 535–547. https://doi.org/10.1083/jcb.200102084 PMID: 11481344

43. Hilfenhaus S, Cohen BJ, Bates C, Kajigaya S, Young NS, Zambon M, et al. Antibody capture haemadherence tests for parvovirus B19-specific IgM and IgG. J Virol Methods. 1993; 45: 27–37. https://doi.org/10.1016/0166-0934(93)90137-g PMID: 8270653

44. Modi S, Swetha MG, Goswami D, Gupta GD, Mayor S, Krishnan Y. A DNA nanomachine that maps spatial and temporal pH changes inside living cells. Nat Nanotechnol. 2009; 4: 325–330. https://doi.org/10.1038/nnano.2009.83 PMID: 19421220

45. Padilla-Parra S, Matos PM, Kondo N, Marin M, Santos NC, Melikyan GB. Quantitative imaging of endosome acidification and single retrovirus fusion with distinct pools of early endosomes. Proc Natl Acad Sci U S A. 2012; 109: 17627–17632. https://doi.org/10.1073/pnas.1211714109 PMID: 23047692

46. Albrecht T, Zhao Y, Nguyen TH, Campbell RE, Johnson JD. Fluorescent biosensors illuminate calcium levels within defined beta-cell endosome subpopulations. Cell Calcium. 2015; 57: 263–274. https://doi.org/10.1016/j.ceca.2015.01.008 PMID: 25682167

47. Scott CC, Gruenberg J. Ion flux and the function of endosomes and lysosomes: PH is just the start: The flux of ions across endosomal membranes influences endosome function not only through regulation of the luminal pH. BioEssays. 2011; 33: 103–110. https://doi.org/10.1002/bies.201000108 PMID: 21140470

48. Simpson AA, Chipman PR, Baker TS, Tijssen P, Rossmann MG. The structure of an insect parvovirus (Galleria mellonella densovirus) at 3.7 Å resolution. Structure. 1998; 6: 1355–1367. https://doi.org/10.1016/s0969-2126(98)00136-1

49. Cotmore SF, Hafenstein S, Tattersall P. Depletion of Virion-Associated Divalent Cations Induces Parvovirus Minute Virus of Mice To Eject Its Genome in a 3′-to-5′ Direction from an Otherwise Intact Viral Particle. J Virol. 2010; 84: 1945–1956. https://doi.org/10.1128/JVI.01563-09 PMID: 19955311

50. Caliaro O, Marti A, Ruprecht N, Leisi R, Subramanian S, Hafenstein S, et al. Parvovirus B19 uncoating occurs in the cytoplasm without capsid disassembly and it is facilitated by depletion of capsid-associated divalent cations. Viruses. 2019; 11. https://doi.org/10.3390/v11050430 PMID: 31083301

51. Römer W, Berland L, Chambon V, Gaus K, Windschiegl B, Tenza D, et al. Shiga toxin induces tubular membrane invaginations for its uptake into cells. Nature. 2007; 450: 670–675. https://doi.org/10.1038/nature05996 PMID: 18046403

52. Ewers H, Römer W, Smith AE, Bacia K, Dmitrieff S, Chai W, et al. GM1 structure determines SV40-induced membrane invagination and infection. Nat Cell Biol. 2010; 12: 11–18. https://doi.org/10.1038/ncb1999 PMID: 20023649

53. Rydell GE, Svensson L, Larson G, Johannes L, Römer W. Human GII.4 norovirus VLP induces membrane invaginations on giant unilamellar vesicles containing secretor gene dependent α1,2-fucosylated glycosphingolipids. Biochim Biophys Acta—Biomembr. 2013; 1828: 1840–1845. https://doi.org/10.1016/j.bbamem.2013.03.016 PMID: 23528203

54. Lakshminarayan R, Wunder C, Becken U, Howes MT, Benzing C, Arumugam S, et al. Galectin-3 drives glycosphingolipid-dependent biogenesis of clathrin-independent carriers. Nat Cell Biol. 2014; 16: 592–603. https://doi.org/10.1038/ncb2970 PMID: 24837829

55. Pezeshkian W, Hansen AG, Johannes L, Khandelia H, Shillcock JC, Kumar PBS, et al. Membrane invagination induced by Shiga toxin B-subunit: From molecular structure to tube formation. Soft Matter. 2016; 12: 5164–5171. https://doi.org/10.1039/c6sm00464d PMID: 27070906

56. Kociurzynski R, Beck SD, Bouhon JB, Römer W, Knecht V. Binding of SV40's Viral Capsid Protein VP1 to Its Glycosphingolipid Receptor GM1 Induces Negative Membrane Curvature: A Molecular Dynamics Study. Langmuir. 2019; 35: 3534–3544. https://doi.org/10.1021/acs.langmuir.8b03765 PMID: 30802059

57. Watkins EB, Majewski J, Chi EY, Gao H, Florent JC, Johannes L. Shiga Toxin Induces Lipid Compression: A Mechanism for Generating Membrane Curvature. Nano Lett. 2019; 19: 7365–7369. https://doi.org/10.1021/acs.nanolett.9b03001 PMID: 31538793

58. Kabbani AM, Raghunathan K, Lencer WI, Kenworthy AK, Kelly CV. Structured clustering of the glycosphingolipid GM1 is required for membrane curvature induced by cholera toxin. Proc Natl Acad Sci U S A. 2020; 117: 14978–14986. https://doi.org/10.1073/pnas.2001119117 PMID: 32554490

59. Pallier C, Greco A, Le Junter J, Saib A, Vassias I, Morinet F. The 3' untranslated region of the B19 parvovirus capsid protein mRNAs inhibits its own mRNA translation in nonpermissive cells. J Virol. 1997; 71: 9482–9489. https://doi.org/10.1128/JVI.71.12.9482-9489.1997

60. Brunstein J, Soderlund-Venermo M, Hedman K. Identification of a novel RNA splicing pattern as a basis of restricted cell tropism of erythrovirus B19. Virology. 2000; 274: 284–291. https://doi.org/10.1006/viro.2000.0460 PMID: 10964772

61. Gallinella G, Manaresi E, Zuffi E, Venturoli S, Bonsi L, Bagnara GP, et al. Different patterns of restriction to B19 parvovirus replication in human blast cell lines. Virology. 2000; 278: 361–367. https://doi.org/10.1006/viro.2000.0673 PMID: 11118359

62. Guan W, Cheng F, Yoto Y, Kleiboeker S, Wong S, Zhi N, et al. Block to the Production of Full-Length B19 Virus Transcripts by Internal Polyadenylation Is Overcome by Replication of the Viral Genome. J Virol. 2008; 82: 9951–9963. https://doi.org/10.1128/JVI.01162-08 PMID: 18684834

63. Chen AY, Kleiboeker S, Qiu J. Productive parvovirus B19 infection of primary human erythroid progenitor cells at hypoxia is regulated by STAT5A and MEK signaling but not HIFα. PLoS Pathog. 2011; 7. https://doi.org/10.1371/journal.ppat.1002088 PMID: 21698228

64. Wolfisberg R, Ruprecht N, Kempf C, Ros C. Impaired genome encapsidation restricts the in vitro propagation of human parvovirus B19. J Virol Methods. 2013; 193: 215–225. https://doi.org/10.1016/j.jviromet.2013.06.003 PMID: 23764418

65. Chehadeh W, Halim MA, Al-Nakib W. Antibody-mediated opsonization of red blood cells in parvovirus B19 infection. Virology. 2009; 390: 56–63. https://doi.org/10.1016/j.virol.2009.04.016 PMID: 19450862

66. Verma M, Dahiya K. Effect of Blood Storage on Complete Biochemistry. J Blood Disord Transfus. 2015; 06: 8–11. https://doi.org/10.4172/2155-9864.1000329

67. Lee T, Kleinman SH, Wen L, Montalvo L, Todd DS, Wright J, et al. Persistence of Virus in Blood Donors. 2013; 51: 1896–1908. https://doi.org/10.1111/j.1537-2995.2010.03035.x Distribution PMID: 21303368

68. Van Meer G, Voelker DR, Feigenson GW. Membrane lipids: Where they are and how they behave. Nat Rev Mol Cell Biol. 2008; 9: 112–124. https://doi.org/10.1038/nrm2330 PMID: 18216768

69. Sharma DK, Choudhury A, Singh RD, Wheatley CL, Marks DL, Pagano RE. Glycosphingolipids internalized via caveolar-related endocytosis rapidly merge with the clathrin pathway in early endosomes and form microdomains for recycling. J Biol Chem. 2003; 278: 7564–7572. https://doi.org/10.1074/jbc.M210457200 PMID: 12482757

70. Schulze H, Sandhoff K. Lysosomal lipid storage diseases. Cold Spring Harb Perspect Biol. 2011; 3: 1–19. https://doi.org/10.1101/cshperspect.a004804 PMID: 21502308

71. D'Angelo G, Capasso S, Sticco L, Russo D. Glycosphingolipids: Synthesis and functions. FEBS J. 2013; 280: 6338–6353. https://doi.org/10.1111/febs.12559 PMID: 24165035

Fig. S1

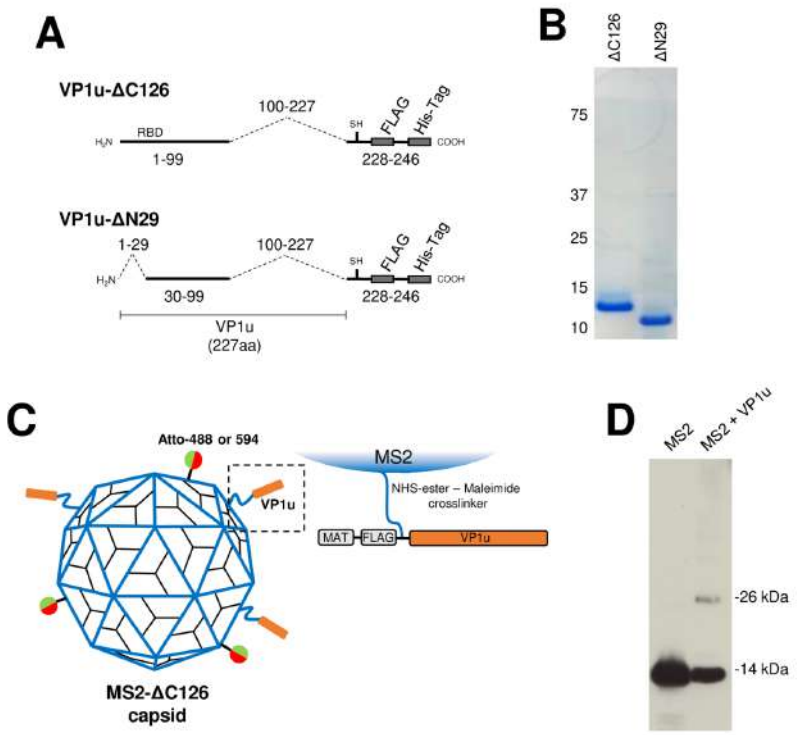

S1 Fig. B19V VP1u constructs and engineered MS2 particles. (A) Schematic depiction of the functional (ΔC126) and non-functional (ΔN29) recombinant VP1u constructs. (B) SDS-PAGE of purified recombinant VP1u constructs under reducing conditions. (C) Schematic depiction of an MS2 particle showing Atto fluorophores and VP1u constructs incorporated on the capsid surface. (D) Crosslinking between recombinant MS2 capsid proteins and VP1u constructs was verified by Western blot using an anti-MS2 antibody.

Fig. S2

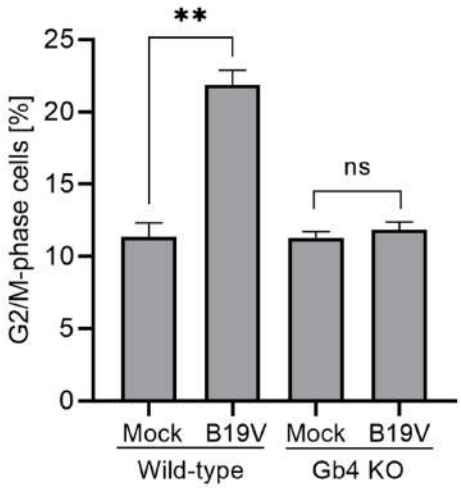

S2 Fig. B19V induces cell cycle arrest in WT but not in Gb4 KO UT7/Epo cells.
Cells were fixed 3d pi and cellular DNA was stained with DAPI. Cell cycle progression was analyzed using flow cytometry. The results are presented as the mean ± SD of three independent experiments. **, $p<0.01$; ns, not significant.

Fig. S3

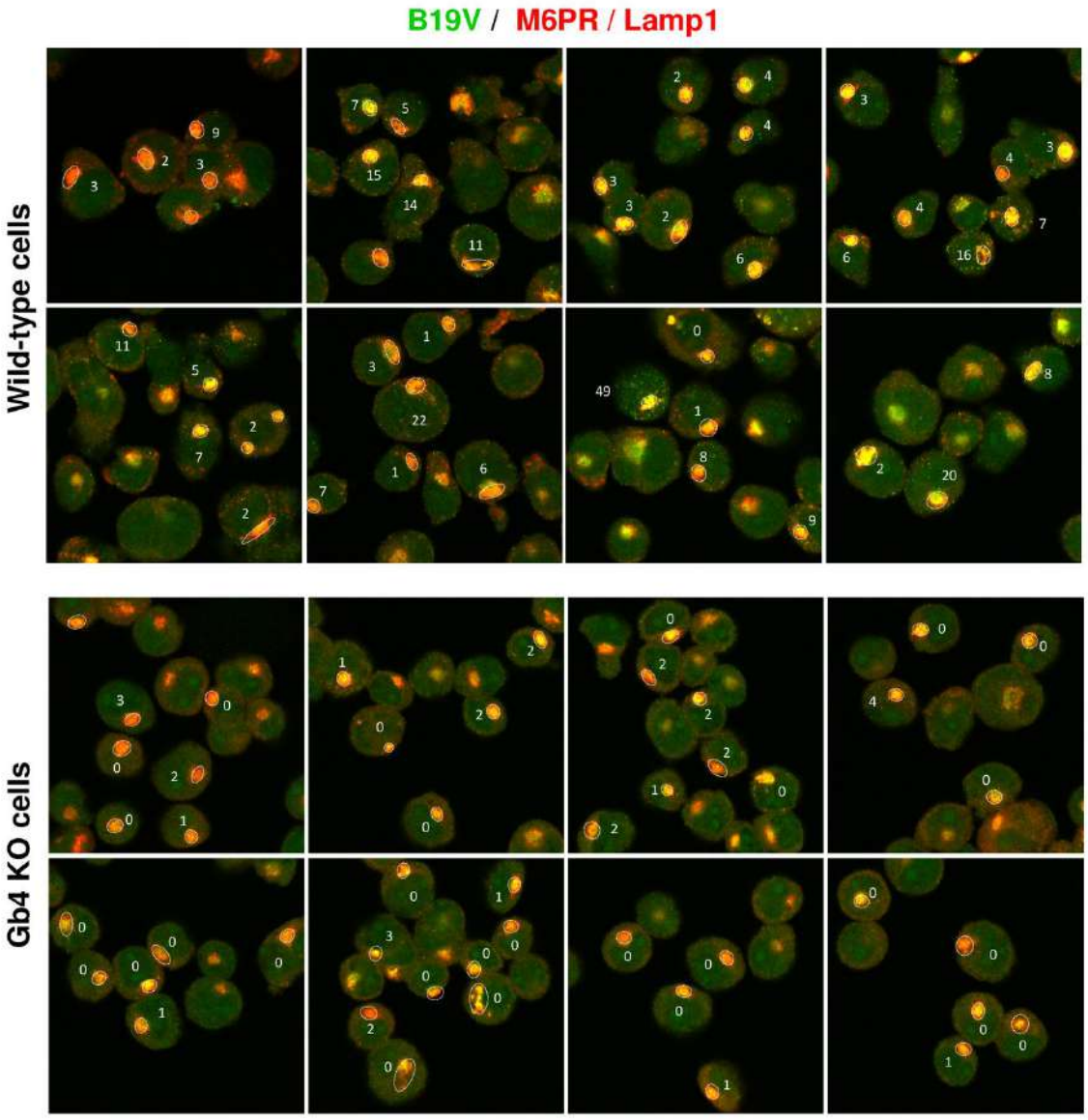

S3 Fig. Quantitative analysis of intracellular fluorescent foci per cell.

Cells exhibiting perinuclear cluster of endosomes in focus (encircled by a dotted line) were selected for analysis. Distinct, clearly visible fluorescent spots (B19V capsids; green) not colocalizing with endocytic markers (red) were counted.

Fig. S4

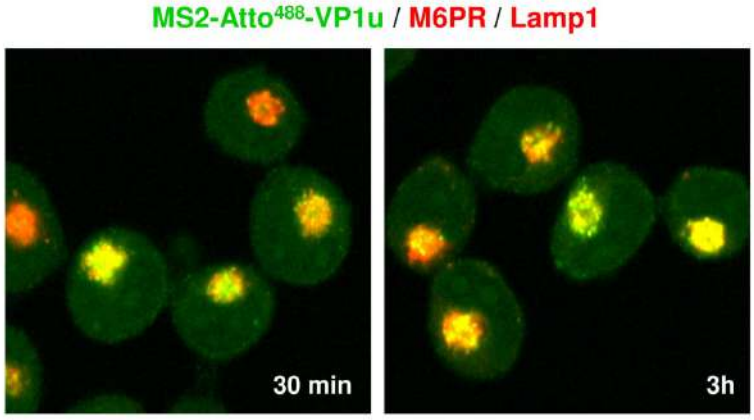

S4 Fig. Internalized MS2-VP1u particles remain sequestered inside the endosomes.
UT7/Epo cells ($3x10^5$) were incubated with 2 µl Atto 488-labeled MS2-VP1u at 4°C for 1h, washed and further incubated at 37°C for 30 min and 3h. Cells were fixed and labeled with antibodies against late endosomes (M6PR) and lysosomes (Lamp1) and visualized under confocal microscopy.

Fig. S5

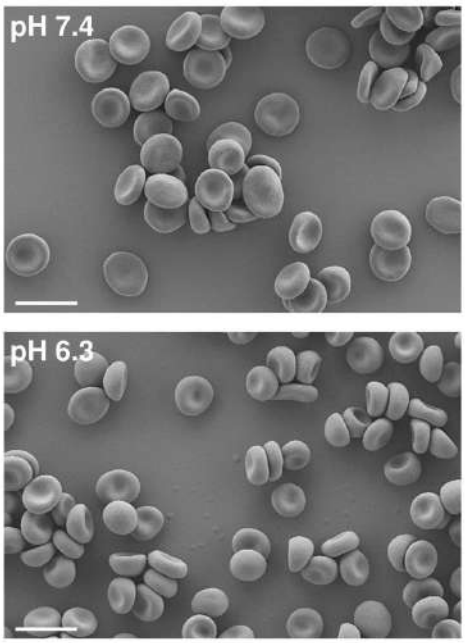

S5 Fig. RBCs integrity is not compromised by exposure to mild acidic conditions.
Scanning electron microscopy of RBCs exposed to pH 7.4 or 6.3 for 2h. RBCs were fixed with 1% glutaraldehyde, dehydrated by subsequent treatment with increasing concentrations of ethanol. Specimen were mounted and analyzed on a scanning electron microscope (Zeiss) with a 100'000-fold magnification. Bar, 10 µm.

Fig. S6

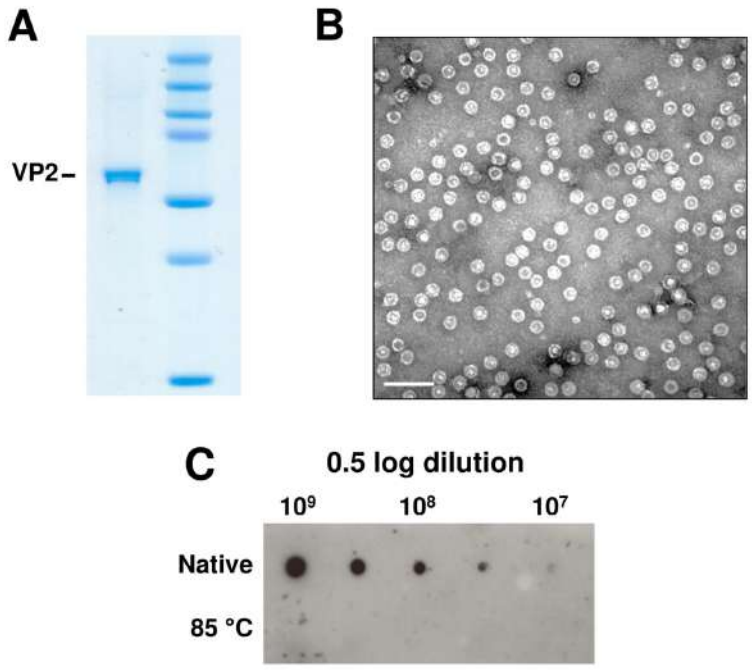

S6 Fig. Purity and integrity of B19 VLPs.
(A) Capsid protein purity of VLPs (VP2-only particles) was verified by SDS-PAGE. Capsid integrity was analyzed by electron microscopy (B), and by dot blot hybridization with an antibody against intact capsids (860-55D) (C). Bar; 100 µm.

Fig. S7

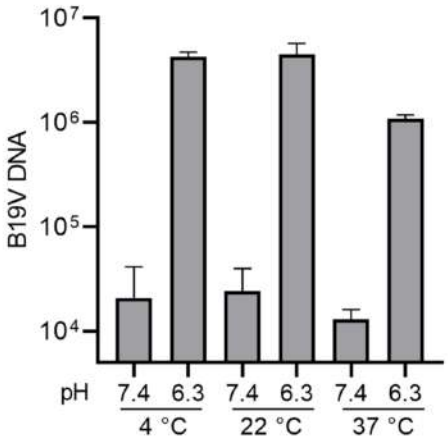

S7 Fig. Effect of temperature on the low pH-mediated interaction of B19V with Gb4.
RBCs (0.5% in 100 µl PiBS) were incubated with B19V ($5x10^9$) at pH 7.4 or 6.3 at different temperatures for 1h. The cells were subsequently washed at room temperature or at 4°C and viral DNA was extracted and quantified by qPCR.

Fig. S8

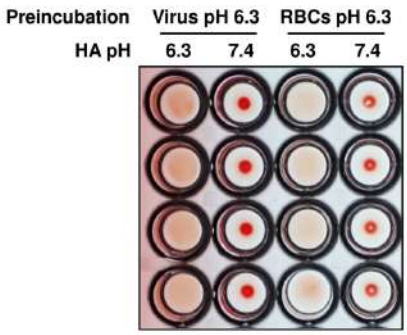

S8 Fig. Preincubation of viruses or RBCs separately at acid pH does not support hemagglutination at neutral pH.
B19V ($5x10^9$) and RBCs (0.5% in 100 µl PiBS) were incubated separately at acidic pH for 1h. Subsequently, the HA was performed at neutral (7.4) of acidic (6.3) pH. HA, hemagglutination assay.

2.1 Additional results: Attempting the identi cation of VP1uR

2.1.1 Introduction

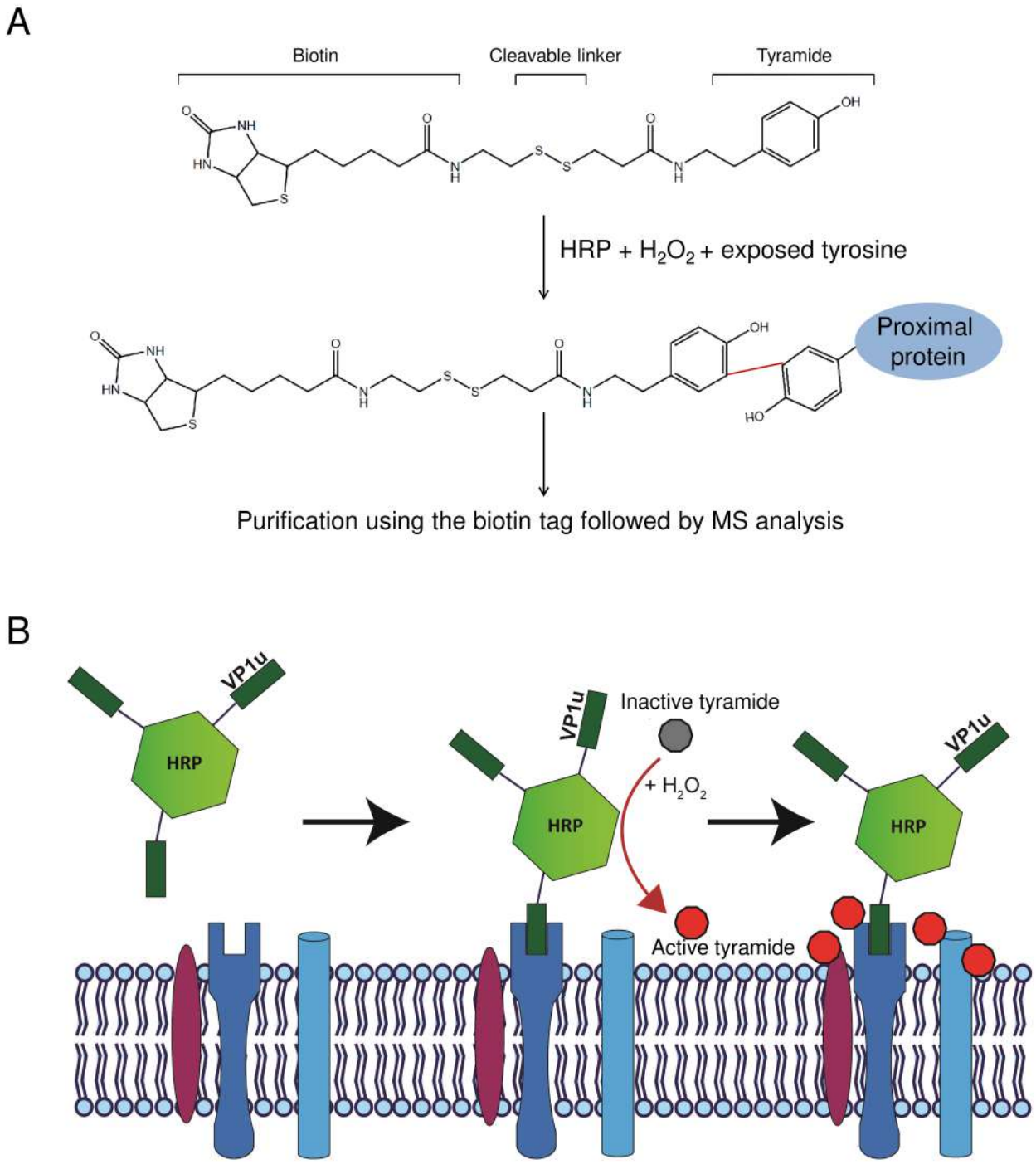

Figure 12: Overview of the strategy employed to identify the VP1uR. (A) HRP attaches Tyramide-SS-Biotin covalently to tyrosine residues of proteins that are in spatial proximity to the enzyme. The biotin tag permits purification of marked proteins with the help of neutravidin beads. The disulfide bond allows elution from the beads with the help of a reducing agent without the need to break the biotin-neutravidin bond. (B) Scheme of the experimental approach. The interaction of VP1u-HRP with the VP1uR on target cells allows labeling of proteins in the proximity of HRP with the Tyramide-SS-Biotin.

The RBD in the VP1u interacts with an as yet unknown receptor molecule (VP1uR) expressed exclusively on permissive EPCs to facilitate virus uptake [70]. Identification of VP1uR would yield many benefits both for B19V research specifically but also for other related applications. Concerning the virus, knowledge of the receptor would allow a deeper understanding of B19V tropism and pathogenesis and pave the way for the development of antiviral drugs and vaccines. Moreover, considering the erythroid-specific expression profile of the VP1uR [224], its identification would facilitate the development of a specific biomarker for Epo-dependent erythroid differentiation stages. As an example, the presence of immature nucleated RBCs in the bloodstream is an indicator of various health disorders such as leukemia and cancer [225][226]. Currently, many biomarkers are employed simultaneously in order to identify hematopoietic cells. Using the VP1uR as a marker can simplify the technique, making it faster, cheaper and more sensitive [227]. Another useful application of the VP1uR is the specific delivery of drugs to erythroid cells. With recombinant VP1u as a guide, a payload can be delivered specifically to erythroid progenitors in the bone marrow. Drug delivery to these cells can be valuable for diseases such as erythroleukemia and sickle cell disease which specifically affect EPCs [228][229]. A promising option for treatments would be the delivery of drugs to cancer cells or the repair of faulty genes with the help of gene editing. The identification of the VP1uR can help spur the development of the aforementioned techniques and treatments.

Previous attempts in our lab to identify the VP1uR by cross-linking and pull-down approaches failed due to the instability of the receptor-ligand complex in detergents typically used for receptor solubilization, emphasizing the limitations of these traditional techniques. The recombinant VP1u was allowed to bind to the cells followed by cross-linking to the VP1uR and pull-down through tags incorporated into the VP1u (unpublished results). A novel approach based on proximity labeling (PL) allows selective tagging of molecules in close spatial proximity to a ligand. To this end, the recombinant VP1u of B19V can be fused to a labeling enzyme, bringing the enzyme close to the cellular receptor. This in turn allows labeling of the unknown receptor as well as any nearby, possible interaction partners. This approach has some marked advantages compared to a classical cross-linking procedure. Specifically, PL approaches do not require long-lasting, stable interaction between the ligand and receptor. labeling takes place in real-time as the interaction takes place, even if it is only transient. This can then be followed by a pull-down of tagged proteins and mass spectrometry (MS) analysis to identify labeled molecules. BioID and APEX2 are two frequently used PL methods for tagging proximal molecules with biotin. While BioID uses the *E. coli* biotin ligase BirA [230], APEX2 uses ascorbate peroxidase [231]. For both methods, the enzyme and ligand are usually expressed as fusion proteins within a cell in order to tag intracellular interaction partners [230][231]. BioID is not optimized for labeling cell surface receptors, as it functions optimally in the reducing intracellular environment [231]. APEX2

could be used for surface tagging, but activated ascorbate peroxidase for cross-linking is difficult to obtain. For this reason, a novel method based on APEX2 has recently been developed. The technique, "selective proteomic proximity labeling using tyramide" (SPPLAT), only differs from APEX2 in the use of HRP instead of ascorbate peroxidase [232][233]. HRP shows strong activity outside of cells and can thus be used to efficiently label cell surface molecules. Figure 12A shows how in the presence of H_2O_2, HRP converts tyramide molecules into radicals, which diffuse a short distance (10-100 nm) before attaching covalently to exposed tyrosines [234][235]. It is therefore crucial that the HRP is brought as close as possible to the VP1uR, which is achieved by the coupling to VP1u (Figure 12B). The tyramide reagent is coupled to biotin which allows the pull-down and isolation of labeled proteins by neutravidin-based affinity purification.

2.1.2 Methods

Cell culture

UT7/Epo cells were cultured in Eagles 59-B medium, a special MEM (Minimum Essential Medium, Gibco) containing neomycin (20 µg/ml), streptomycin (20 µg/ml), penicillin (10 µg/ml) and 5 % fetal calf serum (FCS, AMIMED) at 37 °C in 5 % CO_2. Additionally, the cells were supplemented with 2 U/ml recombinant human erythropoietin (Epo, Janssen-Cilag). Ku812Ep6 cells were maintained in RPMI 1640 (ThermoFisher Scientific, 11875093) with 10 % FCS and 6 U/ml Epo. HuDEP cells are reprogrammed and immortalized from umbilical cord blood CD34+ hematopoietic stem cells [236]. They were grown in in IMDM (ThermoFisher Scientific, 12440053) with 15 % BIT 9500 (Stemcell Technologies, 09500), 50 ng/ml SCF (Gibco, PHC2115), 1µM dexamethasone (Sigma-Aldrich, D2915-100MG), 1 µg/ml doxycycline (Sigma-Aldrich, D9891-5G) and 3 U/ml Epo.

Generation of an HRP-VP1u construct

The recombinant VP1u are truncated at their C-terminus (−C128), contain an artificial cysteine for cross-linking, and carry a FLAG-tag for detection. A total of 10 mg recombinant lyophilized VP1u were added to a 15 ml falcon tube and dissolved in 1 ml dH2O (final concentration: 10 mg/ml). Proteins were reduced by the addition of 5µl 1 M TCEP (Lucerna-Chem, P1021). The solution was incubated at room temperature for 30 min and 100 µl of a 10 mg/ml solution of HRP-Maleimide (ImmunoChemistry Technologies, 6294) were added to the reduced VP1u. The cross-linking reaction was allowed to proceed for 1 h at RT followed by overnight incubation at 4°C. After the coupling, the reaction was loaded onto an ÄKTA size exclusion column (Superdex 200 increase 10/300) in order to separate reacted from free components. Fractions of 400 µl were collected and proteins were separated by SDS-PAGE. Fractions containing the construct were pooled and subsequently concentrated using spin columns with a 30 kDa molecular weight cut-off (Merck Millipore, UFC503008). Concentrated

VP1u-HRP was frozen at -80℃ in small aliquots.

Immuno uorescence analysis

For each condition, 3×10^5 cells were harvested and washed with PBS. For each sample, 0.5 µg of VP1u-HRP were incubated with 2 µg of rat anti-FLAG (Agilent, 200474) for 30 min at 4 ℃. Afterwards, the cells were resuspended with the labeled VP1u-HRP and incubated for 1 h at 4℃ under constant agitation. Cells were washed three times with ice-cold PBS and xed with a 1:1 mixture of methanol and acetone. Fixed samples were blocked with 10 % goat serum (Agilent, X0907) in PBS for 20 min. Subsequently, samples were incubated for 1 h with 1 µl goat anti-rat Alexa Fluor 488 (ThermoFisher Scienti c, A-11006) in 500 µl 2% goat serum in PBS. Samples were washed multiple times with PBS and mounted on a microscopy slide.

Proximity-based biotinylation of VP1uR

All the steps were performed at 4℃ or on ice unless stated otherwise. Recipes of bu ers are listed below. For each cell line, two samples with up to 15×10^6 cells each were prepared in a 15 ml falcon tube blocked with PBSA 1 %. Cells were washed twice with PBS at room temperature to remove residual medium and then resuspended in PBS to a nal concentration of 5×10^6 cells per ml. VP1u-HRP (5 µg/ml) was added to one sample followed by incubation for 2 h shaking at 60 rpm. The other sample was used as a control and 4 µg/ml VP1u and 1 µg/ml HRP were added (unconjugated). Cells were pelleted at 700× g for 5 min, washed once with ice-cold PBSA 0.2 %, then resuspended in tyramide labeling bu er (equal volume as for the incubation with VP1u-HRP) and incubated for 2 min. Catalase (Sigma-Aldrich, C9322) was added to a nal concentration of 100 U/ml to stop the reaction, followed by incubation for 5 min, shaking at 60 rpm. Cells were then washed three times with ice-cold PBSA 0.2 %, using 1 ml per 5×10^6 cells. Cells were lysed by the addition of ice-cold lysis bu er (500 µl per 5×10^6 cells) to the pellet. Samples were vortexed brie y and incubated for 15 min. Benzonase (1 µl, Millipore, E1014) was added and incubated for 30 min followed by brief vortexing. Samples were spun at 12'000× g for 10 min to remove insoluble material. In the meantime, a total of 100 µl per 5×10^6 cells of neutravidin bead slurry (ThermoFisher Scienti c, 29200) were transferred to a fresh 1.5 ml tube and washed once with PBSA 1 % and twice with lysis bu er for 1 min at 500 × g (100 µl of slurry per 15×10^6 initial cells). The lysate supernatant was added to the beads and incubated for 1 h under constant agitation. The beads were then transferred to a mini spin column and washed four times with wash bu er 1 and twice with wash bu er 2 by centrifuging for 1 min at 500 × g. Beads were subsequently resuspended in elution bu er (60 µl per 100 µl of bead slurry) and incubated for 20 min under agitation. Eluted proteins were separated from the beads by centrifugation. The elution step was repeated once and the fractions were combined. Proteins were concentrated by vacuum drying.

Bu ers

All bu ers were prepared as freshly as possible and stored at 4°C for no more than one month. Protein inhibitor cocktails were added immediately before use.

Tyramide labeling bu er:

- 50 mM Tris-HCl pH 7.4
- 0.03 % H2O2, freshly added
- 80 ug/ml Tyramide-SS-Biotin from 10 mg/ml stock in DMSO, 0.45 µm ltered (Iris Biotech, LS-3570.0250)

Lysis bu er:

- 20 mM Tris-HCl pH 7.4
- 5 mM EDTA pH 8.0
- 150 mM NaCl
- 1 % Triton X-100 v/v
- 0.1 M sodium thiocyanate
- 1 × Protease inhibitor cocktail (Roche, 11836153001)

Wash bu er 1:

- 10 mM Tris-HCl pH 7.4
- 1 % Triton X-100
- 1 mM EDTA pH 8.0
- 0.5 % SDS w/v
- 500 mM NaCl
- 0.1 M Sodium thiocyanate
- 1 × Protease inhibitor cocktail

Wash bu er 2:

- 10 mM Tris-HCl pH 7.4
- 1 % Triton X-100
- 1 mM EDTA pH 8.0
- 0.5 % SDS w/v
- 0.1 M Sodium thiocyanate
- 1 × Protease inhibitor cocktail

Elution bu er:

- 5 mM TCEP
- 100 mM Tris pH 7.4
- 1 % SDS w/v
- 0.1 M sodium thiocyanate
- 1 $\times$ Protease inhibitor cocktail

Identi cation of proteins

Puri ed biotinylated proteins were separated on an SDS-PAGE over roughly 1.5 cm. Fixation and staining of proteins were performed using Coomassie gel stain (ThermoFisher Scienti c, 24615). After destaining with dH_2O, a sterile scalpel was used to cut the resolved bands into three or four horizontal slices. The slices were collected and stored in separate 1.5 ml tubes. Gel pieces were overlaid with a mixture of 20:80 dH_2O and ethanol and stored at 4°C. Proteins were identi ed by MS analysis at the Core Facility Proteomics & Mass Spectrometry in Bern.

2.1.3 Results

VP1u-HRP construct can e ciently bind susceptible cells

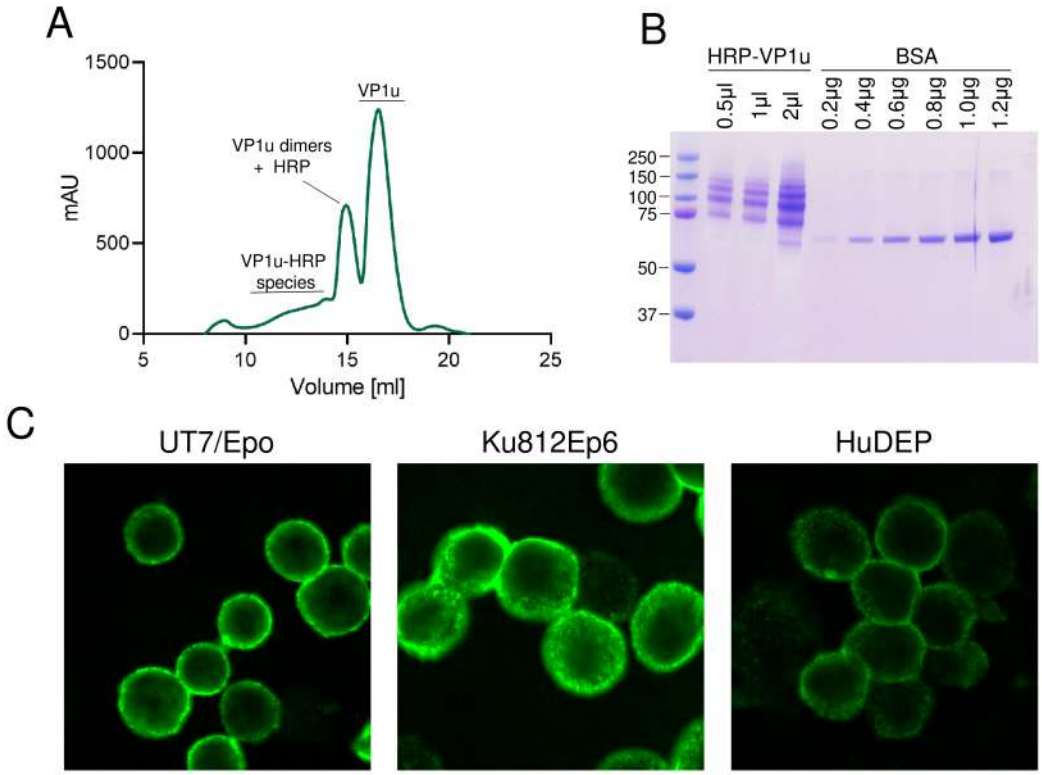

Figure 13: (A) Absorbance graph of eluted proteins from an ÄKTA column. Peaks represent the various protein species present after the cross-linking. mAU: Milli-absorbance units. (B) SDS-PAGE analysis of VP1u-HRP after concentrating desired fractions using a spin column. BSA at various concentrations was used to allow quantification of individual VP1u-HRP bands. (C) Visualization of VP1u-HRP on the cell surface of cells known to express VP1uR after allowing binding at 4 ℃.

The VP1u-HRP construct was generated through maleimide cross-linking. In order to remove unreacted VP1u and HRP from active constructs, size-exclusion chromatography was performed. Elution was performed with PBS and the elution pro le is depicted in Figure 13A. The nal construct was analyzed for quantity and quality on an SDS-PAGE (Figure 13B). Bands of various molecular weights can be observed on the gel, indicating a heterogeneous degree of labeling. The molecular weight of HRP with the cross-linkers is 45 kDa, the one of the recombinant VP1u is 14 kDa. The majority of the HRP seems to harbor two, three, or four VP1u subunits (73, 86, 101 kDa respectively). It was reported that HRP contains six lysine side chains but not all of them are readily accessible for labeling [237][238]. The observed degree of labeling was deemed satisfactory, as VP1u dimers are already very e cient at binding to VP1uR compared to monomers [69]. Importantly, the HRP was still

active after the cross-linking as con rmed by colorimetric reaction with luminol (not shown). It was then investigated whether the VP1u-HRP could actually bind the VP1uR on susceptible cells (Figure 13C). Tested were the megakaryoblastic UT7/Epo, the monocytes Ku812Ep6 as well as HuDEP (Human umbilical cord blood-derived erythroid progenitors). The VP1u-HRP construct was able to e ciently bind all three cell lines, con rming that the VP1u remains functional. Binding appeared to be exceptionally e cient in Ku812Ep6 cells and somewhat weaker in the HuDEP cells.

Proximity-based labeling unveils multiple VP1uR candidates

After verifying that the construct was able to bind the VP1uR, we set out to enzymatically tag cell surface proteins in proximity to the binding site, as described in the "Methods". Initially, UT7/Epo cells were analyzed due to the simplicity of culturing and good VP1uR expression. With the help of MS analysis, over 1000 proteins were found to be enriched compared to the control, most of them surface membrane proteins. As the labeling radius of this technique is estimated to be up to 100 nm around the HRP [234][235], it is expected that not only VP1uR is biotinylated, but also neighboring proteins. To narrow down the list of possible candidates, two additional cell lines, Ku812Ep6 and HuDEP, were used. We theorized that while the VP1uR will be a common denominator in all tested cells, other unrelated proteins may not be labeled to the same degree. Additionally, a technical replicate of UT7/Epo cells was performed to further increase robustness. The selection process was then carried out as follows: First of all, the relative abundance of each protein was established using the "MaxQuant" scoring algorithm. Then, the ratio of relative abundance of the sample of interest and its control was calculated. All proteins that were less than tenfold enriched (vefold in the case of HuDEP cells) were removed. Common hits among all experiments were then selected. Further, proteins that were above fteen times more or less abundant in a given cell line compared to the other two cell lines were also discarded. Lastly, hits for mitochondrial, ribosomal, and nuclear proteins, as well as other proteins that were evidently not membrane receptors, were sorted out manually. This narrowed down the list to less than 100. In table 1, the top ten hits, sorted by relative abundance in UT7/Epo or Ku812Ep6 cells, are listed.

	Protein list UT7/Epo
1	Leukosialin / CD43
2	Integrin beta-1, Isoform 2-5 of Integrin beta-1
3	Junctional adhesion molecule A, Isoform 2 of Junctional adhesion molecule A
4	Integrin alpha-5
5	CD81 antigen
6	4F2 cell surface antigen heavy chain, Isoform 3+4 of 4F2 cell surface antigen heavy chain
7	55 kDa erythrocyte membrane protein, Isoform 2+3 of 55 kDa erythrocyte membrane protein
8	Myeloid-associated di erentiation marker
9	Integrin alpha-4
10	Isoforms OA3-293, OA3-305 and OA3-312 of Leukocyte surface antigen CD47

	Protein list Ku812Ep6
1	Leukosialin / CD43
2	Junctional adhesion molecule A, Isoform 2 of Junctional adhesion molecule A
3	55 kDa erythrocyte membrane protein, Isoform 2+3 of 55 kDa erythrocyte membrane protein
4	Integrin beta-1, Isoform 2-5 of Integrin beta-1
5	CD44 antigen
6	4F2 cell surface antigen heavy chain, Isoform 3+4 of 4F2 cell surface antigen heavy chain
7	Cadherin-1, Isoform 2 of Cadherin-1
8	Intercellular adhesion molecule 2
9	Isoforms OA3-293, OA3-305 and OA3-312 of Leukocyte surface antigen CD47
10	Nectin-1, Isoform Gamma+Alpga of Nectin-1

Table 1: VP1uR candidates. All proteins listed are common in all three cell lines tested and were strongly enriched compared to control samples. The two lists show candidates ordered according to their relative abundance in UT7/Epo and Ku812Ep6 cells respectively.

3 Discussion

Preface

While each of the two publications already contain a dedicated discussion section, I believe it is important to bring together all the key findings of my thesis with a more in-depth interpretation of my results, including the work to identify the VP1uR. Another purpose of this chapter is to revisit the two goals of my thesis and critically evaluate how far those questions have been answered.

3.1 Globoside is an intracellular receptor required for endosomal escape

Globoside has been the proposed receptor of B19V since 1993 [57]. Confounding data in the years following this discovery challenged the seemingly clear-cut receptor role of globoside [183][60][59]. The first goal of this thesis was to elucidate the role of globoside in B19V infection by generating a globoside knockout cell line. Genetic disruption of the B3GalNT1 gene encoding for globoside synthase in the semi-permissive UT7/Epo cell line led to the complete elimination of globoside. B19V binding and internalization were not altered in the globoside knockout cell line, however, the infection was blocked. In sharp contrast, blocking the VP1uR with recombinant VP1u abolished virus internalization, confirming that the VP1uR, and not globoside, is the entry receptor for the virus.

Although globoside was not required for binding and uptake, its presence was essential at a post internalization step. Transfection of the viral genome showed that the presence or absence of globoside does not impact the replication of the virus in the nucleus, nor the production of viral proteins. Accordingly, globoside must be required at a trafficking step after VP1uR-mediated uptake and before translocation of the virus to the nucleus. Indeed, we found that in cells lacking globoside the virus was unable to reach the nucleus and remained sequestered in the late endosomes and lysosomes. In contrast, in cells expressing globoside, an increasing proportion of incoming viruses were found in isolated vesicles devoid of markers for endosomes, lysosomes, Golgi or ER [239]. These results suggested that B19V may interact with globoside inside the acidic endosomes as an essential step for endosomal escape.

Globoside is constantly internalized from the cell surface and is transported to early endosomes [211][212], where it can interact with incoming B19V [117]. Accordingly, acidic pH may play a critical role by increasing the affinity of the virus for globoside. In line with this hypothesis, we confirmed that B19V interacts with globoside exclusively under acidic conditions similar to those present in early endosomes (pH 6.0) [239]. It is well known that low pH in the endosomal compartments is crucial for the infection of many viruses, including parvoviruses [117][120][240]. The acidic pH leads

to conformational changes in the capsid and subsequent endosomal escape of the virus, presumably assisted by the PLA2 activity present in the VP1u. However, besides the PLA2 activity, our findings suggest that B19V exploits the acidic endosomal pH to change the affinity for receptors. At acidic pH, the affinity for VP1uR decreases (unpublished results) and increases for globoside [239]. It is therefore likely that the virus swaps VP1uR for globoside in the acidic early/late endosomes. The interaction of B19V with globoside inside the endocytic compartments may induce membrane curvature and invaginations, leading to the formation of budding vesicles, as observed by confocal microscopy [239]. This phenomenon has already been described following the binding of certain ligands with glycosphingolipids. The bacterial Shiga toxins 1 and 2 (Stx1 and Stx2) bind Gb3, the precursor of globoside, and have a low affinity for globoside [241][242]. Certain subtypes, such as Stx2e, show inverse behavior and preferentially bind globoside [243][244]. GM1, a ganglioside with a similar base structure as globoside, acts as the receptor for cholera toxin (Ctx) of$Vibrio\ cholerae$ [245], as well as for simian virus 40 (SV40) [246]. Binding of Stx, Ctx or SV40 to their respective receptor induces GSL rearrangement and membrane bending [247][248][208]. This occurs due to the multimeric nature of the binding, meaning that many cellular receptors bind each toxin molecule or viral capsid protein. The cell membrane adopts a slightly negative curvature to allow the equidistant binding of multiple receptors [247][248][249]. Elongated tubular structures are formed and scission leads to the formation of budded vesicles [247][248][249]. The fate of SV40 after uptake is the ER [250], while Ctx and Stx traffick through the Golgi to the ER [251][252]. Likely, B19V can also establish such powerful multimeric interaction with globoside in the endosomal membrane, which triggers the formation of tubular structures and budding vesicles containing the virus.

Although globoside may assist endosomal escape by the formation of budding vesicles, the following trafficking steps remain unclear. Brefeldin A (BFA), a drug that disturbs transport from ER to Golgi, was shown to disturb the infection of SV40 [253]. We have also observed that BFA strongly disturbs the intracellular trafficking of B19V (unpublished results). This result suggests that the vesicles budding from endosomes may transport the virus to the Golgi apparatus, which in contrast to the endosomes has the optimal pH and calcium ion concentration required for the lipolytic activity of PLA2 [61](unpublished results).

For many years, globoside has been considered the primary cellular receptor of B19V, notably supported by the observation that individuals lacking globoside cannot be infected and the capacity of soluble globoside to inhibit the hemagglutination activity of B19V[57][58]. Our findings are not in conflict with these observations. We found that globoside is required for the infection and accordingly, individuals without globoside should be resistant to the infection. The assays that revealed the capacity of globoside to inhibit hemagglutination were performed at acidic pH, which promotes the

interaction. Other findings, such as the blocking of infection with anti-globoside antibodies or with soluble globoside [60][57] could not be reproduced in our studies and are likely a result of non-specific interactions. Taken together, we revealed that globoside is not the cellular receptor of B19V required for uptake into permissive cells, a function that corresponds to the VP1uR. Instead, globoside is an essential intracellular factor required for endosomal escape.

3.2 Globoside as a gateway for transmission and dissemination

The binding of B19V to globoside expressed on the plasma membrane can be induced in cells exposed to acidic conditions and results in virus uptake without productive infection [239]. These findings suggest that, although globoside does not function as the primary receptor for virus uptake into permissive cells, it may still serve as a receptor in cells exposed to acidic conditions to allow entry. The airway epithelial cells are exposed to an acidic environment [254][255][256][257][258][259] and although they do not express the VP1uR, they do express globoside (unpublished results). Preliminary results indicate that B19V does not infect these cells but can breach the epithelial barrier in a globoside and pH-dependent manner (unpublished results). These findings suggest that globoside and low pH mediate the transmission of B19V through the respiratory tract and explain the absence of B19V antibodies in individuals lacking globoside [58], as their respiratory epithelium would be impermeable to the virus.

The fact that the affinity for globoside is tightly controlled by the pH explains how a virus with such a strict erythroid tropism can utilize the ubiquitously expressed globoside for infection. The neutral pH of the blood prohibits the interaction with globoside expressed on the nonpermissive RBCs. If B19V would bind globoside on nonpermissive RBCs, the virus would not be able to efficiently target the permissive erythroid cells in the bone marrow.

Acidic niches are also established in the placenta through the activity of sodium/proton exchangers [260]. Similar to the airway epithelial cells, the human placenta does not express the VP1uR (unpublished results). However, globoside is expressed in trophoblast cells, which represent the main cellular barrier of the placenta [191][261]. Globoside expression depends on the gestational age, being particularly detectable in the first and second trimester, and low or undetectable in the third trimester [261]. Perinatal complications due to B19V infection are more frequent in the first and second trimester [262], and thus correlates with the expression of globoside on the placenta. Similar to the airway epithelium, the presence of globoside in the trophoblasts may serve as an entry portal to invade the placenta and spread to the fetus. However, it cannot be excluded that vertical transmission to the fetus is mechanistically different from the passage of the virus through the airway epithelial cells.

This possibility is supported by the fact that the viral a nity for globoside is strongly reduced in the presence of plasma, even at acidic pH values [194][239].

Globoside-dependent uptake of the virus could occur similarly to Stx or Ctx, where the interaction of the lectins with the receptor can lead to internalization in a clathrin-independent manner [263][264][265][249][266]. Due to the lack of EpoR signaling in the airway epithelial cells and trophoblasts, it is improbable that B19V can establish a productive infection in those cells. Rather, globoside facilitates the transport of B19V across the host cellular barrier by transcytosis. Other parvoviruses, such as AAV, are known to utilize transcytosis in a serotype- and host-speci c manner [267][268][269].

Since globoside is a ubiquitous molecule, every acidic niche in the body can become a potential target for the virus. Expanding upon this concept, acidic conditions can also be found in the lymph nodes (LN) [270]. T-cells themselves are the source of this acidity through the production of lactic acid, leading to a mean extracellular pH of 6.3 [270]. Ordinarily, the low pH is an important mechanism to inhibit T-cell e ector functions while still within the LN [270]. Since T-cells express globoside [187], they could represent another important cellular target for B19V. After crossing the airway barrier, the virus may accumulate in the interstitial uid, eventually being transported to the LN via lymphatic vessels. There, interaction with T-cells could be relevant for the spread of the virus within the body.

3.3 Identity of the VP1uR

The uptake receptor of B19V, VP1uR, is expressed exclusively on cells during the Epo-dependent stages of erythropoiesis, mainly on CFU-E, proerythroblasts, and early basophilic erythroblasts (see Figure 3)[70][72]. Previous attempts to identify the receptor by classical cross-linking and pull-down assays were unsuccessful, probably due to the instability of the interaction complex. Here, we utilized a PL-based approach, SPPLAT. With the aid of a functional VP1u-HRP construct, we were able to tag proteins in close proximity to the VP1u binding site on the cell. The HRP activates Tyramide-SS-Biotin in the presence of H_2O_2, which in turn covalently binds exposed tyrosine residues of nearby proteins. Proteins were then solubilized, and puri ed with the aid of the biotin tag, followed by MS analysis. The whole experiment was performed at 4°C in order to prevent the internalization of the VP1u-HRP construct. The initial experiment using UT7/Epo cells did not yield a candidate receptor with the expected restricted erythroid expression. A likely explanation is that speci c post-translational modi cations (PTM) in the VP1uR are involved in the interaction with the virus. Alternatively, the VP1uR may consist of two or more cell surface molecules that arrange in a

di erentiation-stage speci c manner.

To narrow down the receptor candidates, additional cell types were analyzed. As selection criteria, the cell should express detectable levels of the VP1uR but di er considerably from the UT7/Epo cells. This was important to facilitate the identi cation of irrelevant, nonspeci c hits. For this reason, Ku812Ep6, cells from monocytopoiesis, as well as HuDEP, immortalized late-stage EPCs from CD34+ umbilical cord blood, were chosen. Fewer than 100 common hits remained after the selection process described in section 2.1. Proteins with the highest relative abundance in either UT7/Epo or Ku812Ep6 cells can be found in table 1. Importantly, all of the proteins listed are present in the proerythroblast stages of erythropoiesis [271]. At the same time, none are signi cantly enriched in the proerythroblast stage compared to earlier or later points of di erentiation [271]. In short, there does not seem to be a clear candidate with the expression pro le of the VP1uR. This further increases the likelihood that an erythroid-related isoform or PTM may be involved in the interaction. Still, some of the more interesting candidates are worth discussing. As an example, leukosialin (CD43) is present on a multitude of hematopoietic cells, including those permissive for B19V replication [272][273]. Moreover, it is heavily glycosylated, a process that is tightly regulated and is lineage-speci c [274][275][276][277][278][279]. Other interesting candidates are the various alpha and beta integrins. Integrins have already previously been proposed as co-receptor required for B19V attachment [66] and therefore represent promising candidates. The junctional adhesion molecule A was also found to possess di erent possible glycosylation patterns [280] and is already known to serve as a receptor for reoviruses [281]. The 4F2 cell-surface antigen heavy chain (SLC3A2) and nectin-1 also represent candidates with known receptor functions. SLC3A2 has been shown to act as a cofactor necessary for HCV entry via clathrin-mediated endocytosis [282]. Nectin-1 has already been shown to ful ll an important function for herpes simplex virus and pseudorabies virus uptake [283]. Strikingly, nectin-1 is expressed almost exclusively at the proerythroblast stages of EPC di erentiation, albeit at low levels [271]. Interestingly, EpoR was not detected in any of the experiments, suggesting that it is exclusively involved in essential signaling pathways but not located in close spatial proximity to the VP1uR. The di culty to identify the VP1uR by PL methods emphasizes the limitations of the technique. Namely, the target needs to be both a protein and have an exposed tyrosine residue for tagging. Moreover, if the protein is very hydrophobic or present in lipid rafts, solubilization may not be possible despite labeling it with biotin. Furthermore, there is an inherent bias for ubiquitous proteins, as there is an increased likelihood of them being present in the vicinity of the VP1uR. Lastly, the labeling radius of activated tyramide increases with incubation time with the labeling bu er, up to 100 nm [235][234]. Tagging of non-speci c proteins is therefore unavoidable. More selective tests will be necessary to assess the involvement of each possible candidate in B19V uptake. Recently, an

analogous approach to SPPLAT, based on the prokaryotic ubiquitin-like protein (Pup), was shown to be a useful alternative for cell surface receptor labeling [284]. This method holds the advantage of a shorter tagging radius of roughly 6 nm, signi cantly reducing the risk of labeling non-speci c molecules [284].

3.4 Outlook

Today, there is an urgent need to understand the mechanism of parvovirus B19 transmission, infection, and dissemination to the fetus. The lack of knowledge regarding B19V infection can be largely attributed to the long-lasting confusion concerning the cellular receptors of the virus. The results of this thesis clarify the role of globoside in B19V infection, which should not be viewed as the primary cellular receptor required for uptake and productive infection. Instead, globoside is an interacting cellular partner facilitating the breaching of cell membrane barriers under the strict control of the environmental pH. Those barriers can be the endosomal membrane during virus entry into permissive cells, or host cellular barriers, such as the airway epithelium, or the placenta.

An important topic for further research is the mechanistic understanding of the membrane curvature and vesicle formation induced by the multimeric interaction of B19V capsids with globoside molecules. The goal here is to understand how the capsid-globoside complex induces local changes in the physical properties of membranes resulting in uptake if the interaction occurs at the cell surface, or endosomal escape if the interaction occurs inside endosomes. The use of giant multilamellar vesicles (GUVs) decorated with globoside may be an interesting approach for studying the process in a simpli ed model.

B19V infection poses a signi cant risk for pregnant mothers. Only half of the pregnant women show antibodies against B19V [77] and infection with B19V occurs in at least 1 % of pregnancies [88][89]. This in turn can eventually lead to $hydrops\ fetalis$ in roughly 10 % of those pregnancies [92][85][90]. Understanding the cellular process involved in globoside-mediated virus uptake and transport across host epithelial and placental barriers will facilitate the rational development of novel antiviral medi-cation and vaccination.

Cellular receptors are essential for virus entry and spread. Thus, their identi cation is fundamental to understanding the tropism and pathogenesis of the infection. Unveiling the nature of the VP1uR has proven to be an ambitious project. Still, initial results yielded promising results and several receptor candidates were identi ed. Alternative approaches based on proximity labeling can narrow down the list of candidates. Finally, the use of speci c antibodies or genetic knockouts will facilitate the identi cation of the VP1uR.

4 Methods

Preface

In this chapter, I would like to highlight the most central and crucial techniques that were used to conduct my experiments. While the general methodology is already described in the above publications, this chapter allows me to present a more in-depth view of some of the key methods applied in my PhD studies. This means that the focus lies mostly on techniques that have not yet been well established in our lab or where the corresponding publications do not go into sufficient detail. Hopefully, this will prove to be helpful for future scientists that attempt similar experiments so they will have a solid foundation and good reproducibility for their research.

4.1 Southern blot

UT7/Epo WT or KO cells (3×10^6) were seeded in 10 ml culture medium in a 75 cm^2 flask. B19V containing plasma was diluted in 10 ml culture medium without FCS and added to the seeded cells, resulting in 4×10^4 genome equivalents per cell. Cells were harvested after 1 h or after 72 h. Harvested cells were washed 4× with PBS at RT. Cells were resuspended in 50 µl TBS, followed by the addition of 750 µl lysis buffer (0.6 % SDS, 10 mM Tris-HCl pH 7.5, 10 mM EDTA) and 10 µl Proteinase K (600 mAU/ml, Qiagen, 19157). The tubes were inverted 10× and incubated at RT for 1 h. To precipitate the SDS and the chromosomal DNA along with it, 200 µl 5 M NaCl solution were added. Tubes were inverted ten times and incubated for 16 h at 4 °C. The lysates were spun at 16'000× g for 30 min at 4 °C, followed by the extraction of 600 µl supernatant using the DNeasy Blood & Tissue kit (Qiagen, 69506). The enrichment of viral DNA compared to genomic DNA was verified by RT-qPCR (NS1 primer pair for viral DNA, ACTBL2 primer pair for cellular DNA, see subsection 6.2 & 6.3). The extracted DNA (20 µl) was mixed with 5 µl 6× DNA loading dye (New England Biolabs, B7024S), loaded and resolved along with a 2-Log DNA ladder (New England Biolabs, N3200S) on a 0.8 % agarose gel in TAE overnight at 25 V. The ladder was cut off, stained with GelRed (Biotium, 41003) and photographed under UV light next to a ruler. The rest of the gel was cut to a size that preserved the desired molecular weight range, depurinated for 10 min in 0.125 M HCl, rinsed with dH_2O and TAE followed by a denaturation step for 2 × 15 min in 0.5 M NaOH, 1.5 M NaCl. The gel was neutralized 2× for 15 min in 1 M NaCl, 0.5 M Tris-HCl pH 7.4. A positively charged nylon membrane (GE Healthcare, RPN203B) was floated in dH_2O for 1 min and later submerged in 20X SSC (3 M NaCl, 0.3 M sodium citrate) for 5 min. The transfer to the positively charged nylon membrane was performed with 650 ml 20X SSC through upward capillary blotting for 16 h (the membrane was placed above the gel, followed by three soaked filter papers and an 8 cm tall stack of paper towels). A 500 g weight was placed on top of the towels to facilitate the transfer. The membrane was dried on

Component	Final concentration
Tris-HCl pH 7.8	50 mM
$MgCl_2$	5 mM
BSA	50 µg/ml
DTT	10 mM
d(GAT)TP	0.04 mM
α-^{32}P-dCTP	100 µCi
DNA template (773-1716 bases, J35 isolate)	1µg

Table 2: Components of the Southern blot probe for hybridization to B19V DNA.

paper towels until mostly dry. In an oven, the membrane was baked at 90℃ for 1 h to immobilize the DNA. The membrane was prehybridized in a hybridization oven at 42℃ for 90 min with 8 ml hybridization bu er (7 % SDS (w/v), 0.125 M sodium phosphate pH 7.2, 0.25 M NaCl, 1 mM EDTA, 45 % formamide (v/v)) containing 50 pg/ml salmon sperm DNA (Invitrogen, 15632011) which was boiled at 95℃ for 10 min beforehand. The bu er was then replaced with an identical bu er containing a radiolabeled probe for overnight incubation at 42℃. The probe was prepared by nick-translation at 15 ℃ for 1 h, using the reaction components from table 2. This was followed by puri cation of the probe using a PCR clean-up kit (Promega, A9281). The membrane was subsequently washed at 42 ℃ for 2 × 5 min with 2X SSC + 0.1 % SDS and 2× 15 min with 0.1X SSC + 0.1 % SDS. The semi-dry membrane was subsequently sealed in a plastic membrane and exposed to a phosphor image screen overnight. Visualization was carried out with a phosphorimager (Typhoon FLA 9500).

4.2 Transfection of UT7/Epo cells and generation of Gb4 KO cells

The UT7/Epo cell line was transfected with lipofectamine 3000 (Invitrogen, L3000001) due to the low cytotoxicity of the reagent for the cells. Cells (10^6 for a 6-well plate, 2×10^5 for a 12-well plate) were prepared one day before the transfection growth medium. Transfection for CRIPSR/Cas KO was performed using 5µg of DNA (2.5 µg of CRISPR KO plasmid [Santa Cruz Biotechnology, sc-424114] + 2.5 µg of HDR plasmid [Santa Cruz Biotechnology, sc-424114-HDR]). The CRISPR KO and HDR plasmids encode GFP and RFP respectively, which was used to di erentiate between positive and negative transfected cells. For transfection reactions with the B19V infectious clone, 1µg of DNA was used. Two solutions were prepared as indicated in table 3 and mixed well. The contents of solution 2 were added to solution 1 and incubated for 5 min. The DNA-lipid complexes were then added

drop-wise to the cells and incubated for up to three days at 37°C and 5 % CO_2.

Solution 1:	
Opti-MEM	125 µl
Lipofectamine 3000	3.75µl

Solution 2:	
Opti-MEM	125 µl
Plasmid DNA	1-5 µg
P3000 reagent	2µl/ µg DNA

Table 3: Composition of transfection solutions.

Cells transfected with the B19V infectious clone were subsequently harvested, washed at 700g with PBS and analyzed either by RT-qPCR or fixed for immunofluorescence staining. CRISPR/Cas KO transfected cells were then selected by fluorescence-activated cell sorting (FACS). Cells were harvested from the transfection well and spun at 700 × g for 3 min to pellet them. The pellet was washed with 10 ml PBS and the centrifugation step was repeated. The pellet was carefully resuspended in 1 ml ice-cold PBS containing 2 % FCS. Cells expressing both RFP and GFP were sorted into a tube containing 3 ml FCS. Sorted cells were then pelleted and seeded out into a new flask containing fresh culture medium. For the generation of clones, single cells expressing RFP (the GFP signal is lost after a few passages) were sorted into 96-well plate wells containing conditioned medium. For the next two weeks, cells were maintained in conditioned medium followed by the expansion of positive colonies into cell culture flasks. Successful knock-outs were verified by RT-qPCR for the presence of B3GalNT1 mRNA transcripts (see subsection 6.2 & 6.3).

4.3 Baculovirus recombinant protein expression system

Preparation of a pfastBac1-VP2 construct

The baculovirus protein expression system allows for the production of recombinant virus-like particles. This method is especially useful due to its safety, scalability, and high protein expression level. The VP2 ORF of the B19V infectious clone was amplified in a PCR using a primer pair which introduced restriction sites for EcoRI and HindIII (see subsection 6.2 & 6.3). The PCR amplicon was purified using a PCR clean-up kit (Promega, A9281). The purified PCR amplicon was quantified using nanodrop and prepared for cloning into a pfastBac1 plasmid (ThermoFisher Scientific, A38841, see subsection

6.4). To this end, 10 µg of the amplicon were digested with 20 u each of EcoRI-HF (NEB, R3101S), HindIII-HF (NEB, R3104S) and DpnI (NEB, R0176S) in 1X CutSmart Buffer in a heat block for 2 h at 37 °C, 500 rpm. The digested DNA was once more purified with the PCR clean-up kit. pfastBac1 (1 µg) was digested with 20 u each of EcoRI-HF and HindIII-HF in 5 µl in 1X CutSmart Buffer in a heat block for 1 h at 37 °C, 300 rpm. Enzymes were heat-inactivated at 80 °C for 20 min. Further, the plasmid was dephosphorylated by the addition of 0.65 µl of 10X antarctic phosphatase (AnP) buffer and 5 u AnP (NEB, M0289S). Incubation at 37 °C for 1 h was followed by heat-inactivation at 80 °C for 2 min. Ligation was carried out in a total of 20 µl with the 6.5 µl dephosphorylated plasmid, 2 µl 10X T4 ligation buffer, 1 µg digested VP2 ORF, and 1 µl T4 ligase (NEB, M0202S). The mixture was incubated at 4 °C for 30 min, at 16 °C for 30 min, and at RT for 10 min followed by heat-inactivation at 65 °C for 10 min. For transformation, 10-beta *E. coli* (NEB, C3019H) were thawed on ice and transferred to a pre-cooled 14 ml bacterial-culture tube. 2 µl ligation mix (100 ng) were added to the cells and incubated on ice for 30 min. The tube was subsequently transferred to a 42 °C water bath for 30 sec followed by 5 min on ice. SOC medium (500 µl, NEB, B9020S) were added to the cells, followed by incubation at 37 °C, 225 rpm for 1 h. The bacterial suspension (250 µl) and a 1:10 dilution thereof was then spread on pre-warmed agar plates (40 g/l Miller Agar) containing 100 µg/ml ampicillin (Merck, A5354). The plates were incubated overnight at 37 °C. Growing colonies were isolated and diluted in 100 µl PBS. 2 µl of this solution were analyzed by PCR with the "Insert Check" primer pair, using the ligated plasmid as a positive control (see subsection 6.2 & 6.3). Positive colonies were added to 5 ml LB-Medium containing 100 µg/ml ampicillin and incubated overnight at 37 °C, 225 rpm. The following day 700 µl of overnight culture were transferred to a 1.5 ml Eppendorf tube and mixed with a 300 µl solution of glycerol and H_2O (1:1) and stored at -70 °C. Plasmid DNA was isolated from the remainder of the culture using a miniprep kit (Promega, A1460). 1 µg of plasmid was sent for sequencing using the "F check insert" primer as well as the primer "FW-4" (see subsection 6.2 & 6.3).

Generation of a B19V VP2 bacmid

DH10Bac cells (ThermoFisher Scientific, A38841) were thawed on ice and transferred to a pre-cooled 14 ml bacterial-culture tube. pFastBac-VP2 (5 µl, 0.2 ng/µl) was added and the cells were incubated on ice for 30 min. Subsequently, cells were heat-shocked in a water bath at 42 °C for 45 seconds. Cells were chilled on ice for 2 min followed by the addition of 900 µl SOC medium. The cells were transferred to 37 °C, 225 rpm for 4 h. Dilution series of 10^{-1}, 10^{-2} and 10^{-3} of the cells in PBS were created and 100 µl were distributed to agar plates containing kanamycin (50 µg/ml), gentamycin (7 µg/ml), tetracycline (10 µg/ml), 100 µg/ml X-Gal (Millipore, BG-3-G) and IPTG (40 µg/ml). Plates were incubated at 37 °C for 24-48 h. White colonies were picked, added to 100 µl H_2O and restreaked on an identical plate overnight. White colonies were once again picked and dissolved in 100 µl H_2O. Of

each colony, 2µl were analyzed by PCR using "F Transposition" and "R Insert Check" primers (see subsection 6.2 & 6.3). PCR-positive colonies were used to inoculate 200 ml LB-Medium containing kanamycin (50 µg/ml), gentamycin (7 µg/ml,) and tetracycline (10 µg/ml). Incubation for 16 h at 37 ℃, 225 rpm. Bacmids were isolated from the bacteria with the "HiPure Plasmid Maxiprep Kit" (ThermoFisher Scienti c, K210006) using the following protocol:

- 200 ml overnight culture of $E.\ coli$ containing recombinant baculovirus genome were pelleted at 4000 × g at 4 ℃ for 10 min. The supernatant was removed.
- Bacterial pellets were resuspended in 20 ml Resuspension Bu er (R3). Cells were thoroughly homogenized.
- 10 ml Lysis Bu er (L7) were added to each tube. Tubes were then carefully inverted ten times and incubated at RT for 5 min (and not longer).
- 10 ml Precipitation Bu er (N3) were added to each tube. Tubes were inverted ten times to mix contents.
- Mixtures were centrifuged at 12'000 × g at RT for 10 min. The supernatant was centrifuged again to ensure that no more debris was present.
- 30 ml Equilibration Bu er (EQ1) were added to a Maxi Column and allowed to ow through by gravity.
- Bacterial lysates were loaded on the equilibrated column and allowed to drain by gravity.
- 60 ml Wash Bu er (W8) were added and allowed to elute by gravity. A new sterile 50 ml tube was placed under the column.
- 15 ml Elution Bu er (E4) were added to the column to elute bacmid DNA. The column was discarded afterward.
- 10.5 ml isopropanol were added to the elution tube and the solution was mixed well. The tube was centrifuged at 12'000× g at 4 ℃ for 30 min and the supernatant was carefully removed.
- The DNA pellet was carefully resuspended in 5 ml 70 % ethanol.
- The tube was centrifuged at 12'000 × g at 4 ℃ for 5 min. The supernatant was carefully removed and the pellet was air-dried for no more than 10 min.
- The pellet was resuspended in 0.2 ml TE Bu er (TE) without pipetting to avoid shearing the DNA. The tube was stored on ice for at least 10 min to allow DNA to dissolve.

The puri ed bacmid was analyzed by PCR using the "Transposition F/R" primers and Q5 polymerase (see subsection 6.2 & 6.3). The generated amplicons were puri ed with a PCR clean-up kit and 5µl were run on a 1 % agarose gel in 1× TAE bu er and GelRed (Biotium, 41003). The expected size of the amplicon was 4000 bp. The remaining amplicon was used for sequencing using the "Insert Check" and "FW-4" primers ((see subsection 6.2 & 6.3).

Generation of P0 stock of recombinant baculovirus

ExpiSf9 insect cells were cultured in ExpiSF CD medium (ThermoFisher Scientific, A3767801) on an orbital shaker at 125 rpm and 27°C. The cells were grown until they reached a density between 5×10^6 and 10×10^6. For transfection with the bacmid, 62.5×10^6 cells were pelleted at 300× g for 5 min and resuspended in 25 ml of fresh medium. The transfection mixture was prepared in 1 ml Opti-MEM I Reduced Serum Medium (ThermoFisher Scientific, 31985062). 30 µl ExpiFectamine Sf Transfection Reagent (ThermoFisher Scientific, A38841) were added to the medium and the mixture was inverted eight times and incubated for 5 min at RT. 75 µg of bacmid were added to the mixture, which was again inverted eight times and incubated for 5 min at RT. The mixture was then added drop-wise to the ExpiSf9 cells. The cells were allowed to grow for roughly 96 h until a clear increase in the average diameter of the insect cells was observed. The cell suspension was transferred to a 50 ml falcon tube and centrifuged at 300× g for 5 min. The supernatant contained the P0 stock of recombinant baculovirus and was stored at -80°C in aliquots. The P0 stock was quantified by PCR: The supernatant containing the P0 stock was diluted in dH_2O (1:10^2 - 1:10^5) and boiled for 5 min at 90 °C. 2 µl were amplified in a PCR using primers against the gp64 region of the virus (see section 6).

Production of recombinant VP2

ExpiSf9 cells were seeded in fresh, prewarmed medium in a new flask to a final density of 5×10^6/ml one day before infection. ExpiSf Enhancer solution (100 µl) (ThermoFisher Scientific, A38841) were added to the cells immediately after seeding. After 16-24 h, cells were infected with 100-1000 µl of P0 stock (optimal quantities have to be determined empirically). Cell density should not exceed 7×10^6/ml at the time of infection. After the addition of the virus, the cells were incubated at 27 °C for three days or until viability of the cells had dropped to roughly 60-70 % and cells show clear cytopathic effects. The cell suspension was then transferred to a 50 ml falcon tube and cells were pelleted for 20 min at 1000 × g, 4 °C. The pellet fraction was resuspended in 7.5 ml TNTM buffer (25 mM Tris-HCl pH 8.0, 100 mM NaCl, 0.2 % Triton X-100, 2 mM $MgCl_2$). The cell suspension was freeze-thawed three times. Benzonase (Merck, E1014-5KU) was added (1:10'000) and the cell lysate was incubated for 30 min at room temperature. Debris was pelleted by centrifugation for 15 min at 12'000× g, 4 °C. The supernatant was filtered consecutively through a 0.45 µm and 0.1 µm filter. The cleared lysate was loaded on top of a sucrose cushion consisting of 20 % sucrose in TNET buffer (50 mM Tris-HCl pH 8.0, 100 mM NaCl, 1 mM EDTA, 0.2 % Triton X-100). Centrifugation was performed in a Beckman 70-Ti rotor, for 3 h at 45'000 rpm, 4 °C. The lowest 1.5 ml of the centrifugation was used to resuspend the pellet, which was then diluted in an equal amount of TNE buffer (TNET buffer without Triton X-100). Gradient centrifugation was performed with a Beckman SW41 rotor. The 10 % sucrose solution containing the VLPs was layered on top of an OptiPrep gradient (Sigma-Aldrich, D1556-250ML). The OptiPrep (60 %) was diluted in MEM, starting from the bottom: 1 ml 55 %,

then 1.5 ml each of 45-15 % (in 10 % increments). Centrifugation was performed overnight for 16 h at 30'000 $\times$ rpm, 4 ℃. Starting from the top of the gradient, 750 µl fractions were collected in tubes with low protein binding. A dot blot was performed to identify fractions containing the VLPs by using the 3113-81C antibody (see subsection 6.1). A bu er exchange of positive fractions was performed using a PD10 column (GE Healthcare, 17-0851-01). The columns were equilibrated with ve column volumes of TNM bu er (20 mM Tris-HCl pH 7.8, 10 mM NaCl, 2mM $MgCl_2$). The VLPs were loaded on top of the column and allowed to enter, followed by TNM until 2.5 ml total volume had entered the column. The VLPs were eluted by continuous addition of 0.5 ml TNM bu er. Fractions were collected and quanti ed by nanodrop and SDS-PAGE. The VLPs were frozen and stored at -80℃.

4.4 Immuno uorescence

Before xation, a coverslip was placed in a 12-well plate for each condition and rinsed once with ethanol and twice with PBS. An appropriate number of cells were resuspended in roughly 20µl PBS and spotted on a washed coverslip. Cells were allowed to settle for 5 min before the addition of a -20 ℃ chilled solution of methanol and acetone (1:1). The plate was transferred to a -20℃ freezer for 4 min. The xation solution was then removed and the slides were allowed to air-dry. From here onwards, all steps were performed at room temperature. The dried slides were rehydrated by addition of 500 µl PBS and incubation for 5 min. This rehydration step was repeated once. The samples were subsequently blocked for 20 min with 300µl of a 10 % goat serum solution (Agilent, X0907) in PBS. The slides were then incubated for 1 h upside down on a 30µl drop of 2 % goat serum in PBS containing the primary antibody. A list of antibodies can be found in subsection 6.1. The coverslips were replaced to the 12-well plate and washed ve times with PBS over the course of 1 h. Secondary antibodies (Alexa Fluor 488 or 594 antibodies, ThermoFisher) were diluted 1:500 in 500µl of 2 % goat serum in PBS. Incubations with the secondary antibody were performed in the dark for 1 h, shaking. The coverslips were washed once more over the course of 1 h. When working with UT7/Epo cells, the samples were quenched of endosomal auto uorescence by addition of 300µl 2 mM $CuSO_4$ in 50 mM ammonium acetate followed by a 5 min incubation (see Figure 14). The quenching solution was removed and the xed cells were rinsed twice with PBS. The coverslips were subsequently rinsed with dH_2O and ethanol and allowed to dry. The dry coverslips were mounted cell-side down on a 12µl drop of mounting agent (ThermoFisher, P36962) placed on a glass slide.

When staining globoside, cells were blocked with PBSA 1 % and incubated with the primary antibody at 4 ℃ before to xation. Unbound antibody was washed away by sequential centrifugations performed at 4 ℃. Cells were then xed and processed as described above.

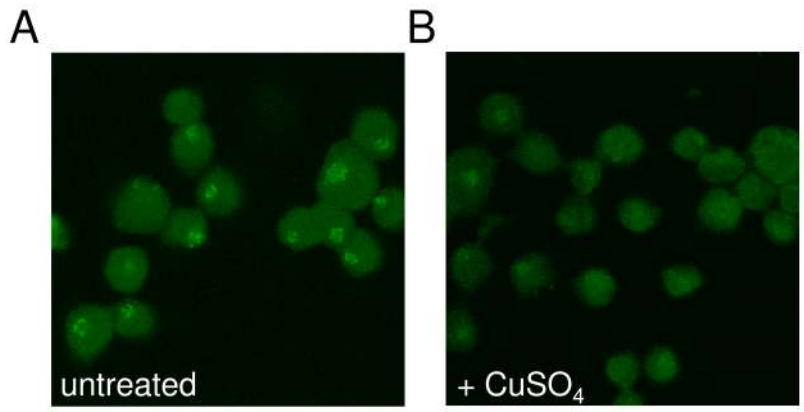

Figure 14: Fixed UT7/Epo cells without (A) and with (B) $CuSO_4$ treatment. The background fluorescence is roughly localized to the endosomal compartments and is also present in live cells. Copper ions were found to be the acting component of the quenching buffer, efficiently reducing the background fluorescence without affecting specific signals from antibodies [285].

4.5 Hemagglutination

Hemagglutination was used to analyze the interaction (or lack thereof) of RBCs with an antigen. RBCs were obtained from complete blood containing EDTA as an anticoagulant (Blutspendezentrum Bern). The whole blood was centrifuged to separate RBCs and plasma. All centrifugations were performed at 400 × g for 3 min. The plasma was removed and the cells were washed ×3 with PBS. For storage, the cells were resuspended in Alsever's solution (4.2 g/l NaCl, 8 g/l sodium citrate, 0.55 g/l citric acid, 20.5 g/l dextrose) equal to the cell volume and stored at 4 ℃ for up to 2 weeks. Before a hemagglutination experiment, the RBCs were washed 2× with PBS and once with the buffer used for the experiment. Each hemagglutination reaction was performed in a round-bottom 96-well plate (ThermoFisher, 262162). The wells of the plate were blocked with 150 µl PBSA 1 % before any experiment to improve the settling of the RBCs. The PBSA 1 % was then completely removed and 50 µl reaction buffer containing the desired antigen were added to the wells. After establishing the desired dilution series of the antigens, 50 µl of a 1 % solution (v/v) of RBCs in the desired buffer were added to each well, for a total volume of 100 µl. The plate was incubated without any agitation at RT for at least 1 h. Images were obtained by photographing the plate on top of a transilluminator.

5 References

[1] Mya Breitbart and Forest Rohwer. Here a virus, there a virus, everywhere the same virus? *Trends in microbiology*, 13(6):278{284, 2005.

[2] Editorial. Microbiology by numbers. *Nat Rev Microbiol*, 9:628, 2011.

[3] Marc P Girard, Thomas Cherian, Yuri Pervikov, and Marie Paule Kieny. A review of vaccine research and development: human acute respiratory infections. *Vaccine*, 23(50):5708{5724, 2005.

[4] CA Suttle. The signi cance of viruses to mortality in aquatic microbial communities. *Microbial ecology*, 28(2):237{243, 1994.

[5] Ken Cadwell. The virome in host health and disease. *Immunity*, 42(5):805{813, 2015.

[6] Clare L Jolly and Quentin J Sattentau. Attachment factors. In *Viral Entry into Host Cells*, pages 1{23. Springer, 2006.

[7] Mark Marsh and Ari Helenius. Virus entry: open sesame. *Cell*, 124(4):729{740, 2006.

[8] Joe Grove and Mark Marsh. The cell biology of receptor-mediated virus entry. *J Cell Biol*, 195(7):1071{1082, 2011.

[9] George Orthopoulos, Kathy Trianta lou, and Martha Trianta lou. Coxsackie b viruses use multiple receptors to infect human cardiac cells. *Journal of medical virology*, 74(2):291{299, 2004.

[10] Wenqiang Wang and Guan-Zhu Han. Pervasive positive selection on virus receptors driven by host-virus con icts in mammals. *Journal of Virology*, 95(20):e01029{21, 2021.

[11] Andrea Reischl, Manuela Reithmayer, Gabriele Winsauer, Rosita Moser, Irene Goesler, and Dieter Blaas. Viral evolution toward change in receptor usage: adaptation of a major group human rhinovirus to grow in icam-1-negative cells. *Journal of virology*, 75(19):9312{9319, 2001.

[12] Eric Baranowski, Carmen M Ruiz-Jarabo, and Esteban Domingo. Evolution of cell recognition by viruses. *Science*, 292(5519):1102{1105, 2001.

[13] Shuai Lu, Xi-xiu Xie, Lei Zhao, Bin Wang, Jie Zhu, Ting-rui Yang, Guang-wen Yang, Mei Ji, Cui-ping Lv, Jian Xue, et al. The immunodominant and neutralization linear epitopes for sars-cov-2. *Cell reports*, 34(4):108666, 2021.

[14] Gunther Spohn and Martin F Bachmann. Therapeutic vaccination to block receptor{ligand interactions. *Expert opinion on biological therapy*, 3(3):469{476, 2003.

[15] L Kilham and LJ Olivier. A latent virus of rats isolated in tissue culture. *Virology*, 7(4):428{437, 1959.

[16] LV Crawford. A minute virus of mice. *Virology*, 29(4):605{612, 1966.

[17] YE Cossart, B Cant, AM Field, and D Widdows. Parvovirus-like particles in human sera. *The Lancet*, 305(7898):72{73, 1975.

[18] Neil R Blacklow, M David Hoggan, and Wallace P Rowe. Isolation of adenovirus-associated viruses from man. *Proceedings of the National Academy of Sciences of the United States of America*, 58(4):1410, 1967.

[19] Tobias Allander, Martti T Tammi, Margareta Eriksson, Annelie Bjerkner, Annika Tiveljung-Lindell, and Bjorn Andersson. Cloning of a human parvovirus by molecular screening of respiratory tract samples. *Proceedings of the National Academy of Sciences*, 102(36):12891{12896, 2005.

[20] Tuomas Jartti, Klaus Hedman, Laura Jartti, Olli Ruuskanen, Tobias Allander, and Maria Soderlund-Venermo. Human bocavirus|the rst 5 years. *Reviews in medical virology*, 22(1):46{64, 2012.

[21] Tung G Phan, Nguyen P Vo, Isidore JO Bonkoungou, Amit Kapoor, Nicolas Barro, Miguel O'Ryan, Beatrix Kapusinszky, Chunling Wang, and Eric Delwart. Acute diarrhea in west african children: diverse enteric viruses and a novel parvovirus genus. *Journal of virology*, 86(20):11024{11030, 2012.

[22] Tung G Phan, Khira Sdiri-Loulizi, Mahjoub Aouni, Katia Ambert-Balay, Pierre Pothier, Xutao Deng, and Eric Delwart. New parvovirus in child with unexplained diarrhea, tunisia. *Emerging infectious diseases*, 20(11):1911, 2014.

[23] Tung G Phan, Brigitte Dreno, Antonio Charlys Da Costa, Linlin Li, Patricia Orlandi, Xutao Deng, Beatrix Kapusinszky, Juliana Siqueira, Anne-Chantal Knol, Franck Halary, et al. A new protoparvovirus in human fecal samples and cutaneous t cell lymphomas (mycosis fungoides). *Virology*, 496:299{305, 2016.

[24] Morris S Jones, Amit Kapoor, Vladimir V Lukashov, Peter Simmonds, Frederick Hecht, and Eric Delwart. New dna viruses identi ed in patients with acute viral infection syndrome. *Journal of virology*, 79(13):8230{8236, 2005.

[25] J Kisary, B Nagy, and Z Bitay. Presence of parvoviruses in the intestine of chickens showing stunting syndrome. *Avian pathology*, 13(2):339{343, 1984.

[26] Herman Tse, Hoi-Wah Tsoi, Jade LL Teng, Xin-Chun Chen, Haiying Liu, Boping Zhou, Bo-Jian Zheng, Patrick CY Woo, Susanna KP Lau, and Kwok-Yung Yuen. Discovery and genomic characterization of a novel ovine partetravirus and a new genotype of bovine partetravirus. *PLoS One*, 6(9), 2011.

[27] FC Wong, JG Spearman, MA Smolenski, and PC Loewen. Equine parvovirus: initial isolation and partial characterization. *Canadian journal of comparative medicine*, 49(1):50, 1985.

[28] Francis R Abinanti and Mildred S War eld. Recovery of a hemadsorbing virus (haden) from the gastrointestinal tract of calves. *Virology*, 14:288, 1961.

[29] HS Joo, CR Donaldson-Wood, and RH Johnson. Observations on the pathogenesis of porcine parvovirus infection. *Archives of virology*, 51(1-2):123{129, 1976.

[30] Laszlo Zsak, Ra Mi Cha, and J Michael Day. Chicken parvovirus{induced runting-stunting syndrome in young broilers. *Avian diseases*, 57(1):123{127, 2013.

[31] Robert B Morrison and Han S Joo. Acute reproductive losses due to porcine parvovirus infection in a swine herd: Herd observations and economic analysis of the losses. *Preventive Veterinary Medicine*, 2(5):699{706, 1984.

[32] TA Cave, H Thompson, SWJ Reid, DR Hodgson, and DD Addie. Kitten mortality in the united kingdom: a retrospective analysis of 274 histopathological examinations (1986 to 2000)*Veterinary Record*, 151(17):497{501, 2002.

[33] Romane A Awad, Wagdy KB Khalil, and Ashraf G Attallah. Epidemiology and diagnosis of feline panleukopenia virus in egypt: Clinical and molecular diagnosis in cats.*Veterinary world*, 11(5):578, 2018.

[34] RH Johnson, GEORGE MARGOLIS, and LAWRENCE KILHAM. Identity of feline ataxia virus with feline panleucopenia virus.*Nature*, 214(5084):175{177, 1967.

[35] WF Robinson, GE Wilcox, and RLP Flower. Canine parvoviral disease: experimental reproduction of the enteric form with a parvovirus isolated from a case of myocarditis. *Veterinary pathology*, 17(5):589{599, 1980.

[36] WF Robinson, GE Wilcox, RL Flower, and JR Smith. Evidence for a parvovirus as the aetiologic agent in the myocarditis of puppies. *Australian veterinary journal*, 55(6):294, 1979.

[37] Elisabeth M Siedek, Holger Schmidt, Gordon H Sture, and Ruediger Raue. Vaccination with canine parvovirus type 2 (cpv-2) protects against challenge with virulent cpv-2b and cpv-2c.*Berliner und Munchener Tierarztliche Wochenschrift*, 124(1-2):58{64, 2011.

[38] John A Wagner, Thomas Reynolds, Mary Lynn Moran, Richard B Moss, Je rey J Wine, Terence R Flotte, and Phyllis Gardner. E cient and persistent gene transfer of aav-cftr in maxillary sinus. *The Lancet*, 351(9117):1702{1703, 1998.

[39] Richard B Moss, David Rodman, L Terry Spencer, Moira L Aitken, Pamela L Zeitlin, David Waltz, Carlos Milla, Alan S Brody, John P Clancy, Bonnie Ramsey, et al. Repeated adeno-associated virus serotype 2 aerosol-mediated cystic brosis transmembrane regulator gene transfer to the lungs of patients with cystic brosis: a multicenter, double-blind, placebo-controlled trial. *Chest*, 125(2):509{521, 2004.

[40] Dongsheng Duan. Systemic aav micro-dystrophin gene therapy for duchenne muscular dystrophy*Molecular Therapy*, 26(10):2337{2356, 2018.

[41] Assia Angelova, Tiago Ferreira, Clemens Bretscher, Jean Rommelaere, and Antonio Marchini. Parvovirus-based combinatorial immunotherapy: A reinforced therapeutic strategy against poor-prognosis solid cancers. *Cancers*, 13(2):342, 2021.

[42] Karsten Geletneky, Jacek Hajda, Assia L Angelova, Barbara Leuchs, David Capper, Andreas J Bartsch, Jan-Oliver Neumann, Tilman Schöning, Johannes Hüsing, Birgit Beelte, et al. Oncolytic h-1 parvovirus shows safety and signs of immunogenic activity in a rst phase i/iia glioblastoma trial. *Molecular Therapy*, 25(12):2620{2634, 2017.

[43] Remo Leisi, Jan Bieri, Nathan J Roth, and Carlos Ros. Determination of parvovirus retention pro les in virus lter membranes using laser scanning microscopy.*Journal of Membrane Science*, page 118012, 2020.

[44] ICTV international commitee on taxonomy of viruses. `https://talk.ictvonline.org/taxonomy/`. Accessed: 2020-04-16.

[45] N Nicolay and S Cotter. Clinical and epidemiological aspects of parvovirus b19 infections in ireland, january 1996-june 2008. *Eurosurveillance*, 14(25):19249, 2009.

[46] Uniprot protein sequence database - genome sequences. https://www.uniprot.org/uniprot/Q784T0. Accessed: 2020-04-24.

[47] Lynette Sawyer, Deborah Hanson, Grace Castro, William Luckett, Thomas W Dubensky Jr, and Adonis Stassinopoulos. Inactivation of parvovirus b19 in human platelet concentrates by treatment with amotosalen and ultraviolet a illumination. *Transfusion*, 47(6):1062{1070, 2007.

[48] BJ Cohen and KE Brown. Laboratory infection with human parvovirus b19. *The Journal of infection*, 24(1):113{114, 1992.

[49] Johannes Blümel, Ivo Schmidt, Hannelore Willkommen, and Johannes Löwer. Inactivation of parvovirus b19 during pasteurization of human serum albumin. *Transfusion*, 42(8):1011{1018, 2002.

[50] M Yunoki, M Tsujikawa, T Urayama, Y Sasaki, M Morita, H Tanaka, S Hattori, K Takechi, and K Ikuta. Heat sensitivity of human parvovirus b19. *Vox sanguinis*, 84(3):164{169, 2003.

[51] Mikihiro Yunoki, Takeru Urayama, Muneo Tsujikawa, Yoshie Sasaki, Shunichi Abe, Kazuo Takechi, and Kazuyoshi Ikuta. Inactivation of parvovirus b19 by liquid heating incorporated in the manufacturing process of human intravenous immunoglobulin preparations. *British journal of haematology*, 128(3):401{404, 2005.

[52] Jesse Summers, SE Jones, and MJ Anderson. Characterization of the genome of the agent of erythrocyte aplasia permits its classi cation as a human parvovirus. *Journal of General Virology*, 64(11):2527{2532, 1983.

[53] Giampaolo Zuccheri, Anna Bergia, Giorgio Gallinella, Monica Musiani, and Bruno Samor. Scanning force microscopy study on a single-stranded dna: The genome of parvovirus b19. *Chembiochem*, 2(3):199{204, 2001.

[54] Matthew C Blundell, Caroline Beard, and Caroline R Astell. In vitro identi cation of a b19 parvovirus promoter. *Virology*, 157(2):534{538, 1987.

[55] Mili Jain, Gurleen Oberoi, Rashmi Kumar, and Ashutosh Kumar. Erythrovirus b19 induced persistent bicytopenia in a healthy child. *Revista brasileira de hematologia e hemoterapia*, 39:278{280, 2017.

[56] Senthil Velan Bhoopalan, Lily Jun-shen Huang, and Mitchell J Weiss. Erythropoietin regulation of red blood cell production: From bench to bedside and back. *F1000Research*, 9, 2020.

[57] Kevin E Brown, Stacie M Anderson, and Neal S Young. Erythrocyte p antigen: cellular receptor for b19 parvovirus. *Science*, 262(5130):114{117, 1993.

[58] Kevin E Brown, Jonathan R Hibbs, Giorgio Gallinella, Stacie M Anderson, Elton D Lehman, Peggy McCarthy, and Neal S Young. Resistance to parvovirus b19 infection due to lack of virus receptor (erythrocyte p antigen). *New England Journal of Medicine*, 330(17):1192{1196, 1994.

[59] Waqas Nasir, Jonas Nilsson, Sigvard Olofsson, Marta Bally, and Gustaf E Rydell. Parvovirus b19 vlp recognizes globoside in supported lipid bilayers. *Virology*, 456:364{369, 2014.

[60] Barbel Kaufmann, Ulrich Baxa, Paul R Chipman, Michael G Rossmann, Susanne Modrow, and Robert Seckler. Parvovirus b19 does not bind to membrane-associated globoside in vitro. *Virology*, 332(1):189{198, 2005.

[61] Carlos Ros, Marco Gerber, and Christoph Kempf. Conformational changes in the vp1-unique region of native human parvovirus b19 lead to exposure of internal sequences that play a role in virus neutralization and infectivity. *Journal of virology*, 80(24):12017{12024, 2006.

[62] Dong Xu and Yang Zhang. Ab initio protein structure assembly using continuous structure fragments and optimized knowledge-based force eld. *Proteins: Structure, Function, and Bioinformatics*, 80(7):1715{1735, 2012.

[63] Keiya Ozawa, Gary Kurtzman, and Neal Young. Replication of the b19 parvovirus in human bone marrow cell cultures. *Science*, 233(4766):883{886, 1986.

[64] Keiya Ozawa, Gary Kurtzman, and Neal Young. Productive infection by b19 parvovirus of human erythroid bone marrow cells in vitro. 1987.

[65] Yasuhiko Munakata, Takako Saito-Ito, Keiko Kumura-Ishii, Jie Huang, Takao Kodera, Tomonori Ishii, Yasuhiko Hirabayashi, Yoshio Koyanagi, and Takeshi Sasaki. Ku80 autoantigen as a cellular coreceptor for human parvovirus b19 infection. *Blood*, 106(10):3449{3456, 2005.

[66] Kirsten A Weigel-Kelley, Mervin C Yoder, and Arun Srivastava. $\alpha 5\beta 1$ integrin as a cellular coreceptor for human parvovirus b19: requirement of functional activation of $\beta 1$ integrin for viral entry. *Blood*, 102(12):3927{3933, 2003.

[67] Kirsten A Weigel-Kelley, Mervin C Yoder, and Arun Srivastava. Recombinant human parvovirus b19 vectors: erythrocyte p antigen is necessary but not su cient for successful transduction of human hematopoietic cells. *Journal of virology*, 75(9):4110{4116, 2001.

[68] Claudia Bonsch, Christoph Zuercher, Patricia Lieby, Christoph Kempf, and Carlos Ros. The globoside receptor triggers structural changes in the b19 virus capsid that facilitate virus internalization. *Journal of virology*, 84(22):11737{11746, 2010.

[69] Remo Leisi, Chiarina Di Tommaso, Christoph Kempf, and Carlos Ros. The receptor-binding domain in the vp1u region of parvovirus b19. *Viruses*, 8(3):61, 2016.

[70] Remo Leisi, Nico Ruprecht, Christoph Kempf, and Carlos Ros. Parvovirus b19 uptake is a highly selective process controlled by vp1u, a novel determinant of viral tropism. *Journal of virology*, 87(24):13161{13167, 2013.

[71] Remo Leisi, Marcus von Nordheim, Christoph Kempf, and Carlos Ros. Speci c targeting of proerythroblasts and erythroleukemic cells by the vp1u region of parvovirus b19. *Bioconjugate chemistry*, 26(9):1923{1930, 2015.

[72] Remo Leisi, Marcus Von Nordheim, Carlos Ros, and Christoph Kempf. The vp1u receptor restricts parvovirus b19 uptake to permissive erythroid cells. *Viruses*, 8(10):265, 2016.

[73] MJ Anderson, PG Higgins, LR Davis, JS Willman, SE Jones, IM Kidd, JR Pattison, and DAJ Tyrrell. Experimental parvoviral infection in humans. *Journal of Infectious Diseases*, 152(2):257{265, 1985.

[74] Francis A Plummer, Gregory W Hammond, Kevin Forward, Leila Sekla, Linda M Thompson, SE Jones, IM Kidd, and Mary J Anderson. An erythema infectiosum|like illness caused by human parvovirus infection. *New England Journal of Medicine*, 313(2):74{79, 1985.

[75] JR Pattison et al. Parvovirus infections and hypoplastic crisis in sickle-cell anaemia.*Parvovirus infections and hypoplastic crisis in sickle-cell anaemia.*, 1:664{665, 1981.

[76] Helen M Faddy, Elise C Gorman, Veronica C Hoad, Francesca D Frentiu, Sarah Tozer, and RLP Flower. Seroprevalence of antibodies to primate erythroparvovirus 1 (b19v) in australia.*BMC infectious diseases*, 18(1):1{7, 2018.

[77] Richard Yomi Akele, Jennifer Tamuno Abelekum, Bernard Oluwapelumi Oluboyo, Janet Funmilayo Akinseye, Seyi Samson Enitan, Olusola Ayodeji Olayanju, and Emmanuel Jide Akele. Prevalence of human parvovirus b19 igg and igm antibodies among pregnant women attending antenatal clinic at federal teaching hospital ido-ekiti, nigeria. *African Journal of Infectious Diseases*, 15(2):10, 2021.

[78] C Rohrer, B Gartner, A Sauerbrei, S Bohm, B Hottentrager, U Raab, W Thierfelder, P Wutzler, and Susanne Modrow. Seroprevalence of parvovirus b19 in the german population.*Epidemiology & Infection*, 136(11):1564{1575, 2008.

[79] MJ Anderson, SEyt Jones, SP Fisher-Hoch, et al. Human parvo virus, the cause of erythema infectiosum (fth disease)? *Human parvo virus, the cause of erythema infectiosum (fifth disease)?*, 1, 1983.

[80] DM Reid, T Brown, TMS Reid, JAN Rennie, and CJ Eastmond. Human parvovirus-associated arthritis: a clinical and laboratory description. *The Lancet*, 325(8426):422{425, 1985.

[81] GJ Kurtzman, BJ Cohen, AM Field, R Oseas, RM Blaese, NS Young, et al. Immune response to b19 parvovirus and an antibody defect in persistent viral infection. *The Journal of clinical investigation*, 84(4):1114{1123, 1989.

[82] Prasad Rao Koduri. Parvovirus b19-related anemia in hiv-infected patients.*AIDS patient care and STDs*, 14(1):7{11, 2000.

[83] Nguyen L Toan, Bui T Sy, Le H Song, Hoang V Luong, Nguyen T Binh, Vu Q Binh, Reinhard Kandolf, Thirumalaisamy P Velavan, Peter G Kremsner, and C-Thomas Bock. Co-infection of human parvovirus b19 with plasmodium falciparum contributes to malaria disease severity in gabonese patients.*BMC infectious diseases*, 13(1):1{10, 2013.

[84] Rakesh Agarwal, Rashmi Baid, Rajarshi Datta, Manjari Saha, and Nirmalendu Sarkar. Falciparum malaria and parvovirus b19 coinfection: A rare entity. *Tropical parasitology*, 7(1):47, 2017.

[85] Stanley J Naides and Carl P Weiner. Antenatal diagnosis and palliative treatment of non-immune hydrops fetalis secondary to fetal parvovirus b19 infection. *Prenatal diagnosis*, 9(2):105{114, 1989.

[86] Kathleen E Simpson, Gregory A Storch, Caroline K Lee, Kent E Ward, Saar Danon, Catherine M Simon, Je rey W Delaney, Alan Tong, and Charles E Canter. High frequency of detection by pcr of viral nucleic acid in the blood of infants presenting with clinical myocarditis. *Pediatric cardiology*, 37(2):399{404, 2016.

[87] Laura A Adamson-Small, Igor V Ignatovich, Monica G Laemmerhirt, and Jacqueline A Hobbs. Persistent parvovirus b19 infection in non-erythroid tissues: possible role in the in ammatory and disease process. *Virus research*, 190:8{16, 2014.

[88] Anne Kristine Valeur-Jensen, Carsten B Pedersen, Tine Westergaard, Inge P Jensen, Morten Lebech, Per K Andersen, Peter Aaby, Bent N rgaard Pedersen, and Mads Melbye. Risk factors for parvovirus b19 infection in pregnancy. *Jama*, 281(12):1099{1105, 1999.

[89] Centers for Disease Control (CDC et al. Risks associated with human parvovirus b19 infection.*MMWR. Morbidity and mortality weekly report*, 38(6):81{97, 1989.

[90] T Brown, A Anand, LD Ritchie, JP Clewley, and TMS Reid. Intrauterine parvovirus infection associated with hydrops fetalis. *The Lancet*, 324(8410):1033{1034, 1984.

[91] Nobuo Yaegashi. Pathogenesis of nonimmune hydrops fetalis caused by intrauterine b19 infection.*The Tohoku journal of experimental medicine*, 190(2):65{82, 2000.

[92] Deborah M Feldman, Diane Timms, and Adam F Borgida. Toxoplasmosis, parvovirus, and cytomegalovirus in pregnancy. *Clinics in laboratory medicine*, 30(3):709{720, 2010.

[93] Wolfgang Holzgreve, Cynthia JR Curry, Mitchell S Golbus, Peter W Callen, Roy A Filly, and J Charles Smith. Investigation of nonimmune hydrops fetalis. *American journal of obstetrics and gynecology*, 150(7):805{812, 1984.

[94] Public Health Laboratory Service Working Party on Fifth Disease. Prospective study of human parvovirus (b19) infection in pregnancy. *BMJ: British Medical Journal*, pages 1166{1170, 1990.

[95] LARRY J ANDERSON. Role of parvovirus b19 in human disease. *The Pediatric infectious disease journal*, 6(8):711{718, 1987.

[96] MJ Anderson, E Lewis, IM Kidd, SM Hall, and BJ Cohen. An outbreak of erythema infectiosum associated with human parvovirus infection. *Epidemiology & Infection*, 93(1):85{93, 1984.

[97] Sally A Baylis, Nita Shah, and Philip D Minor. Evaluation of di erent assays for the detection of parvovirus b19 dna in human plasma. *Journal of virological methods*, 121(1):7{16, 2004.

[98] Jun Yi Sim, Luan-Yin Chang, Jong-Min Chen, Ping-Ing Lee, Li-Min Huang, and Chun-Yi Lu. Human parvovirus b19 infection in patients with or without underlying diseases. *Journal of Microbiology, Immunology and Infection*, 52(4):534{541, 2019.

[99] Ulla M Saarinen, Terence L Chorba, Peter Tattersall, Neal S Young, Larry J Anderson, Erskine Palmer, and Peter F Coccia. Human parvovirus b19-induced epidemic acute red cell aplasia in patients with hereditary hemolytic anemia. 1986.

[100] LJ Anderson, C Tsou, RA Parker, TL Chorba, H Wul , P Tattersall, and PP Mortimer. Detection of antibodies and antigens of human parvovirus b19 by enzyme-linked immunosorbent assay. *Journal of clinical microbiology*, 24(4):522{526, 1986.

[101] Jonathan R Kerr. Pathogenesis of human parvovirus b19 in rheumatic disease. *Annals of the rheumatic diseases*, 59(9):672{683, 2000.

[102] Maria Soderlund, Caroline S Brown, Willy JM Spaan, Lea Hedman, and Klaus Hedman. Epitope type-speci c igg responses to capsid proteins vp1 and vp2 of human parvovirus b19. *Journal of Infectious Diseases*, 172(6):1431{1436, 1995.

[103] Stacie Anderson, Mikio Momoeda, Masako Kawase, Sachiko Kajigaya, and Neal S Young. Peptides derived from the unique region of b19 parvovirus minor capsid protein elicitneutralizing antibodies in rabbits. *Virology*, 206(1):626{632, 1995.

[104] Elisa Zu , Elisabetta Manaresi, Giorgio Gallinella, Giovanna A Gentilomi, Simona Venturoli, Marialuisa Zerbini, and Monica Musiani. Identi cation of an immunodominant peptide in the parvovirus b19 vp1 unique region able to elicit a long-lasting immune response in humans. *Viral immunology*, 14(2):151{158, 2001.

[105] TOMOKO Saikawa, STACIE Anderson, MIKIO Momoeda, SACHIKO Kajigaya, and NEAL S Young. Neutralizing linear epitopes of b19 parvovirus cluster in the vp1 unique and vp1-vp2 junction regions. *Journal of virology*, 67(6):3004{3009, 1993.

[106] Nancy L Meyer, Guiqing Hu, Omar Davulcu, Qing Xie, Alex J Noble, Craig Yoshioka, Drew S Gingerich, Andrew Trzynka, Larry David, Scott M Stagg, et al. Structure of the gene therapy vector, adeno-associated virus with its cell receptor, aavr. *Elife*, 8:e44707, 2019.

[107] Laura B Goodman, Sangbom M Lyi, Natalie C Johnson, Javier O Cifuente, Susan L Hafenstein, and Colin R Parrish. Binding site on the transferrin receptor for the parvovirus capsid and e ects of altered a nity on cell uptake and infection. *Journal of virology*, 84(10):4969{4978, 2010.

[108] Lin-Ya Huang, Ami Patel, Robert Ng, Edward Blake Miller, Sujata Halder, Robert McKenna, Aravind Asokan, and Mavis Agbandje-McKenna. Characterization of the adeno-associated virus 1 and 6 sialic acid binding site. *Journal of virology*, 90(11):5219{5230, 2016.

[109] Alberto Lopez-Bueno, Mari-Paz Rubio, Nathan Bryant, Robert McKenna, Mavis Agbandje-McKenna, and Jose M Almendral. Host-selected amino acid changes at the sialic acid binding pocket of the parvovirus capsid modulate cell binding a nity and determine virulence. *Journal of virology*, 80(3):1563{1573, 2006.

[110] JR Kerr and VS Cunni e. Antibodies to parvovirus b19 non-structural protein are associated with chronic but not acute arthritis following b19 infection. *Rheumatology*, 39(8):903{908, 2000.

[111] Andreas von Poblotzki, Andrea Hemauer, Andreas Gigler, Elisabeth Puchhammer-Stockl, Franz Xaver Heinz, Jorg Pont, Klaus Laczika, Hans Wolf, and Susanne Modrow. Antibodies to the nonstructural protein of parvovirus b19 in persistently infected patients: implications for pathogenesis. *Journal of Infectious Diseases*, 172(5):1356{1359, 1995.

[112] Erik D Heegaard, Cecilie J Rasksen, and Jesper Christensen. Detection of parvovirus b19 ns1-speci c antibodies by elisa and western blotting employing recombinant ns1 protein as antigen. *Journal of medical virology*, 67(3):375{383, 2002.

[113] Kristina von Kietzell, Tanja Pozzuto, Regine Heilbronn, Tobias Grossl, Henry Fechner, and Stefan Weger. Antibody-mediated enhancement of parvovirus b19 uptake into endothelial cells mediated by a receptor for complement factor c1q. *Journal of virology*, 88(14):8102{8115, 2014.

[114] Yasuhiko Munakata, Ichiro Kato, Takako Saito, Takao Kodera, Keiko Kumura Ishii, and Takeshi Sasaki. Human parvovirus b19 infection of monocytic cell line u937 and antibody-dependent enhancement. *Virology*, 345(1):251{257, 2006.

[115] JSM Peiris, S Gordon, JC Unkeless, and JS Porter eld. Monoclonal anti-fc receptor igg blocks antibody enhancement of viral replication in macrophages. *Nature*, 289(5794):189{191, 1981.

[116] Brian J Mady, David V Erbe, Ichiro Kurane, Michael W Fanger, and Francis A Ennis. Antibody-dependent enhancement of dengue virus infection mediated by bispeci c antibodies against cell surface molecules other than fc gamma receptors. *The journal of immunology*, 147(9):3139{3144, 1991.

[117] Silva Quattrocchi, Nico Ruprecht, Claudia Bonsch, Sven Bieli, Christoph Zurcher, Klaus Boller, Christoph Kempf, and Carlos Ros. Characterization of the early steps of human parvovirus b19 infection. *Journal of virology*, 86(17):9274{9284, 2012.

[118] Bernhard Mani, Claudia Baltzer, Noelia Valle, Jose M Almendral, Christoph Kempf, and Carlos Ros. Low ph-dependent endosomal processing of the incoming parvovirus minute virus of mice virion leads to externalization of the vp1 n-terminal sequence (n-vp1), n-vp2 cleavage, and uncoating of the full-length genome. *Journal of Virology*, 80(2):1015{1024, 2006.

[119] Zoltan Zadori, Jozsef Szelei, Marie-Claude Lacoste, Yi Li, Sebastien Gariepy, Philippe Raymond, Marc Allaire, Ivan R Nabi, and Peter Tijssen. A viral phospholipase a2 is required for parvovirus infectivity. *Developmental cell*, 1(2):291{302, 2001.

[120] Susan F Cotmore, Anthony M D'Abramo Jr, Christine M Ticknor, and Peter Tattersall. Controlled conformational transitions in the mvm virion expose the vp1 n-terminus and viral genome without particle disassembly. *Virology*, 254(1):169{181, 1999.

[121] Glen A Farr, Susan F Cotmore, and Peter Tattersall. Vp2 cleavage and the leucine ring at the base of the vefold cylinder control ph-dependent externalization of both the vp1 n terminus and the genome of minute virus of mice. *Journal of Virology*, 80(1):161{171, 2006.

[122] Carlos Ros, Christoph J Burckhardt, and Christoph Kempf. Cytoplasmic tra cking of minute virus of mice: low-ph requirement, routing to late endosomes, and proteasome interaction. *Journal of virology*, 76(24):12634{12645, 2002.

[123] Judit J Penzes, Paul Chipman, Nilakshee Bhattacharya, Allison Zeher, Rick Huang, Robert McKenna, and Mavis Agbandje-McKenna. Adeno-associated virus 9 structural rearrangements induced by endosomal tra cking ph and glycan attachment. *Journal of Virology*, 95(19):e00843{21, 2021.

[124] Claudia Filippone, Ning Zhi, Susan Wong, Jun Lu, Sachiko Kajigaya, Giorgio Gallinella, Laura Kakkola, Maria Söderlund-Venermo, Neal S Young, and Kevin E Brown. Vp1u phospholipase activity is critical for infectivity of full-length parvovirus b19 genomic clones. *Virology*, 374(2):444{452, 2008.

[125] Glen A Farr, Li-guo Zhang, and Peter Tattersall. Parvoviral virions deploy a capsid-tethered lipolytic enzyme to breach the endosomal membrane during cell entry. *Proceedings of the National Academy of Sciences*, 102(47):17148{17153, 2005.

[126] Stefanie Stahnke, Kerstin Lux, Silke Uhrig, Florian Kreppel, Marianna Hösel, Oliver Coutelle, Manfred Ogris, Michael Hallek, and Hildegard Büning. Intrinsic phospholipase a2 activity of adeno-associated virus is involved in endosomal escape of incoming particles. *Virology*, 409(1):77{83, 2011.

[127] Maija Vihinen-Ranta, Sanna Suikkanen, and Colin R Parrish. Pathways of cell infection by parvoviruses and adeno-associated viruses. *Journal of virology*, 78(13):6709{6714, 2004.

[128] Severine Bär, Jean Rommelaere, and Jürg PF Nüesch. Vesicular transport of progeny parvovirus particles through er and golgi regulates maturation and cytolysis. *PLoS pathogens*, 9(9):e1003605, 2013.

[129] Oliver Caliaro, Andrea Marti, Nico Ruprecht, Remo Leisi, Suriyasri Subramanian, Susan Hafenstein, and Carlos Ros. Parvovirus b19 uncoating occurs in the cytoplasm without capsid disassembly and it is facilitated by depletion of capsid-associated divalent cations. *Viruses*, 11(5):430, 2019.

[130] Nelly Panté and Michael Kann. Nuclear pore complex is able to transport macromolecules with diameters of 39 nm. *Molecular biology of the cell*, 13(2):425{434, 2002.

[131] Eleuterio Lombardo, Juan C Ramirez, Javier Garcia, and Jose M Almendral. Complementary roles of multiple nuclear targeting signals in the capsid proteins of the parvovirus minute virus of mice during assembly and onset of infection. *Journal of virology*, 76(14):7049{7059, 2002.

[132] Joshua C Grieger, Stephen Snowdy, and Richard J Samulski. Separate basic region motifs within the adeno-associated virus capsid proteins are essential for infectivity and assembly. *Journal of virology*, 80(11):5199{5210, 2006.

[133] Maija Vihinen-Ranta, Laura Kakkola, Anne Kalela, Pekka Vilja, and Matti Vuento. Characterization of a nuclear localization signal of canine parvovirus capsid proteins. *European journal of biochemistry*, 250(2):389{394, 1997.

[134] Yong Luo, Steve Kleiboeker, Xuefeng Deng, and Jianming Qiu. Human parvovirus b19 infection causes cell cycle arrest of human erythroid progenitors at late s phase that favors viral dna replication. *Journal of virology*, 87(23):12766{12775, 2013.

[135] Tarig Bashir, Rita Hörlein, Jean Rommelaere, and Kurt Willwand. Cyclin a activates the dna polymerase δ-dependent elongation machinery in vitro: a parvovirus dna replication model. *Proceedings of the National Academy of Sciences*, 97(10):5522{5527, 2000.

[136] SF Cotmore and P Tattersall. In vivo resolution of circular plasmids containing concatemer junction fragments from minute virus of mice dna and their subsequent replication as linear molecules. *Journal of Virology*, 66(1):420{431, 1992.

[137] Yong Luo and Jianming Qiu. Human parvovirus b19: a mechanistic overview of infection and dna replication. *Future virology*, 10(2):155{167, 2015.

[138] M Lo chelt, H Delius, and O-R Kaaden. A novel replicative form dna of aleutian disease virus: the covalently closed linear dna of the parvoviruses. *Journal of general virology*, 70(5):1105{1116, 1989.

[139] LOIS A Salzman and PHYLLIS Fabisch. Nucleotide sequence of the self-priming 3'terminus of the single-stranded dna extracted from the parvovirus kilham rat virus. *Journal of virology*, 30(3):946{950, 1979.

[140] Andreas Q Baldauf, Kurt Willwand, Eleni Mumtsidu, JP N esch, and Jean Rommelaere. Speci c initiation of replication at the right-end telomere of the closed species of minute virus of mice replicative-form dna. *Journal of Virology*, 71(2):971{980, 1997.

[141] Wuxiang Guan, Susan Wong, Ning Zhi, and Jianming Qiu. The genome of human parvovirus b19 can replicate in nonpermissive cells with the help of adenovirus genes and produces infectious virus. *Journal of virology*, 83(18):9541{9553, 2009.

[142] Gloria Bua, Elisabetta Manaresi, Francesca Bonvicini, and Giorgio Gallinella. Parvovirus b19 replication and expression in di erentiating erythroid progenitor cells. *PLoS One*, 11(2):e0148547, 2016.

[143] Yuko Yoto, Jianming Qiu, and David J Pintel. Identi cation and characterization of two internal cleavage and polyadenylation sites of parvovirus b19 rna. *Journal of virology*, 80(3):1604{1609, 2006.

[144] Wuxiang Guan, Fang Cheng, Qinfeng Huang, Steve Kleiboeker, and Jianming Qiu. Inclusion of the central exon of parvovirus b19 precursor mrna is determined by multiple splicing enhancers in both the exon and the downstream intron. *Journal of virology*, 85(5):2463{2468, 2011.

[145] Wuxiang Guan, Qinfeng Huang, Fang Cheng, and Jianming Qiu. Internal polyadenylation of the parvovirus b19 precursor mrna is regulated by alternative splicing. *Journal of Biological Chemistry*, 286(28):24793{24805, 2011.

[146] Keiya Ozawa and NEAL Young. Characterization of capsid and noncapsid proteins of b19 parvovirus propagated in human erythroid bone marrow cell cultures. *Journal of virology*, 61(8):2627{2630, 1987.

[147] Ning Zhi, Ian P Mills, Jun Lu, Susan Wong, Claudia Filippone, and Kevin E Brown. Molecular and functional analyses of a human parvovirus b19 infectious clone demonstrates essential roles for ns1, vp1, and the 11-kilodalton protein in virus replication and infectivity. *Journal of virology*, 80(12):5941{5950, 2006.

[148] Peng Xu, Zhe Zhou, Min Xiong, Wei Zou, Xuefeng Deng, Safder S Ganaie, Steve Kleiboeker, Jianxin Peng, Kaiyu Liu, Shengqi Wang, et al. Parvovirus b19 ns1 protein induces cell cycle arrest at g2-phase by activating the atr-cdc25c-cdk1 pathway. *PLoS pathogens*, 13(3):e1006266, 2017.

[149] Stanley Mo att, Nobuo Yaegashi, Kohtaro Tada, Nobuyuki Tanaka, and Kazuo Sugamura. Human parvovirus b19 nonstructural (ns1) protein induces apoptosis in erythroid lineage cells. *Journal of virology*, 72(4):3018{3028, 1998.

[150] Mikio Momoeda, Susan Wong, Masako Kawase, Neal S Young, and Sachiko Kajigaya. A putative nucleoside triphosphate-binding domain in the nonstructural protein of b19 parvovirus is required for cytotoxicity. *Journal of Virology*, 68(12):8443{8446, 1994.

[151] Sunil Kumar Tewary, Haiyan Zhao, Xuefeng Deng, Jianming Qiu, and Liang Tang. The human parvovirus b19 non-structural protein 1 n-terminal domain speci cally binds to the origin of replication in the viral dna. *Virology*, 449:297{303, 2014.

[152] CHRISTIAN Doerig, B Hirt, JEAN-PHILIPPE Antonietti, and PETER Beard. Nonstructural protein of parvoviruses b19 and minute virus of mice controls transcription. *Journal of virology*, 64(1):387{396, 1990.

[153] Masako Nomaguchi, Mikako Fujita, Yasuyuki Miyazaki, and Akio Adachi. Viral tropism. *Frontiers in microbiology*, 3:281, 2012.

[154] Aaron Yun Chen, Wuxiang Guan, Sai Lou, Zhengwen Liu, Steve Kleiboeker, and Jianming Qiu. Role of erythropoietin receptor signaling in parvovirus b19 replication in human erythroid progenitor cells. *Journal of virology*, 84(23):12385{12396, 2010.

[155] Steven G Elliott, MaryAnn Foote, and Graham Molineux. *Erythropoietins, erythropoietic factors, and erythropoiesis: molecular, cellular, preclinical, and clinical biology*. Springer Science & Business Media, 2009.

[156] Safder S Ganaie, Wei Zou, Peng Xu, Xuefeng Deng, Steve Kleiboeker, and Jianming Qiu. Phosphorylated stat5 directly facilitates parvovirus b19 dna replication in human erythroid progenitors through interaction with the mcm complex. *PLoS pathogens*, 13(5):e1006370, 2017.

[157] Aaron Yun Chen, Steve Kleiboeker, and Jianming Qiu. Productive parvovirus b19 infection of primary human erythroid progenitor cells at hypoxia is regulated by stat5a and mek signaling but not hifα. *PLoS Pathog*, 7(6):e1002088, 2011.

[158] Alison Sinclair, Sarah Yarranton, and Celine Schelcher. Dna-damage response pathways triggered by viral replication. *Expert reviews in molecular medicine*, 8(5):1{11, 2006.

[159] Yong Luo, Sai Lou, Xuefeng Deng, Zhengwen Liu, Yi Li, Steve Kleiboeker, and Jianming Qiu. Parvovirus b19 infection of human primary erythroid progenitor cells triggers atr-chk1 signaling, which promotes b19 virus replication. *Journal of virology*, 85(16):8046{8055, 2011.

[160] Richard O Adeyemi, Sebastien Landry, Meredith E Davis, Matthew D Weitzman, and David J Pintel. Parvovirus minute virus of mice induces a dna damage response that facilitates viral replication.*PLoS pathogens*, 6(10):e1001141, 2010.

[161] Sai Lou, Yong Luo, Fang Cheng, Qinfeng Huang, Weiran Shen, Steve Kleiboeker, John F Tisdale, Zhengwen Liu, and Jianming Qiu. Human parvovirus b19 dna replication induces a dna damage response that is dispensable for cell cycle arrest at phase g2/m.*Journal of virology*, 86(19):10748{10758, 2012.

[162] Giuseppina Giglia-Mari, Angelika Zotter, and Wim Vermeulen. Dna damage response.*Cold Spring Harbor perspectives in biology*, 3(1):a000745, 2011.

[163] K Ozawa, Jamshed Ayub, and Neal Young. Translational regulation of b19 parvovirus capsid protein production by multiple upstream aug triplets. *Journal of Biological Chemistry*, 263(22):10922{10926, 1988.

[164] Eleuterio Lombardo, Juan C Ramrez, Mavis Agbandje-McKenna, and Jose M Almendral. A beta-stranded motif drives capsid protein oligomers of the parvovirus minute virus of mice into the nucleus for viral assembly. *Journal of Virology*, 74(8):3804{3814, 2000.

[165] Pavel Plevka, Susan Hafenstein, Lei Li, Anthony D'Abrgamo Jr, Susan F Cotmore, Michael G Rossmann, and Peter Tattersall. Structure of a packaging-defective mutant of minute virus of mice indicates that the genome is packaged via a pore at a 5-fold axis*Journal of virology*, 85(10):4822{4827, 2011.

[166] Susan F Cotmore and Peter Tattersall. Genome packaging sense is controlled by the e ciency of the nick site in the right-end replication origin of parvoviruses minute virus of mice and luiii. *Journal of virology*, 79(4):2287{2300, 2005.

[167] Jianke Wang, Safder S Ganaie, Fang Cheng, Peng Xu, Kang Ning, Xiaomei Wang, Steve Kleiboeker, Shipeng Cheng, and Jianming Qiu. Rna binding motif protein rbm45 regulates expression of the 11-kilodalton protein of parvovirus b19 through binding to novel intron splicing enhancers. *Mbio*, 11(2):e00192{20, 2020.

[168] Weixing Luo and Caroline R Astell. A novel protein encoded by small rnas of parvovirus b19.*Virology*, 195(2):448{455, 1993.

[169] Mannie MY Fan, Lillian Tamburic, Cynthia Shippam-Brett, Darren B Zagrodney, and Caroline R Astell. The small 11-kda protein from b19 parvovirus binds growth factor receptor-binding protein 2 in vitro in a src homology 3 domain/ligand-dependent manner.*Virology*, 291(2):285{291, 2001.

[170] Safder S Ganaie and Jianming Qiu. Recent advances in replication and infection of human parvovirus b19. *Frontiers in cellular and infection microbiology*, 8:166, 2018.

[171] N Sol, J Le Junter, I Vassias, JM Freyssinier, A Thomas, AF Prigent, BB Rudkin, S Fichelson, and F Morinet. Possible interactions between the ns-1 protein and tumor necrosis factor alpha pathways in erythroid cell apoptosis induced by human parvovirus b19.*Journal of virology*, 73(10):8762{8770, 1999.

[172] Eiji Morita and Kazuo Sugamura. Human parvovirus b19-induced cell cycle arrest and apoptosis. In *Seminars in Immunopathology*, volume 24, page 187. Springer Nature BV, 2002.

[173] Aaron Yun Chen, Elizabeth Yan Zhang, Wuxiang Guan, Fang Cheng, Steve Kleiboeker, Thomas M Yankee, and Jianming Qiu. The small 11kda nonstructural protein of human parvovirus b19 plays a key role in inducing apoptosis during b19 virus infection of primary erythroid progenitor cells. *Blood, The Journal of the American Society of Hematology*, 115(5):1070{1080, 2010.

[174] Satoshi Shimomura, Norio Komatsu, Norbert Frickhofen, Stacie Anderson, Sachiko Kajigaya, and Neal S Young. First continuous propagation of b19 parvovirus in a cell line. 1992.

[175] NC Munshi, S Zhou, MJ Woody, DA Morgan, and A Srivastava. Successful replication of parvovirus b19 in the human megakaryocytic leukemia cell line mb-02.*Journal of virology*, 67(1):562{566, 1993.

[176] T Takahashi, K Ozawa, K Takahashi, Y Okuno, Y Muto, F Takaku, and S Asano. Dna replication of parvovirus b 19 in a human erythroid leukemia cell line (jk-1) in vitro. *Archives of virology*, 131(1):201{208, 1993.

[177] Eiji Miyagawa, Tsutomu Yoshida, Hirohiko Takahashi, Kazuhito Yamaguchi, Tohko Nagano, Yoshiko Kiriyama, Kazuo Okochi, and Hiroyuki Sato. Infection of the erythroid cell line, ku812ep6 with human parvovirus b19 and its application to titration of b19 infectivity. *Journal of virological methods*, 83(1-2):45{54, 1999.

[178] Perrine Caillet-Fauquet, Marie-Louise Draps, Mario Di Giambattista, Yvan De Launoit, and Ruth Laub. Hypoxia enables b19 erythrovirus to yield abundant infectious progeny in a pluripotent erythroid cell line. *Journal of virological methods*, 121(2):145{153, 2004.

[179] Raphael Wol sberg, Nico Ruprecht, Christoph Kempf, and Carlos Ros. Impaired genome encapsidation restricts the in vitro propagation of human parvovirus b19. *Journal of virological methods*, 193(1):215{225, 2013.

[180] Chun-Ching Chiu, Ya-Fang Shi, Jiann-Jou Yang, Yuan-Chao Hsiao, Bor-Show Tzang, and Tsai-Ching Hsu. E ects of human parvovirus b19 and bocavirus vp1 unique region on tight junction of human airway epithelial a549 cells. *PLoS One*, 9(9):e107970, 2014.

[181] Yasuto Tonegawa and Sen-itiroh Hakomori. \ganglioprotein and globoprotein": the glycoproteins reacting with anti-ganglioside and anti-globoside antibodies and the ganglioprotein change associated with transformation. *Biochemical and biophysical research communications*, 76(1):9{17, 1977.

[182] Keith S Fletcher, Eric G Bremer, and GA Schwarting. P blood group regulation of glycosphingolipid levels in human erythrocytes. *Journal of Biological Chemistry*, 254(22):11196{11198, 1979.

[183] Laura LW Cooling, Theodore AW Koerner, and Stanley J Naides. Multiple glycosphingolipids determine the tissue tropism of parvovirus b19. *Journal of Infectious Diseases*, 172(5):1198{1205, 1995.

[184] Reiji Kannagi, Thalia Papayannopoulou, Betty Nakamoto, Nancy A Cochran, Takashi Yokochi, George Stamatoyannopoulos, and Sen-itiroh Hakomori. Carbohydrate antigen pro les of human erythroleukemia cell lines hel and k562. 1983.

[185] Bernhard KNIEP, David A MONNER, Udo SCHWUL ERA, and Peter F M ̈UHLRADT. Glycosphingolipids of the globo-series are associated with the monocytic lineage of human myeloid cells. *European journal of biochemistry*, 149(1):187{191, 1985.

[186] Clement P Delannoy, Yoann Rombouts, Sophie Groux-Degroote, Stephanie Holst, Bernadette Coddeville, Anne Harduin-Lepers, Manfred Wuhrer, Elisabeth Elass-Rochard, and Yann Guerardel. Glycosylation changes triggered by the di erentiation of monocytic thp-1 cell line into macrophages. *Journal of proteome research*, 16(1):156{169, 2017.

[187] Kathryn E Stein and Donald M Marcus. Glycosphingolipids of puri ed human lymphocytes. *Biochemistry*, 16(24):5285{5291, 1977.

[188] William MF Lee, John C Klock, and Bruce A Macher. Isolation and structural characterization of human lymphocyte neutral glycosphingolipids. *Biochemistry*, 20(13):3810{3814, 1981.

[189] Dennis E Vance and Charles C Sweeley. Quantitative determination of the neutral glycosyl ceramides in human blood. *Journal of lipid research*, 8(6):621{630, 1967.

[190] G Dawson, AW Kruski, and AM Scanu. Distribution of glycosphingolipids in the serum lipoproteins of normal human subjects and patients with hypo-and hyperlipidemias. *Journal of lipid research*, 17(2):125{131, 1976.

[191] Carole C Wegner and Jeanne A Jordan. Human parvovirus b19 vp2 empty capsids bind to human villous trophoblast cells in vitro via the globoside receptor. *Infectious diseases in obstetrics and gynecology*, 12(2):69{78, 2004.

[192] Y Kamasaki, T Nakamura, Keigo Yoshizaki, T Iwamoto, A Yamada, E Fukumoto, Y Maruya, K Iwabuchi, K Furukawa, T Fujiwara, et al. Glycosphingolipids regulate ameloblastin expression in dental epithelial cells. *Journal of dental research*, 91(1):78{83, 2012.

[193] Eric Coles and J Lindsley Foote. Glycosphingolipids from rabbit aorta, plasma, and red blood cells: e ects of high cholesterol-high fat diets on fatty acid distribution and quantity of glycosphingolipids. *Journal of lipid research*, 15(3):192{199, 1974.

[194] KE Brown and BJ Cohen. Haemagglutination by parvovirus b19. *Journal of general virology*, 73(8):2147{2149, 1992.

[195] BA Macher and John C Klock. Isolation and chemical characterization of neutral glycosphingolipids of human neutrophils. *Journal of Biological Chemistry*, 255(5):2092{2096, 1980.

[196] Lelio Orci, Mariella Ravazzola, Paolo Meda, Cherie Holcomb, Hsiao-Ping Moore, Linda Hicke, and Randy Schekman. Mammalian sec23p homologue is restricted to the endoplasmic reticulum transitional cytoplasm. *Proceedings of the National Academy of Sciences*, 88(19):8611{8615, 1991.

[197] Meir Aridor, Sergei I Bannykh, Tony Rowe, and William E Balch. Sequential coupling between copii and copi vesicle coats in endoplasmic reticulum to golgi transport. *The Journal of cell biology*, 131(4):875{893, 1995.

[198] H Coste, MB Martel, and R Got. Topology of glucosylceramide synthesis in golgi membranes from porcine submaxillary glands. *Biochimica et Biophysica Acta (BBA)-Biomembranes*, 858(1):6{12, 1986.

[199] Giovanni D'Angelo, Takefumi Uemura, Chia-Chen Chuang, Elena Polishchuk, Michele Santoro, Henna Ohvo-Rekila, Takashi Sato, Giuseppe Di Tullio, Antonio Varriale, Sabato D'Auria, et al. Vesicular and non-vesicular transport feed distinct glycosylation pathways in the golgi. *Nature*, 501(7465):116{120, 2013.

[200] Xavier Buton, Paulette Herve, Janek Kubelt, Astrid Tannert, Koert NJ Burger, P Fellmann, Peter Muller, Andreas Herrmann, Michel Seigneuret, and Philippe F Devaux. Transbilayer movement of monohexosylsphingolipids in endoplasmic reticulum and golgi membranes. *Biochemistry*, 41(43):13106{13115, 2002.

[201] Mara Fabiana De Rosa, Daniel Sillence, Cameron Ackerley, and Cli ord Lingwood. Role of multiple drug resistance protein 1 in neutral but not acidic glycosphingolipid biosynthesis. *Journal of Biological Chemistry*, 279(9):7867{7876, 2004.

[202] Tomoko Nomura, Minoru Takizawa, Junken Aoki, Hiroyuki Arai, Keizo Inoue, Etsuji Wakisaka, Naonobu Yoshizuka, Genji Imokawa, Naoshi Dohmae, Koji Takio, et al. Puri cation, cdna cloning, and expression of udp-gal: glucosylceramideβ-1, 4-galactosyltransferase from rat brain. *Journal of Biological Chemistry*, 273(22):13570{13577, 1998.

[203] Tadahiro Kumagai, Takeshi Sato, Shunji Natsuka, Yukito Kobayashi, Dapeng Zhou, Tadashi Shinkai, Satoru Hayakawa, and Kiyoshi Furukawa. Involvement of murine β-1, 4-galactosyltransferase v in lactosylceramide biosynthesis. *Glycoconjugate journal*, 27(7-9):685{695, 2010.

[204] Yoshinao Kojima, Satoshi Fukumoto, Keiko Furukawa, Tetsuya Okajima, Joelle Wiels, Keiko Yokoyama, Yasuo Suzuki, Takeshi Urano, Michio Ohta, and Koichi Furukawa. Molecular cloning of globotriaosylceramide/cd77 synthase, a glycosyltransferase that initiates the synthesis of globo series glycosphingolipids. *Journal of Biological Chemistry*, 275(20):15152{15156, 2000.

[205] Tetsuya Okajima, Yoko Nakamura, Makoto Uchikawa, David B Haslam, Shin-ichiro Numata, Keiko Furukawa, Takeshi Urano, and Koichi Furukawa. Expression cloning of human globoside synthase cdnas identi cation of β3gal-t3 as udp-n-acetylgalactosamine: Globotriaosylceramideβ1, 3-n-acetylgalactosaminyltransferase. *Journal of Biological Chemistry*, 275(51):40498{40503, 2000.

[206] Mariana K Maxud, Jose L Daniotti, and Hugo JF Maccioni. Functional coupling of glycosyl transfer steps for synthesis of gangliosides in golgi membranes from neural retina cells. *Journal of Biological Chemistry*, 270(34):20207{20214, 1995.

[207] Donald M Marcus, Masaharu Naiki, and Samar K Kundu. Abnormalities in the glycosphingolipid content of human pk and p erythrocytes. *Proceedings of the National Academy of Sciences*, 73(9):3263{3267, 1976.

[208] Senthil Arumugam, Stefanie Schmieder, Weria Pezeshkian, Ulrike Becken, Christian Wunder, Dan Chinnapen, John Hjort Ipsen, Anne K Kenworthy, Wayne Lencer, Satyajit Mayor, et al. Ceramide structure dictates glycosphingolipid nanodomain assembly and function. *Nature communications*, 12(1):1{12, 2021.

[209] Gerrit Van Meer, Dennis R Voelker, and Gerald W Feigenson. Membrane lipids: where they are and how they behave. *Nature reviews Molecular cell biology*, 9(2):112{124, 2008.

[210] Gerrit van Meer and Kai Simons. The function of tight junctions in maintaining di erences in lipid composition between the apical and the basolateral cell surface domains of mdck cells. *The EMBO journal*, 5(7):1455{1464, 1986.

[211] James J Miller, Kazuhiro Aoki, Francie Moehring, Carly A Murphy, Crystal L O'Hara, Michael Tiemeyer, Cheryl L Stucky, and Nancy M Dahms. Neuropathic pain in a fabry disease rat model. *JCI insight*, 3(6), 2018.

[212] Konrad Sandho and Thomas Kolter. Topology of glycosphingolipid degradation. *Trends in cell biology*, 6(3):98{103, 1996.

[213] Martine Chatelut, Michele Leruth, Klaus Harzer, Arie Dagan, Sergio Marchesini, Shimon Gatt, Robert Salvayre, Pierre Courtoy, and Thierry Levade. Natural ceramide is unable to escape the lysosome, in contrast to a uorescent analogue. *FEBS letters*, 426(1):102{106, 1998.

[214] S Hakamori. Bifunctional role of glycosphingolipids. *J Biol Chem*, 265(18713):6, 1990.

[215] Seung-Yeol Park, Chan-Yeong Kwak, James A Shayman, and Jung Hoe Kim. Globoside promotes activation of erk by interaction with the epidermal growth factor receptor. *Biochimica et Biophysica Acta (BBA)-General Subjects*, 1820(7):1141{1148, 2012.

[216] Yu Song, Donald A Withers, and Sen-itiroh Hakomori. Globoside-dependent adhesion of human embryonal carcinoma cells, based on carbohydrate-carbohydrate interaction, initiates signal transduction and induces enhanced activity of transcription factors ap1 and creb. *Journal of Biological Chemistry*, 273(5):2517{2525, 1998.

[217] Takashi Nakamura, Yuta Chiba, Masahiro Naruse, Kan Saito, Hidemitsu Harada, and Satoshi Fukumoto. Globoside accelerates the di erentiation of dental epithelial cells into ameloblasts. *International journal of oral science*, 8(4):205{212, 2016.

[218] KR Willison, RA Karol, A Suzuki, SK Kundu, and DM Marcus. Neutral glycolipid antigens as developmental markers of mouse teratocarcinoma and early embryos: an immunologic and chemical analysis. *The Journal of Immunology*, 129(2):603{609, 1982.

[219] Nicole Lund, Martin L Olsson, Stephanie Ramkumar, Darinka Sakac, Vered Yahalom, Cyril Levene, Asa Hellberg, Xue-Zhong Ma, Beth Binnington, Daniel Jung, et al. The human pk histo-blood group antigen provides protection against hiv-1 infection. *Blood, The Journal of the American Society of Hematology*, 113(20):4980{4991, 2009.

[220] R. R. Race and joint author Sanger, Ruth. *Blood groups in man*. Oxford Blackwell Scienti c Publications, 6th ed edition, 1975. Includes bibliographical references and index.

[221] SK Kundu, A Suzuki, Bernice Sabo, Joan McCreary, E Niver, R Harman, and DM Marcus. Erythrocyte glycosphingolipids of four siblings with the rare blood group p phenotype and their parents. *International Journal of Immunogenetics*, 8(5):357{365, 1981.

[222] Hisahiro Yoshida, Kazuhiko Ito, Nobuyuki Emi, Hideharu Kanzaki, and Shunpei Matsuura. A new therapeutic antibody removal method using antigen-positive red cells: Ii. application to a p-incompatible pregnant woman. *Vox sanguinis*, 47(3):216{223, 1984.

[223] R Sue Shirey, Paul Michael Ness, Thomas Stephen Kickler, JA Rock, NA Callan, WD Schla , and J Niebyl. The association of anti-p and early abortion. *Transfusion*, 27(2):189{191, 1987.

[224] Cornelia Bircher, Jan Bieri, Ruben Assaraf, Remo Leisi, and Carlos Ros. A conserved receptor-binding domain in the vp1u of primate erythroparvoviruses determines the marked tropism for erythroid cells. *Viruses*, 14(2):420, 2022.

[225] Paolo Danise, Mariacaterina Maconi, Fabio Barrella, Anna Di Palma, Daniela Avino, Adele Rovetti, Maria Gioia, and Giovanni Amendola. Evaluation of nucleated red blood cells in the peripheral blood of hematological diseases. *Clinical chemistry and laboratory medicine*, 50(2):357{360, 2012.

[226] Axel Stachon, Tim Holland-Letz, and Michael Krieg. High in-hospital mortality of intensive care patients with nucleated red blood cells in blood. *Clinical Chemistry and Laboratory Medicine (CCLM)*, 42(8):933{938, 2004.

[227] Carlos Ros, Jan Bieri, and Remo Leisi. The vp1u of human parvovirus b19: A multifunctional capsid protein with biotechnological applications. *Viruses*, 12(12):1463, 2020.

[228] Blanche P Alter, Liya He, Robert Acosta, Mary Ellen Knobloch, JoAnn C Thomson, Patricia Giardina, and Rona S Weinberg. Sickle and thalassemic erythroid progenitor cells are di erent from normal. *Hemoglobin*, 16(6):447{467, 1992.

[229] Prajwal Boddu, Christopher B Benton, Wei Wang, Gautam Borthakur, Joseph D Khoury, and Naveen Pemmaraju. Erythroleukemia-historical perspectives and recent advances in diagnosis and management. *Blood reviews*, 32(2):96{105, 2018.

[230] Kyle J Roux, Dae In Kim, Manfred Raida, and Brian Burke. A promiscuous biotin ligase fusion protein identi es proximal and interacting proteins in mammalian cells. *The Journal of cell biology*, 196(6):801{810, 2012.

[231] Hyun-Woo Rhee, Peng Zou, Namrata D Udeshi, Je rey D Martell, Vamsi K Mootha, Steven A Carr, and Alice Y Ting. Proteomic mapping of mitochondria in living cells via spatially restricted enzymatic tagging. *Science*, 339(6125):1328{1331, 2013.

[232] Xue-Wen Li, Johanna S Rees, Peng Xue, Hong Zhang, Samir W Hamaia, Bailey Sanderson, Phillip E Funk, Richard W Farndale, Kathryn S Lilley, Sarah Perrett, et al. New insights into the dt40 b cell receptor cluster using a proteomic proximity labeling assay. *Journal of Biological Chemistry*, 289(21):14434{14447, 2014.

[233] Johanna Susan Rees, Xue-Wen Li, Sarah Perrett, Kathryn Susan Lilley, and Antony Philip Jackson. Selective proteomic proximity labeling assay using tyramide (spplat): a quantitative method for the proteomic analysis of localized membrane-bound protein clusters. *Current Protocols in Protein Science*, 88(1):19{27, 2017.

[234] Mark N Bobrow, Thomas D Harris, Krista J Shaughnessy, and Gerald J Litt. Catalyzed reporter deposition, a novel method of signal ampli cation application to immunoassays. *Journal of immunological methods*, 125(1-2):279{285, 1989.

[235] C Schöfer, Klara Weipoltshammer, Marlene Almeder, and Franz Wachtler. Signal ampli cation at the ultrastructural level using biotinylated tyramides and immunogold detection. *Histochemistry and cell biology*, 108(4-5):313{319, 1997.

[236] Ryo Kurita, Noriko Suda, Kazuhiro Sudo, Kenichi Miharada, Takashi Hiroyama, Hiroyuki Miyoshi, Kenzaburo Tani, and Yukio Nakamura. Establishment of immortalized human erythroid progenitor cell lines able to produce enucleated red blood cells. *PloS one*, 8(3):e59890, 2013.

[237] Enda Miland, Malcolm R Smyth, and Ciaran O'Fagain. Modification of horseradish peroxidase with bifunctional n-hydroxysuccinimide esters: effects on molecular stability. *Enzyme and Microbial Technology*, 19(4):242–249, 1996.

[238] NN Ugarova, GD Rozhkova, and IV Berezin. Chemical modification of the ε-amino groups of lysine residues in horseradish peroxidase and its effect on the catalytic properties and thermostability of the enzyme. *Biochimica et Biophysica Acta (BBA)-Enzymology*, 570(1):31–42, 1979.

[239] Jan Bieri, Remo Leisi, Cornelia Bircher, and Carlos Ros. Human parvovirus b19 interacts with globoside under acidic conditions as an essential step in endocytic trafficking. *PLoS Pathogens*, 17(4):e1009434, 2021.

[240] RJ Rodriguez, JF White Jr, AE Arnold, and a RS and Redman. Fungal endophytes: diversity and functional roles. *New phytologist*, 182(2):314–330, 2009.

[241] Clifford A Lingwood, H Law, Susan Richardson, Martin Petric, JL Brunton, S De Grandis, and MOHAMMED Karmali. Glycolipid binding of purified and recombinant escherichia coli produced verotoxin in vitro. *Journal of Biological Chemistry*, 262(18):8834–8839, 1987.

[242] T Waddell, S Head, M Petric, A Cohen, and C Lingwood. Globotriosyl ceramide is specifically recognized by the escherichia coli verocytotoxin 2. *Biochemical and biophysical research communications*, 152(2):674–679, 1988.

[243] S DeGrandis, H Law, James Brunton, C Gyles, and CA Lingwood. Globotetraosylceramide is recognized by the pig edema disease toxin. *Journal of Biological Chemistry*, 264(21):12520–12525, 1989.

[244] Marie E Fraser, Masao Fujinaga, Maia M Cherney, Angela R Melton-Celsa, Edda M Twiddy, Alison D O'Brien, and Michael NG James. Structure of shiga toxin type 2 (stx2) from escherichia coli o157: H7. *Journal of Biological Chemistry*, 279(26):27511–27517, 2004.

[245] Jan Holmgren, I Lönnroth, J Månsson, and Lars Svennerholm. Interaction of cholera toxin and membrane gm1 ganglioside of small intestine. *Proceedings of the National Academy of Sciences*, 72(7):2520–2524, 1975.

[246] Billy Tsai, Joanna M Gilbert, Thilo Stehle, Wayne Lencer, Thomas L Benjamin, and Tom A Rapoport. Gangliosides are receptors for murine polyoma virus and sv40. *The EMBO journal*, 22(17):4346–4355, 2003.

[247] Winfried Römer, Ludwig Berland, Valerie Chambon, Katharina Gaus, Barbara Windschiegl, Daniele Tenza, Mohamed RE Aly, Vincent Fraisier, Jean-Claude Florent, David Perrais, et al. Shiga toxin induces tubular membrane invaginations for its uptake into cells. *Nature*, 450(7170):670–675, 2007.

[248] Helge Ewers, Winfried Römer, Alicia E Smith, Kirsten Bacia, Serge Dmitrieff, Wengang Chai, Roberta Mancini, Jürgen Kartenbeck, Valerie Chambon, Ludwig Berland, et al. Gm1 structure determines sv40-induced membrane invagination and infection. *Nature cell biology*, 12(1):11–18, 2010.

[249] Weria Pezeshkian, Allan Gronhoj Hansen, Ludger Johannes, Himanshu Khandelia, Julian C Shillcock, PB Sunil Kumar, and John Hjort Ipsen. Membrane invagination induced by shiga toxin b-subunit: from molecular structure to tube formation. *Soft matter*, 12(23):5164{5171, 2016.

[250] Jiirgen Kartenbeck, Hans Stukenbrok, and Ari Helenius. Endocytosis of simian virus 40 into the endoplasmic reticulum. *The Journal of cell biology*, 109(6):2721{2729, 1989.

[251] Benjamin J Nichols, Anne K Kenworthy, Roman S Polishchuk, Robert Lodge, Theresa H Roberts, Koret Hirschberg, Robert D Phair, and Jennifer Lippincott-Schwartz. Rapid cycling of lipid raft markers between the cell surface and golgi complex. *Journal of Cell Biology*, 153(3):529{542, 2001.

[252] Frederic Mallard, Claude Antony, Danièle Tenza, Jean Salamero, Bruno Goud, and Ludger Johannes. Direct pathway from early/recycling endosomes to the golgi apparatus revealed through the study of shiga toxin b-fragment transport. *The Journal of cell biology*, 143(4):973{990, 1998.

[253] Leonard C Norkin, Howard A Anderson, Scott A Wolfrom, and Ariella Oppenheim. Caveolar endocytosis of simian virus 40 is followed by brefeldin a-sensitive transport to the endoplasmic reticulum, where the virus disassembles. *Journal of virology*, 76(10):5156{5166, 2002.

[254] Noah D Fabricant. Signi cance of the ph of nasal secretions in situ. *Archives of Otolaryngology*, 34(1):150{163, 1941.

[255] SS Hehar, JDT Mason, AB Stephen, N Washington, NS Jones, SJ Jackson, and D Bush. Twenty-four hour ambulatory nasal ph monitoring. *Clinical Otolaryngology & Allied Sciences*, 24(1):24{25, 1999.

[256] RJA England, JJ Homer, LC Knight, and SR Ell. Nasal ph measurement: a reliable and repeatable parameter. *Clinical Otolaryngology & Allied Sciences*, 24(1):67{68, 1999.

[257] D McShane, JC Davies, MG Davies, A Bush, DM Geddes, and EWFW Alton. Airway surface ph in subjects with cystic brosis. *European Respiratory Journal*, 21(1):37{42, 2003.

[258] H Breuninger. Über das physikalisch-chemische verhalten des nasenschleims. *Archiv für Ohren-, Nasen- und Kehlkopfheilkunde*, 184(2):133{138, 1964.

[259] Charles R Bodem, Lawrence M Lampton, Donald P Miller, Eugene F Tarka, and E Dale Everett. Endobronchial ph: relevance to aminoglycoside activity in gram-negative bacillary pneumonia. *American Review of Respiratory Disease*, 127(1):39{41, 1983.

[260] Joaqun Araos, Luis Silva, Rocio Salsoso, Tamara Saez, Eric Barros, Fernando Toledo, Jaime Gutierrez, Fabian Pardo, Andrea Leiva, Carlos Sanhueza, et al. Intracellular and extracellular ph dynamics in the human placenta from diabetes mellitus. *Placenta*, 43:47{53, 2016.

[261] JA Jordan and JA DeLoia. Globoside expression within the human placenta. *Placenta*, 20(1):103{108, 1999.

[262] Ma'asoumah Makhseed, Alexander Pacsa, Mohammad Abrar Ahmed, and Sahar Sultan Essa. Pattern of parvovirus b19 infection during di erent trimesters of pregnancy in kuwait. *Infectious diseases in obstetrics and gynecology*, 7(6):287{292, 1999.

[263] HA Anderson, Y Chen, and LC Norkin. Bound simian virus 40 translocates to caveolin-enriched membrane domains, and its entry is inhibited by drugs that selectively disrupt caveolae. *Molecular biology of the cell*, 7(11):1825{1834, 1996.

[264] Palmer A Orlandi and Peter H Fishman. Filipin-dependent inhibition of cholera toxin: evidence for toxin internalization and activation through caveolae-like domains. *Journal of Cell Biology*, 141(4):905{915, 1998.

[265] Eva-Maria Damm, Lucas Pelkmans, Jurgen Kartenbeck, Anna Mezzacasa, Teymuras Kurzchalia, and Ari Helenius. Clathrin-and caveolin-1{independent endocytosis: entry of simian virus 40 into cells devoid of caveolae. *The Journal of cell biology*, 168(3):477{488, 2005.

[266] Henri-Francois Renard, Mijo Simunovic, Joel Lemière, Emmanuel Boucrot, Maria Daniela Garcia-Castillo, Senthil Arumugam, Valerie Chambon, Christophe Lamaze, Christian Wunder, Anne K Kenworthy, et al. Endophilin-a2 functions in membrane scission in clathrin-independent endocytosis. *Nature*, 517(7535):493{496, 2015.

[267] Giovanni Di Pasquale and John A Chiorini. Aav transcytosis through barrier epithelia and endothelium. *Molecular therapy*, 13(3):506{516, 2006.

[268] Giovanni Di Pasquale, Lynda Ostedgaard, Daniel Vermeer, William D Swaim, Philip Karp, and John A Chiorini. Bovine aav transcytosis inhibition by tannic acid results in functional expression of cftr in vitro and altered biodistribution in vivo. *Gene therapy*, 19(5):576{581, 2012.

[269] Steven F Merkel, Allison M Andrews, Evan M Lutton, Dakai Mu, Eloise Hudry, Bradley T Hyman, Casey A Maguire, and Servio H Ramirez. Tra cking of aav vectors across a model of the blood-brain barrier; a comparative study of transcytosis and transduction using primary human brain endothelial cells. *Journal of neurochemistry*, 140(2):216, 2017.

[270] Hao Wu, Veronica Estrella, Matthew Beatty, Dominique Abrahams, Asmaa El-Kenawi, Shonagh Russell, Arig Ibrahim-Hashim, Dario Livio Longo, Yana K Reshetnyak, Anna Moshnikova, et al. T-cells produce acidic niches in lymph nodes to suppress their own e ector functions. *Nature communications*, 11(1):1{13, 2020.

[271] Emilie-Fleur Gautier, Sarah Ducamp, Marjorie Leduc, Virginie Salnot, Francois Guillonneau, Michael Dussiot, John Hale, Marie-Catherine Giarratana, Anna Raimbault, Luc Douay, et al. Comprehensive proteomic analysis of human erythropoiesis. *Cell reports*, 16(5):1470{1484, 2016.

[272] Eileen Remold-O'Donnell, Christopher Zimmerman, Dianne Kenney, and Fred S Rosen. Expression on blood cells of sialophorin, the surface glycoprotein that is defective in wiskott-aldrich syndrome. 1987.

[273] Thomas Moore, Shiang Huang, LW Terstappen, Michael Bennett, and Vinay Kumar. Expression of cd43 on murine and human pluripotent hematopoietic stem cells. *The Journal of Immunology*, 153(11):4978{4987, 1994.

[274] SR Carlsson and M Fukuda. Isolation and characterization of leukosialin, a major sialoglycoprotein on human leukocytes. *Journal of Biological Chemistry*, 261(27):12779{12786, 1986.

[275] Sven R Carlsson, H Sasaki, and M Fukuda. Structural variations of o-linked oligosaccharides present in leukosialin isolated from erythroid, myeloid, and t-lymphoid cell lines. *Journal of Biological Chemistry*, 261(27):12787{12795, 1986.

[276] A Bettaieb, F Farace, MT Mitjavila, Z Mishal, MC Dokhelar, T Tursz, J Breton-Gorius, W Vainchenker, and N Kie er. Use of a monoclonal antibody (ga3) to demonstrate lineage restricted o-glycosylation on leukosialin during terminal erythroid di erentiation. 1988.

[277] C Simon Shelley, Eileen Remold-O'Donnell, Alvin E Davis, GA Bruns, Fred S Rosen, Michael C Carroll, and Alexander S Whitehead. Molecular characterization of sialophorin (cd43), the lymphocyte surface sialoglycoprotein defective in wiskott-aldrich syndrome. *Proceedings of the National Academy of Sciences*, 86(8):2819{2823, 1989.

[278] Jason Cyster, Chamorro Somoza, Nigel Killeen, and Alan F Williams. Protein sequence and gene structure for mouse leukosialin (cd43), a t lymphocyte mucin without introns in the coding sequence. *European journal of immunology*, 20(4):875{881, 1990.

[279] Dan Baeckstrom. Post-translational fate of a mucin-like leukocyte sialoglycoprotein (cd43) aberrantly expressed in a colon carcinoma cell line. *Journal of Biological Chemistry*, 272(17):11503{11509, 1997.

[280] Ulhas P Naik, YH Ehrlich, and E Kornecki. Mechanisms of platelet activation by a stimulatory antibody: cross-linking of a novel platelet receptor for monoclonal antibody f11 with the fcγ rii receptor. *Biochemical Journal*, 310(1):155{162, 1995.

[281] Erik S Barton, J Craig Forrest, Jodi L Connolly, James D Chappell, Yuan Liu, Frederick J Schnell, Asma Nusrat, Charles A Parkos, and Terence S Dermody. Junction adhesion molecule is a receptor for reovirus. *Cell*, 104(3):441{451, 2001.

[282] Ngan NT Nguyen, Yun-Sook Lim, Lap P Nguyen, Si C Tran, Trang TD Luong, Tram TT Nguyen, Hang T Pham, Han N Mai, Jae-Woong Choi, Sang-Seop Han, et al. Hepatitis c virus modulates solute carrier family 3 member 2 for viral propagation. *Scientific reports*, 8(1):1{14, 2018.

[283] Morgyn S Warner, Robert J Geraghty, Wanda M Martinez, Rebecca I Montgomery, J Charles Whitbeck, Ruliang Xu, Roselyn J Eisenberg, Gary H Cohen, and Patricia G Spear. A cell surface protein with herpesvirus entry activity (hveb) confers susceptibility to infection by mutants of herpes simplex virus type 1, herpes simplex virus type 2, and pseudorabies virus. *Virology*, 246(1):179{189, 1998.

[284] Qiang Liu, Jun Zheng, Weiping Sun, Yinbo Huo, Liye Zhang, Piliang Hao, Haopeng Wang, and Min Zhuang. A proximity-tagging system to identify membrane protein{protein interactions. *Nature methods*, 15(9):715{722, 2018.

[285] Stephen A Schnell, William A Staines, and Martin W Wessendorf. Reduction of lipofuscin-like auto uorescence in uorescently labeled tissue. *Journal of Histochemistry & Cytochemistry*, 47(6):719{730, 1999.

[286] Johannes Muthing, Ulrich Maurer, Ksenija Sostarie, Ulrich Neumann, Heike Brandt, Sevim Duvar, Jasna Peter-Katalinie, and Sabine Weber-Schurholz. Di erent distributions of glycosphingolipids in mouse and

rabbit skeletal muscle demonstrated by biochemical and immunohistological analyses.*The Journal of Biochemistry*, 115(2):248{256, 1994.

6 Appendix

6.1 Antibodies

Name	Dilution	Source
Human MAb IgG 860-55D	1:100 (IF)	Mikrogen, 94406,
Mouse MAb IgG 3113-81C	1:100 (IF), 1:1500 (WB)	US biological, P3113-81C-100ug
Chicken PAb IgY α-globoside	1:100 (IF)	J. Mühthing [286]
Mouse MAb α-M6PR	1:100 (IF)	Abcam, ab2733
Mouse MAb α-LAMP1	1:50 (IF)	Abcam, ab25630

6.2 Primers

All primers were obtained from Microsynth.

Primer name	Primer sequence
F B3GalNT1 mRNA	5'-CTC CTG AGT TTC TTT GTG ATG TGG-3'
R B3GalNT1 mRNA	5'-CAT TAC GTA CTT GGC ATT GGG G-3'
F B3GalNT1 mRNA nested	5'-CCC CAC TAC AAT GTG ATA GAA CGC-3'
R B3GalNT1 mRNA nested	5'-GGC AAA ACT CAG TTA CCC ACC-3'
F GAPDH mRNA control	5'-GCC AAA AGG GTC ATC ATC TCT G-3'
R GAPDH mRNA control	5'-CCT GCT TCA CCA CCT TCT TG-3'
F ACTBL DNA	5'-GTG GGA TCC ATG AGA CAA CC TC-3'
R ACTBL DNA	5'-GTG GT ATC TGG GTA AGA GCC C-3'
F NS1 / B19V DNA	5'-GGG GCA GCA TGT GTT AA-3'
R NS1 / B19V DNA	5'-CCA TGC CAT ATA CTG GAA CAC T-3'
F Insert Check	5'-GTT GGC TAC GTA TAC TCC GG-3'
R Insert Check	5'-ATG GTG CTC TGG GTC ATA TGG-3'
FW-4	5'-CAA GGA ATT TCT GGA GAC AGC-3'
F Transposition	5'-CCC AGT CAC GAC GTT GTA AAA CG-3'
R Transposition	5'-AGC GGA TAA CAA TTT CAC ACA GG-3'
F gp64	5'-CGG CGT GAG TAT GAT TCT CAA A-3'
R gp64	5'-ATG AGC AGA CAC GCA GCT TTT-3'

6.3 PCR Programs

Genomic PCR: After DNA extraction or, in case of nested PCR, after dilution of the initial amplicon the following mastermix was prepared:

Component	Volume per sample	Final concentration
Luna Universal 2× mix (NEB, M3003)	10 µl	1 ×
Forward Primer	1 µl	500 nM
Reverse Primer	1µl	500 nM
dH_2O	6 µl	
Total volume per sample:	18 µl	

The 2 µl DNA extract or standard were added to the 18 µl mastermix and run with the following protocol. In case of nested PCR, the product of a prior PCR run was diluted 1:10'000 in dH_2O and used instead.

B19 DNA quanti cation

Duration [s]	Temperature [°C]
300	95.0
10	95.0
15	55.0
20	72.0 go to step 3 (39×)
60	95.0
Melting curve	65.0 - 95.0

Nested PCR B3GalNT1

Duration [s]	Temperature [°C]
600	95.0
15	95.0
20	56.0
30	72.0; go to step 3 (39×)
60	95.0
Melting curve	65.0 - 95.0

Colony PCR pFastBac1-VP2

Duration [s]	Temperature [°C]
300	95.0
15	95.0
15	55.0
25	72.0; go to step 2 (39×)
60	95.0
Melting curve	65.0 - 95.0

Bacmid Transposition Colony PCR

Duration [s]	Temperature [°C]
120	95.0
20	95.0
20	55.0
45	72.0; go to step 3 (39×)
60	95.0
Melting curve	65.0 - 95.0

Quanti cation of Baculovirus P0 stock

Duration [s]	Temperature [°C]
120	95.0
10	95.0
35	60.0; go to step 2 (39×)
Melting curve	65.0 - 95.0

RT-qPCR: Reverse transcription was performed in a one-step reaction. Reverse transcription PCR was performed using the following mastermix:

Component	Volume per sample	Final concentration
Luna Universal 2× mix (NEB, M3003)	10 µl	1 ×
Luna Reverse Transcriptase (NEB, E3005)	1µl	1 ×
Forward Primer	1 µl	500 nM
Reverse Primer	1µl	500 nM
dH_2O	5 µl	
Total volume per sample:	18 µl	

2 µl isolated mRNA or standards were added to the 18µl mastermix and run with the following protocol:

B19 NS1 infectivity assay

Duration [s]	Temperature [°C]
600	55.0
300	95.0
10	95.0
15	55.0
20	72.0 go to step 3 (39×)
60	95.0
Melting curve	65.0 - 95.0

B3GalNT1 mRNA / GAPDH mRNA

Duration [s]	Temperature [°C]
600	55.0
60	95.0
10	95.0
20	57.0
30	60.0 go to step 3 (39×)
60	95.0
Melting curve	65.0 - 95.0

Cloning with Q5 Polymerase was performed using the following set-up:

Component	Volume per sample	Final concentration
Q5 High-Fidelity 2 × Master Mix (NEB, M0492)	25 µl	1 ×
Forward Primer	2.5 µl	500 nM
Reverse Primer	2.5µl	500 nM
DMSO	2 µl	4 %
dH_2O	18 - [volume DNA] µl	
Total volume per sample:	50 - [volume DNA] µl	

PCR programs using Q5 polymerase:

Cloning of VP2 ORF

Duration [s]	Temperature [°C]
300	95.0
15	95.0
20	58.0
90	72.0 go to step 2 (1×)
15	95.0
20	68.0
90	72.0 go to step 5 (37×)

Analysis of isolated bacmids

Duration [s]	Temperature [°C]
300	95.0
45	95.0
45	60.0
240	72.0 go to step 2 (1×)
600	72.0

6.4 Plasmids

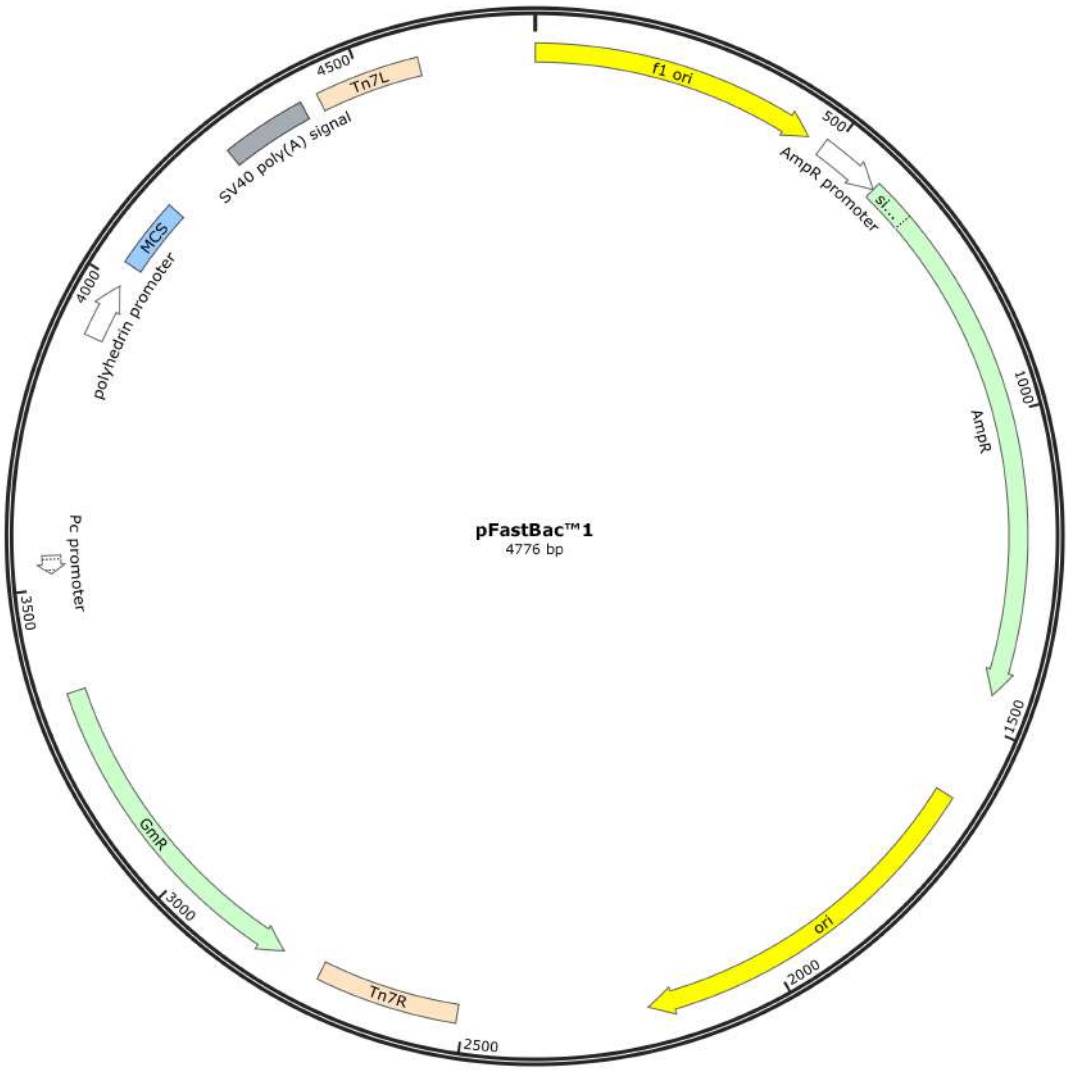

Figure 15: The pFastBac1 plasmid used in the generation of recombinant baculovirus genomes. The multiple cloning site (MCS, marked in blue) contains the necessary restriction sites EcoRI and HindIII for the introduction of the B19V VP2 ORF. The two sequences marked with Tn7L and Tn7R denote the complementary sequences that enclose the part of the plasmid that will be transposed to the bacmid.

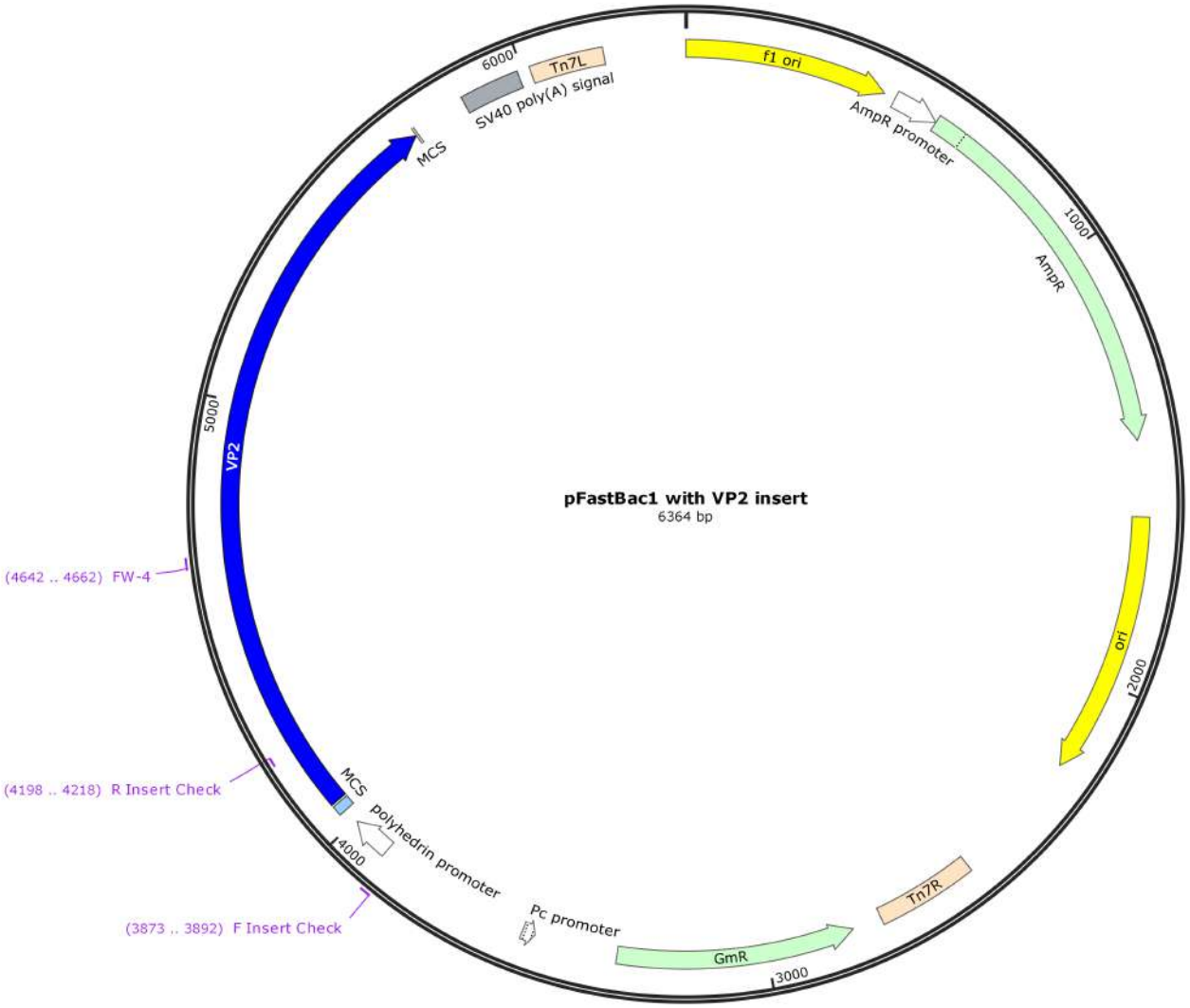

Figure 16: The pFastBac1 with the inserted VP2 gene sequence of B19V. Primers that were used for colony PCR as well as for sequencing are denoted in purple.

Erklärung

gemäss Art. 18 PromR Phil.-nat. 2019

Name/Vorname: Bieri Jan

Matrikelnummer: 13-120-357

Studiengang: PhD - Chemistry and molecular Sciences

Bachelor ☐ Master ☐ Dissertation ☑

Titel der Arbeit: Receptor switching controls human parvovirus B19 tropism and cell entry

LeiterIn der Arbeit: PD Dr. Carlos Ros

Ich erkläre hiermit, dass ich diese Arbeit selbständig verfasst und keine anderen als die angegebenen Quel-len benutzt habe. Alle Stellen, die wörtlich oder sinn-gemäss aus Quellen entnommen wurden, habe ich als solche gekennzeichnet. Mir ist bekannt, dass andern-falls der Senat gemäss Artikel 36 Absatz 1 Buchstabe r des Gesetzes über die Universität vom 5. September 1996 und Artikel 69 des Universitätssta-tuts vom 7. Juni 2011 zum Entzug des Doktortitels be-rechtigt ist.
Für die Zwecke der Begutachtung und der Überprüfung der Einhaltung der Selbständigkeitserklärung bzw. der Reglemente betreffend Plagiate erteile ich der Univer-sität Bern das Recht, die dazu erforderlichen Perso-nendaten zu bearbeiten und Nutzungshandlungen vor-zunehmen, insbesondere die Doktorarbeit zu vervielfäl-tigen und dauerhaft in einer Datenbank zu speichern sowie diese zur Überprüfung von Arbeiten Dritter zu verwenden oder hierzu zur Verfügung zu stellen.

Ort/Datum

Unterschrift